

INVESTIGATIONS ON THE ELECTRICAL CHARACTERISTICS OF CERTAIN SEMICONDUCTOR FILMS AND POLYMERIZED PARA-TOLUIDINE FILMS.

THESIS SUBMITTED IN PARTIAL FULFILMENT OF
THE REQUIREMENTS FOR THE DEGREE OF
DOCTOR OF PHILOSOPHY

NIRMALA PAUL

DEPARTMENT OF PHYSICS
UNIVERSITY OF COCHIN

1981

DECLARATION

Certified that the work presented in this thesis is based on the original work done by me under the guidance of Dr.M.G. Krishna Pillai, Professor, Department of Physics, University of Cochin, and has not been included in any other thesis submitted previously for the award of any degree.

Cochin-22, }
2 December 1981. }


NIRMALA PAUL

CERTIFICATE

Certified that the work reported in the present thesis is based on the bona fide work done by Miss Nirmala Paul, Research Scholar, under my guidance in the Department of Physics, University of Cochin, and has not been included in any other thesis submitted previously for the award of any degree.

Cochin-22, }
2 December 1981. }


Dr. M.G. KRISHNA PILLAI
Professor of Physics
(Supervising Teacher)

SYNOPSIS

INVESTIGATIONS ON THE ELECTRICAL CHARACTERISTICS OF CERTAIN SEMICONDUCTOR FILMS AND POLYMERIZED PARA-TOLUIDINE FILMS

The thesis is a report of the attempts made to prepare semiconducting and dielectric thin films and to study their electrical properties. It consists of (i) studies on the preparation and electrical characteristics of compound semiconductor thin films of silver sulphide and ferric hydroxide, and (ii) investigations on the electrical and dielectric properties of plasma polymerized thin films of para-toluidine.

Compound thin films of both silver sulphide and ferric hydroxide have been prepared by chemical method involving an interfacial chemical reaction of a solution and a gas. A controlled chemical reaction between hydrogen sulphide gas and silver nitrate solution has been used to produce silver sulphide films. The n-type Ag_2S films thus prepared have been used for the electrical conductivity studies. The temperature dependence of electrical conduction in these films has been studied in the temperature range 303K to 473K. The log conductivity versus

temperature curve shows an abrupt change in conductivity at about 443K. In the higher temperature region the resistance of the films shows an almost temperature independent behaviour. At the region where sharp change in conductivity is observed, the curve does not follow exactly the same path for heating and cooling cycles. The activation energies for conduction in the regions have been determined. These studies have been carried out for films of thicknesses ranging from 400 Å to 2200 Å. The dependence of the temperature coefficient of resistance of the silver sulphide films on thickness and temperature has been studied. From the conductivity studies it is concluded that in the temperature range below 450K ionic conduction is predominant whereas in the temperature range above 450K electronic conduction is predominant.

Ferric hydroxide films have been prepared by the chemical reaction between ferrous sulphate solution and ammonia gas in a controlled atmosphere. The ferric hydroxide films thus prepared have been found to be amorphous in nature as revealed by X-ray diffraction studies and they are used for electrical conduction studies. Temperature dependence of electrical resistivity in the temperature range 303K to 473K revealed two types of conduction in

the system. At temperatures above 313K the conduction is due to the intrinsic defects and below 313K the conduction is due to impurities. Studies have been carried out for films in the thickness range 180 \AA to 1500 \AA . The activation energy for conduction, calculated for films of different thicknesses is found to be dependent on the thickness. As the thickness of the film increases the activation energy is found to decrease, which is attributed to the impurity charge carriers giving rise to various energy levels in the band gap.

Polymer thin films of para-toluidine have been prepared in a radiofrequency glow discharge from the monomer para-toluidine in a vacuum of the order of 10^{-2} torr. A radiofrequency oscillator which oscillates at a frequency of ~ 4.5 MHz giving enough power for polymerizing has been designed and fabricated as part of the research work. A vacuum set up together with the plasma zone has also been designed to suit the necessities of polymerization and fabricated using corning glass. The system is able to attain a vacuum better than 10^{-2} torr using a rotary pump. The power from the RF source is fed to the discharge tube by capacitive coupling.

The monomer p-toluidine has been polymerized by the electrodeless glow discharge method in a vacuum of 2×10^{-2} torr. Sodium chloride crystals and microscope glass slides have been used as substrates. The films deposited on the sodium chloride have been used for the infrared studies which give information regarding the structure of the polymer. On comparison of the IR spectra of both the monomer and polymer, it is proposed that the polymerization of p-toluidine is by hydrogen abstraction and the polymer units are linked by polar C-N bonds. The polymer films show good adhesion to the substrate and are found to be chemically inert. The high stability and insoluble nature of the polymer suggest the presence of cross links in it.

The current-voltage characteristics of the glow discharge polymerized p-toluidine films sandwiched between aluminium electrodes have been studied for different film thicknesses. The aluminium electrodes have been pre- and post deposited to prepare the metal-polymer-metal sandwich from a tungsten filament in a high vacuum coating unit. The current-voltage characteristics show an ohmic region at low fields and a square law region at high fields. In

the square law region the current shows an inverse cube dependence on thickness. The $I \propto V^2/d^3$ dependence suggests a space-charge-limited conduction in the film system.

Knowing the trap filled limit voltage V_{TFL} and the crossover voltage V_x from the Ohm's law to square law region, the trap concentration N_t and the trap energy level E_t have been calculated.

The aluminium-polymer-aluminium structures have been used for the dielectric studies. The temperature dependence of dielectric constant and dielectric loss in the temperature range 303K to 473K and the variation of capacitance with film thickness at a fixed frequency 1 KHz have been studied. The dielectric constant shows an increase with increase of temperature which may be attributed to the effects of the impurities and lattice defects. A loss peak has been observed at 423K in the $\tan \delta$ versus temperature curve, which is suggested to be due to the change in crystallinity in the polymer films.

The properties of silver sulphide films have been observed to be comparable with those of the films prepared by other methods especially the vacuum evaporation technique [1]. The polymer films produced by electrodeless

glow discharge method show properties similar to those of high quality GD polymer films [2,3]. Thus it is concluded that semiconducting and dielectric films having desirable properties can be prepared by the rather simple technique used in the present investigation.

References

- [1] A. Ichimescu and L. Constantinescu, Rev. Roum. Phys.,
17, 163 (1972)
- [2] M. Millard in "Techniques and Applications of Plasma
Chemistry" (J.R. Hollahan and A.T. Bell, eds.),
Wiley-Interscience, New York (1974)
- [3] J.M. Tibbit, A.T. Bell and M. Shen in "Plasma Chemistry
of Polymers" (M. Shen, ed.), Marcel Dekker Inter-
science, New York (1976)

CONTENTS

		Page
SYNOPSIS	..	i
INTRODUCTION	..	1
CHAPTER ONE	SEMICONDUCTING AND INSULATING THIN FILMS--A BRIEF REVIEW	5
1.1	Preparation of Thin Films	5
1.2	Polymer Thin Films	11
1.3	Thickness Measurements of Thin Films	22
1.4	Transport Properties of Insulating and Semiconducting Thin Films	26
1.5	Transport Phenomena in Polymeric Materials	38
CHAPTER TWO	PREPARATION AND CHARACTERIZATION OF SILVER SULPHIDE AND FERRIC HYDROXIDE THIN FILMS	42
2.1	Introduction	42
2.2	Preparation of Silver Sulphide Films	43
2.3	Characterization of Silver Sulphide Films	46
2.4	Preparation of Ferric Hydroxide Films	47
2.5	Characterization of Ferric Hydroxide Films	50
CHAPTER THREE	ELECTRICAL CHARACTERIZATION OF SILVER SULPHIDE FILMS	54
3.1	Introduction	54
3.2	Structure Fabrication and Resistance Measurements	58
3.3	Results	60
3.4	Discussion	63
CHAPTER FOUR	ELECTRICAL CHARACTERIZATION OF FERRIC HYDROXIDE AND FERRIC OXIDE THIN FILMS	68
4.1	Structure Fabrication and Measurement Set Up	68
4.2	Results	70
4.3	Discussion	72

	Page
CHAPTER FIVE	
PREPARATION AND CHARACTERIZATION OF GLOW DISCHARGE POLYMERIZED PARA-TOLUIDINE THIN FILMS ..	76
5.1	76
5.2	77
5.3	79
5.4	81
CHAPTER SIX	
DIELECTRIC STUDIES ON GLOW DISCHARGE POLYMERIZED PARA- TOLUIDINE THIN FILMS ..	86
6.1	86
6.2	87
6.3	92
6.4	93
6.5	95
6.6	97
6.7	98
CHAPTER SEVEN	
SPACE CHARGE LIMITED CONDUCTION IN POLYMER FILMS OF PARA- TOLUIDINE ..	100
7.1	100
7.2	100
7.3	102
7.4	103
CHAPTER EIGHT	
SUMMARY AND CONCLUSION ..	107
8.1	107
8.2	112
REFERENCES ..	114
LIST OF SYMBOLS ..	133
ACKNOWLEDGEMENTS ..	137

INTRODUCTION

Thin films play an important role in modern optical and electronic technologies. The advancement of physics of thin films has helped the microminiaturization of electronic components to such an extent that without it the new developments in space physics and communication networks would have been impossible. Even though the earlier investigations were mainly on metallic films [1,2] the later developments brought in its folds semiconducting and insulating films and this paved the way for new branches in this field.

The properties of thin films of a material are found to be much different from those of the parent bulk material. This change in nature itself is responsible to a great extent, for the development of new, compact and efficient thin film devices. Various methods have been developed for the preparation of thin films. Even though evaporation technique is commonly used for the preparation of majority of the films, certain newly developed techniques of chemical deposition are found to be more ideal in the preparation of semiconducting and insulating thin films. Evaporation of the compound semiconductor may result in non-stoichiometry of the resulting films whereas by the chemical deposition method stoichiometric films can be prepared. Several compound semiconducting films such as GaAs [3], CdS [4] etc. have been successfully prepared by

this method. Generally, in thin films, the electrical conduction has been studied both along and across the films. In the case of insulating films the conduction across the films is much treated whereas in the case of semiconducting films the conduction along the plane of the film is more significant [5].

Polymer films are found to be better insulators compared to other insulating films. Polymer films of semiconducting nature also do exist. Of the various methods proposed for the preparation of polymer films, the glow discharge method is widely used. Such films have numerous merits over conventional polymer films both in their preparation and applications [6-9]. Plasma polymerized dielectric films are used in the fabrication of microcapacitors [10]. The main advantage of such films is that they can be obtained as very thin films of high stability, good electrical properties and pin-hole free nature.

In the present thesis, investigations on the preparation and electrical characterization of semiconducting films of silver sulphide and ferric hydroxide are presented along with a detailed study on the glow discharge polymerization of para-toluidine films and their electrical characterization.

The silver sulphide films on glass substrate have been prepared by the chemical deposition method, employing the chemical reaction between silver nitrate solution and hydrogen sulphide gas. The electrical conductivity of these films at different temperatures has been studied and the conduction mechanism explained. Ferric hydroxide films have been prepared by a similar technique utilizing the chemical reaction between ferrous sulphate solution and ammonia gas. The electrical conduction in these films in the temperature range 303K to 473K has been studied.

Polymer films from the monomer para-toluidine have been prepared by the electrodeless glow discharge polymerization technique. The polymer units have been characterized with the help of infra-red studies and possible mechanism of polymerization is suggested. The electrical conduction in these films sandwiched between aluminium electrodes has also been studied. The d.c. conduction revealed a space charge limited electron flow in the system. The dielectric properties of aluminium-polymer-aluminium system have also been investigated and the behaviour has been found to be related to the structure of the film.

Part of the above investigations has been communicated in the form of the following research papers:

- 1) Variation of Electrical Conductivity of Ferric Hydroxide Films with Temperature,
Indian Journal of Pure and Appl. Phys., 18,
311-313 (1980).
- 2) Dielectric Studies of Poly-p-Toluidine Films Produced by the Electrodeless Glow Discharge Method,
Thin Solid Films, 76, 201-205 (1981).
- 3) Electrical Conductivity Studies of Silver Sulphide Films prepared by Chemical Method
(To be published).
- 4) Space Charge Limited Currents in Electrodeless Glow Discharge Polymerized Films of p-Toluidine
(To be published).

CHAPTER ONE

SEMICONDUCTING AND INSULATING THIN FILMS--A BRIEF REVIEW

1.1 Preparation of Thin Films

Number of methods are used for the preparation of thin films. Selection of a particular method is governed by the nature of the films to be obtained and also by the application of these films. Several excellent reviews dealing with the techniques followed in the preparation of thin films are available [11-17]. Broadly all these methods can be classified under two heads: (A) Physical methods and (B) Chemical methods. Sputtering and evaporation are the commonly employed physical methods. The chemical methods consist mainly of chemical vapour deposition (CVD) and electro deposition.

A. Physical Methods

1.1.1 Sputtering

Sputtering refers to the ejection of surface atoms when the surface is bombarded with energetic particles. These ejected atoms, called as the sputtered atoms are condensed on a suitable substrate to form thin film. Low- and high pressure sputterings are employed for the preparation of thin films. The different sputtering techniques are: [11] (1) Glow discharge sputtering, (2) Bias sputtering, (3) Triode sputtering, (4) Ion beam sputtering, (5) R.F. sputtering and (6) Reactive sputtering.

1.1.2 Evaporation

This is the most commonly accepted method for thin film preparation [11,13]. As the evaporation is carried out in high vacuum the presence of impurities in the film will be minimum. The rate of evaporation and the condensation of the vapour depend upon the evaporation source and the material used. The different methods of evaporation are:

(1) Resistive heating, (2) Flash evaporation, (3) Arc evaporation, (4) Laser evaporation, (5) RF heating, (6) Electron bombardment heating and (7) Multiple beam epitaxy. As resistive heating method is used in the present investigation, it is briefly described.

Resistive heating consists of evaporation of the material from a resistively heated filament or boat usually made of refractory metals such as tungsten, molybdenum, tantalum or niobium. Most of the materials can be resistively evaporated choosing suitable sources. Vapour sources of various types, geometries and sizes are used according to the material to be evaporated. The filament material should have structural stability, low vapour pressure and it should not alloy with the evaporant at elevated temperatures.

In the present investigation, resistive heating has been employed for the deposition of silver (99.999%) and aluminium (99.999%) electrodes. Silver gets evaporated from

molybdenum boats of size 6cm x 1.1cm x 0.1mm and aluminium from coiled tungsten filament of 0.05cm diameter. The evaporation has been carried out in a high vacuum coating unit capable of attaining a vacuum better than 10^{-5} torr. The details of the coating unit are given below.

1.1.3 Vacuum Coating Unit

The vacuum coating unit consists mainly of three parts: (1) the pumping system, (2) the vacuum chamber and (3) power supply. The material to be evaporated is kept in the vacuum chamber of diameter 12 inches which stands on a collar, fitted to the cabinet inside which the pumping system is located. The schematic diagram of the coating unit is given in figure (1.1). The pumping system incorporates a four stage, water cooled, fractionating 6 inch oil diffusion pump, having a baffle pumping speed of 1000 litres per second and an oil capacity of 500 ml, (silicon DC 704 oil) backed by a double stage rotary pump having a pumping speed of 540 litres per minute.

The vacuum chamber is connected to the rotary pump through the roughing valve and the backing valve connects the diffusion pump to the rotary pump. The diffusion pump is isolated from the work chamber through the water cooled baffle. The rotary pump evacuation of the work chamber is done keeping the baffle valve closed and for the diffusion evacuation the baffle valve is opened.

- A - Vacuum chamber
- B - Rotary pump
- C - Backing valve
- D - Diffusion pump
- E - Roughing valve
- P₁ - Pirani gauge
- F - Baffle valve
- G - Base plate
- P₂ - Pennig gauge
- V₁ - Rotary pump vent
- V₂ - Vacuum chamber vent
- S - Shutter

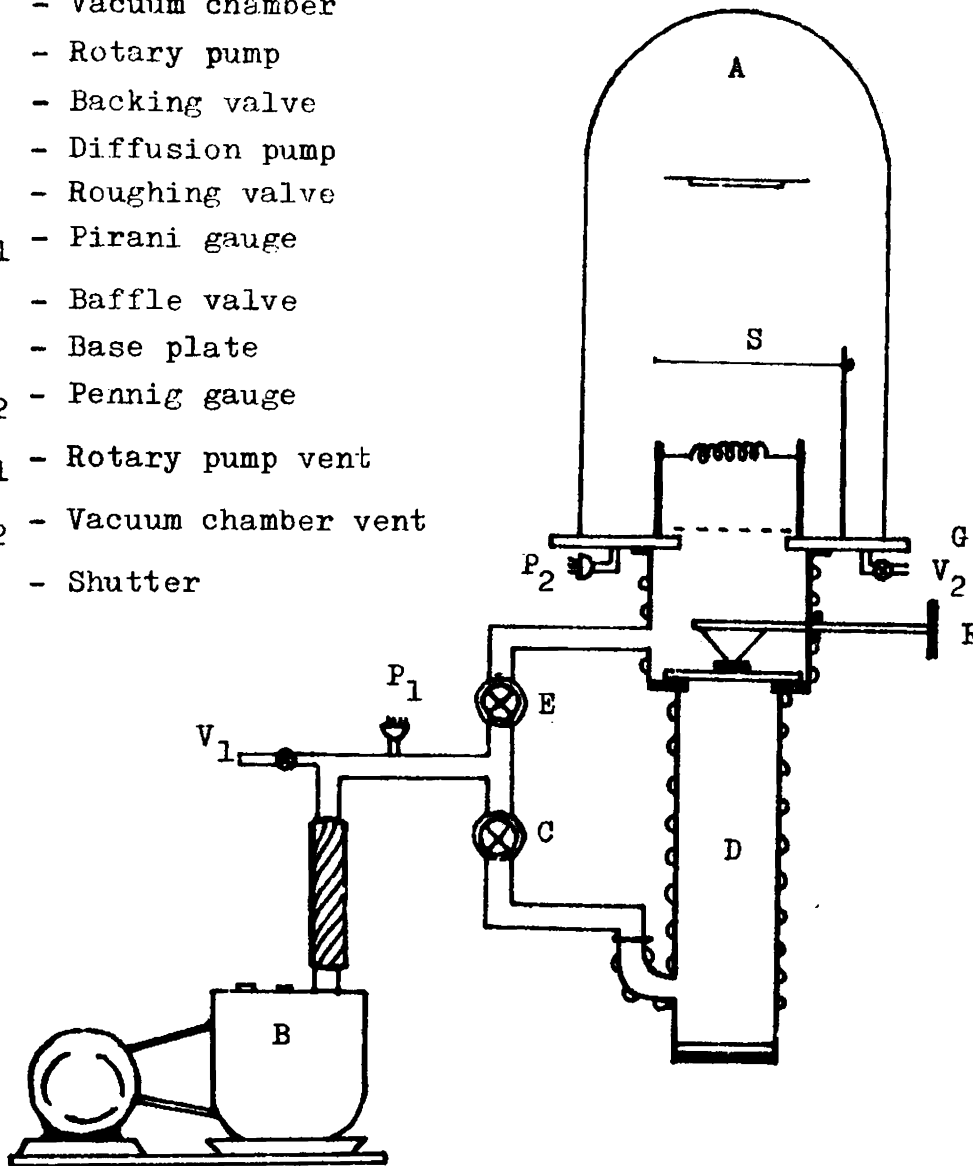


Fig.1.1 Schematic diagram of the vacuum coating unit.

A neoprene gasket encloses the lower portion of the bell jar which makes vacuum seal with the stainless steel base plate. The feed throughs on the base plate include four high current feed throughs insulated with teflon tubes for connecting filaments or boats and two high voltage feed throughs for ion bombardment cleaning. The shutter inside the chamber is fitted on the base plate through Wilson seal. The Pirani gauge (upto 10^{-3} torr) and Pennig gauge (10^{-2} - 10^{-6} torr) are used to measure the vacuum inside the work chamber and they are attached to the base plate with demountable adaptors. Provisions are also given on the base plate for fixing the ion bombardment cleaning unit and substrate holder.

All the interconnections of the vacuum line in the unit are given using one inch diameter copper tubes and all the couplings are made of demountable screw seals which keep the neoprene 'O' rings compressed.

B. Chemical Methods

1.1.4 Chemical Vapour Deposition

In the chemical vapour deposition process the vapour of a volatile compound to be deposited is thermally decomposed or reacted with other gases, vapours or liquids at the substrate forming a nonvolatile deposit [18]. The growth rate of certain semiconductor films are found to be increased by the application of a transverse field [14,19]. The reaction

is also found to be activated by catalytic action of the substrate surface, high energy radiation, heat [20,21] etc.

Metal, semiconductor and insulator films and also single crystal films of semiconducting compounds can be deposited by the CVD process. For most CVD processes working pressure of a few torrs will be sufficient [22,23]. The deposition processes such as pyrolysis [24], transfer reactions, polymerization etc. come under the CVD process.

1.1.5 Electro Deposition

(i) Electrolytic Deposition

In this method the metallic ions in the electrolyte migrate towards the cathode under the influence of an applied electric field and get deposited there. The deposition rate is proportional to the electrolysis time and current density. The deposition rate also depends on the geometry of the cathode, the temperature and agitation of the electrolyte. The structure of the deposit depends sensitively on the rate of deposition and also on the solution characteristics [25,26].

(ii) Electroless Deposition

Here the deposition occurs by a chemical reduction process without the application of an external field [27]. Metallic films of Ni, Co and Pb have been deposited by this process. Reaction temperature influences the rate of growth of film [28].

(iii) Anodization

In the anodization process the deposit is obtained on the substrate of the parent material. In an electrolytic cell the anode is made of the material to be deposited so that negative ions get deposited on the anode [29]. The rate of growth of anodic films depends on the current density and temperature of the electrolyte [30].

1.1.6 Other Methods

(i) Chemical Spray Method

Another method for deposition of certain photo-conducting and electroluminescent films of II-VI compounds is by chemical spraying of the material vapour on a suitable substrate on which the film may get deposited [31].

(ii) Langmuir-Blodgett Technique

The building-up of crystalline molecular films, having the desired number of monolayers on substrate is called Langmuir-Blodgett technique [32-34]. Films of known and controllable thickness can be formed by this method. Built-up films of barium stearate, stearic acid, chlorophyll etc. have been prepared by the Langmuir-Blodgett technique [35].

1.1.7 Substrates

Because of the availability and good insulating nature of microscope glass slides they are used as substrates

for the conductivity studies. They are of size 7.5cm x 2.5cm x 0.12cm. For infra-red studies the substrates used are sodium chloride crystals.

The cleanness of the substrate has a very profound influence on the growth and adhesion of the films. Different cleaning procedures have been described in literature [36-38]. For the present study the substrates are cleaned in the following way.

Sodium chloride crystals are well polished using ethyl alcohol. The glass substrates are cleaned chemically using dilute HCl, teepole, distilled water and isopropyl alcohol, by which majority of the contaminants are removed. The substrates are then agitated ultrasonically in distilled water for 20 minutes. Then they are rinsed in distilled water and dried in hot air. After drying the substrates are subjected to ion bombardment for about 10 minutes in a vacuum of $\sim 10^{-2}$ torr which removes the last trace of impurities.

1.2 Polymer Thin Films

1.2.1 Basic Concepts of Polymers

The name polymer is derived from the Greek *polymeros* which means many parts. Polymer molecule has a number of repeating units which are linked by covalent

bonds to form a large molecule or a macromolecule. These chemical units can be of the same kind or of different kinds. In the former case the polymer is called homopolymer and in the latter, hetro- or co-polymer. These repeat units will be equivalent or nearly equivalent to the starting material [39-42]. The repeat units are called monomeric units. These monomeric units are joined to form linear chains, branched chains or interconnected to form three dimensional networks. The degree of polymerization (D_p) of a polymer is the number of repeat units present in it. Knowing the molecular weight (M_r) of the repeat unit and the degree of polymerization the molecular weight of the polymer (M_p) can be found out as the product of D_p and M_r .

Polymerization processes are divided into condensation or step reaction polymerization and addition or chain reaction polymerization [41-45]. Condensation polymerization occurs due to the condensation or step-wise addition of monomer molecules. In addition or chain reaction the active centre may be a free radical or an ion leading to radical polymerization or ionic polymerization, respectively. The ions can be positive or negative [43-45].

Many substances do form polymers. Organic, organometallic and inorganic substances may undergo polymerization under suitable conditions. There are insulating and semiconducting polymers. Insulating ones can be made semiconducting by doping.

Several methods such as photolythic process [46,47] pyrolysis [48], subjecting to high energy radiation [46,49], gaseous discharge or plasma polymerization, [47,50-52], chemical methods [45] etc. are used for the production of polymers.

1.2.2 Preparation of Polymer Thin Films

The chemical methods used for preparing the polymer films are solution casting and pyrolytic method. The physical methods are evaporation, sputtering, photolysis, radiation induction and plasma polymerization.

(i) Solution Casting

In this method the polymer is dissolved in a volatile solvent and the substrate is kept immersed in the solution. When the volatile solvent gets evaporated, the polymer film will be formed on the substrate. In another method the solution of the polymer in a suitable volatile solvent is spread on water surface and the solvent is allowed to evaporate. Then the polymer film will be obtained on the glass substrate immersed in water. In suitable cases the solution of the polymer in a volatile solvent is spread on the surface of the substrate itself and the film will be obtained when the solvent gets evaporated [53-55]. The films formed in this method are often porous. Epitaxial films of homopolymers have been prepared by this method [56].

(ii) Pyrolytic Method

In the pyrolytic method the monomer vapour is heated in a low vacuum system and the vapour is allowed to flow over a catalyst. The monomer polymerizes and condenses on a substrate which is kept at a lower temperature [46]. Polymer films of p-xylene [48,57] produced in this way is a typical example.

(iii) Evaporation

Polymer thin films can be prepared by evaporation method in the same way as inorganic films are produced. The evaporant can be heated resistively [58] or using electron beams [59]. The vapour coming out will be fragmented material with a molecular weight less than the bulk polymer [58,60]. It has been reported that when electron beam heating is employed bombardment of the substrate with scattered electrons aids polymerization [60].

(iv) Sputtering

In the sputtering process the polymer fragments are ejected from the target polymer and these fragments undergo dissociation due to excitation by the plasma [61-64]. The local heating of the polymer target gives rise to a thermal evaporation of the material [65]. It has been noticed that the sputtered films depart more from stoichiometry [66] of the target polymer.

(v) Radiation Induced Polymerization

Here the polymerization is achieved by the high temperature electron bombardment of [49,67] the monomer surface or by exposure to high energy radiations such as γ -rays, UV rays etc. in which case it is called photolytic process [46,47,67-69]. Polymer films of DC 704 pump oil, siloxanes [70-73], butadiene [67,74], styrene [67,75] epoxy resin films [76] etc. have been produced by electron bombardment method. Polymer films of methyl methacrylate and methyl vinyl ketone [47], butadiene, styrene, acrylonitrile [67] etc. can be produced by photolytic process. In radiation induced polymerization free radicals are formed by ionization.

(vi) Plasma Polymerization

Organic, organometallic and inorganic materials can be polymerized by the plasma polymerization. Also the properties of plasma polymerized films are superior to those of conventional polymers and polymer films produced by other methods [77]. Hence researchers have given much attention to the plasma polymerized thin films. Bradley and Hammes [78] have reported the plasma polymerization of about 40 monomers. In the present study the polymer films are prepared in a plasma produced by electrodeless glow discharge.

The plasma suitable for polymerization are of four types [79]. They are silent discharges, direct current and low frequency glow discharges, high frequency discharges, and microwave discharges.

(a) Silent Discharges

The silent discharge tube is usually made of glass or quartz. It consists of a coaxial section and the inner and outer surfaces of the coaxial section are connected to a high voltage power supply ($> 1000\text{KV}$) by means of metal electrodes or conducting liquids. Organic reactants frequently form polymers in the silent discharge. It can operate at pressures upto 1 atmosphere.

(b) Microwave Discharges

For plasma experiments microwave generators with outputs between a few watts and a kilowatt can be used. The microwave power is led by coaxial cable or waveguide from magnetron or klystron to a resonant cavity enclosing the reactor. As the dimensions of the reactor are of the order of field wavelength the magnitude of the electric field can vary significantly inside the reaction tube. For this reason the organic substances are normally almost destroyed. Microwave discharges have been found to be successful with inorganic compounds [80]. The microwave experiments are usually done at pressures of several torrs since it is difficult to initiate and sustain microwave discharges at low pressures (≤ 1 torr).

(c) Direct Current Discharges

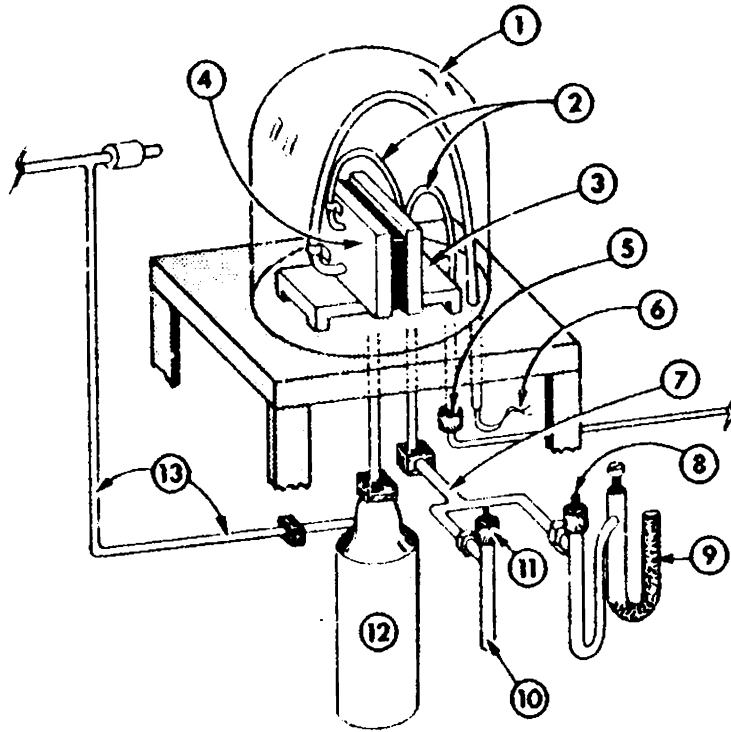
In direct current discharge two metal electrodes are placed inside a reactor and a variable high voltage is applied to produce the plasma [81,82]. To produce polymer films by DC discharge a bell jar type reactor can be used (Fig.1.2). The polymer films deposit mostly on the cathode and on the substrate placed in the close vicinity of the cathode. A smaller amount is deposited on anode also [83].

(d) High Frequency Discharges

High frequency discharge itself can be divided as AC discharge with internal electrodes and electrodeless discharge. The electrodeless discharge is further classified as inductive coupled discharge and capacitive coupled discharge. The three discharges may be treated separately.

i) AC Discharge with Internal Electrodes

AC supply operating in the frequency range 50 Hz to 2450 MHz can be utilized for AC discharge with electrodes. The polymer films get deposited on both the electrodes. Here also a bell jar type reactor can be used for depositing polymer films (Fig.1.2). It has been observed that in AC as well as in DC discharges when the gas in the bell jar is static, the gas pressure rises or falls, when the discharge is first turned on [78,81,84,85]. This increase or decrease of pressure depends upon the monomer used. For a fixed initial



- | | |
|------------------------|---------------------------|
| 1 - Bell jar | 8 - Air bleed valve |
| 2 - Cooling line | 9 - Drierite absorber |
| 3 - Sample holder | 10 - Monomer reservoir |
| 4 - Heat sink | 11 - Metering valve |
| 5 - Thermocouple | 12 - Dry-ice-acetone trap |
| 6 - Electrical leads | 13 - Vacuum line |
| 7 - Monomer feed lines | |

Fig.1.2 Typical experimental set up for deposition of polymer films in a bell-jar plasma reactor.

monomer pressure the polymerization rate increases with increasing discharge power or current density. The cooling of the internal electrodes enhances the rate of deposition. It has been reported that the build up of contaminants can be reduced if the film formation is carried out in the flow through mode rather than in the static mode [86].

ii) Electrodeless Discharge

At frequencies above 1 MHz, energy can be fed to the plasma without the aid of internal electrodes. For laboratory purposes the radio frequency oscillator is best suited because of its great versatility. The energy can be fed to the plasma indirectly either by inductive coupling or by capacitive coupling.

ii)(a) Electrodeless Discharge with Inductive Coupling

Here the discharge tube is located on the axis of a coil and the radio frequency power is fed to the discharge tube through this coil. Figure 1.3(a) shows the arrangement of the discharge tube. Monomer vapour when flowing through the discharge region will get polymerized and will deposit on the substrate placed inside the discharge tube. In some cases of the high frequency discharge polymerization and deposition take place in the tail of the glow discharge [87].

ii)(b) Electrodeless Discharge with Capacitive Coupling

In the capacitive coupling the power is fed to the discharge tube by means of a set of capacitor plates (Fig.1.3(b)). The deposition will be mainly limited to the region between the two external electrodes; but extends slightly to the outer regions also. Here the substrate is placed in the region between the electrodes [88].

Different types of reactors and experimental set up are in use. Figure (1.4) shows a schematic representation of an inductive coupled flow system. In figure (1.5) the capacitive coupled flow system is given.

In the high frequency discharge method of polymerization the monomer vapour can be fed into the plasma zone in three ways: (i) the monomer vapour may be fed directly through the discharge tube [88-96], (ii) the monomer vapour and a carrier gas may be fed through the discharge tube [97,98] and (iii) the monomer vapour may be introduced into the after glow of an inert gas [87,88]. The polymer film formation occurs mainly in the plasma region in the immediate vicinity of the external electrodes where the plasma glow is intense.

In the present investigation polymer films are deposited in a capacitive coupled electrodeless glow discharge and the details are given in chapter 5.

- 1 - Vacuum pump
- 2 - Pressure transducer
- 3 - Monomer
- 4 - Gas
- 5 - RF discharge coil
- 6 - Substrate

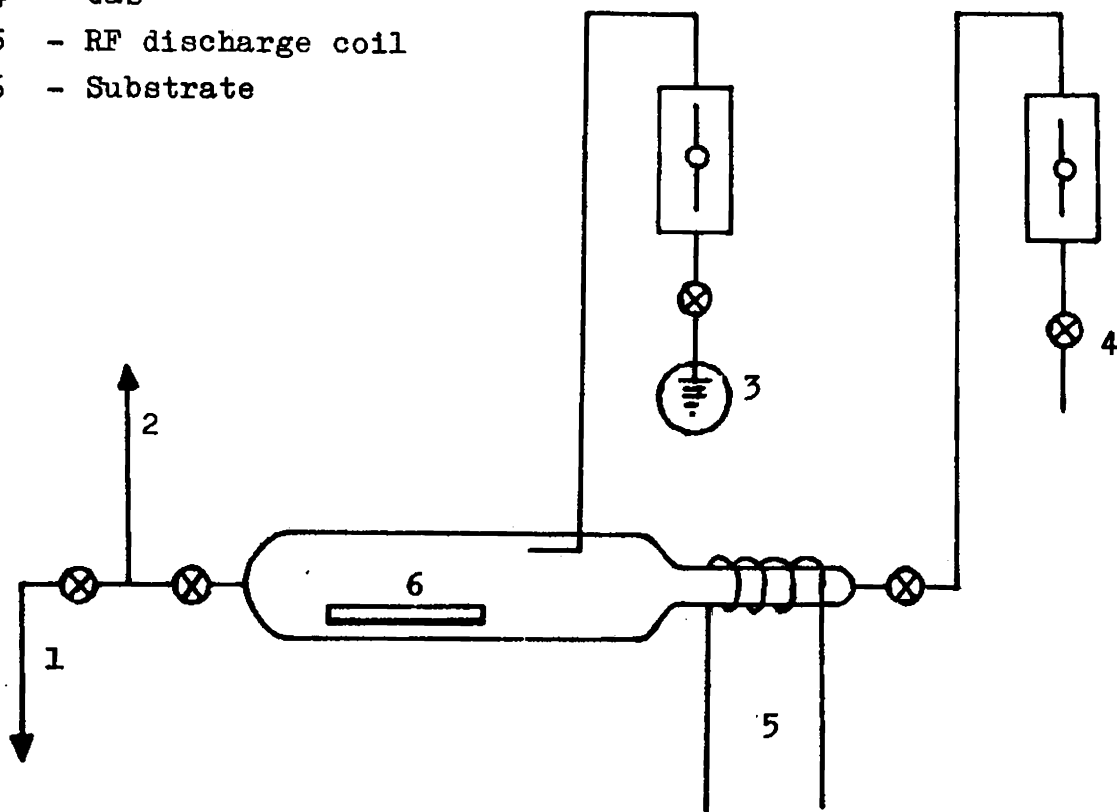
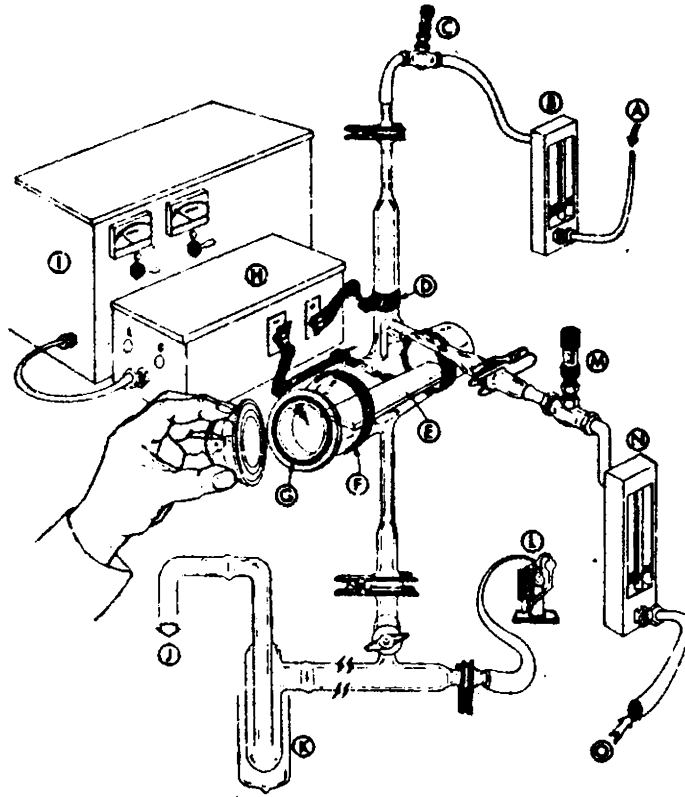


Fig.1.4 Schematic representation of a flow system used with inductive coupled electrodeless system.



- | | |
|------------------------|--------------------------|
| A - From gas cylinder | I - Generator |
| B - Rotometer | J - To pump |
| C - Flow control valve | K - Liquid nitrogen trap |
| D - High voltage | L - McLeod gauge |
| E - Substrate | M - Flow control valve |
| F - Ground | N - Rotometer |
| G - O-ring | O - From gas cylinder |
| H - Coupling unit | |

Fig.1.5 Typical experimental set up used with capacitive coupled electrodeless system for deposition of polymer films.

1.2.3 Mechanism of Plasma Polymerization

Many possible mechanisms are put forward to explain plasma polymerization. No mechanism is solely responsible for plasma polymerization and no mechanism can be completely ruled out as impossible. This is so because it is not possible to isolate these mechanisms. The possible mechanisms are briefly dealt with below.

The action of electric discharge causes the free electrons in the plasma to attain energy and these energetic electrons undergo collisions with neutral gas molecules. This transfer of energy gives rise to new chemically active species such as metastables, atoms, free radicals and ions which may initiate the formation of new materials. Reaction between electrons and molecules, ions and molecules, ions and ions and electrons and ions etc. can take place in the plasma. The energy loss due to collisions which electrons undergo is compensated by the gain of energy from the applied electric field.

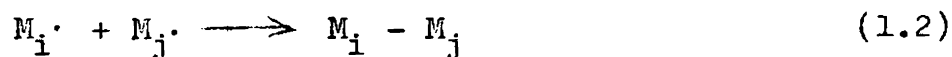
Because of these large number of elementary reactions taking place in a plasma, many species may take part in the polymerization process [99]. Yasud et al. [99-101] have recently suggested a possible mechanism for the polymerization process of organic compounds in an electrodeless glow discharge system. According to them polymerization occurs through the coupling of primary

radicals (or excited species) formed due to the ionization of monomer vapour. The polymerization process may be represented through the following steps:

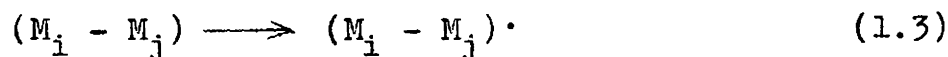
Initiation



Recombination



Reinitiation



where i and j are the numbers of repeating unit; i.e., $i = j = 1$ for monomer $i = j = 2$ for dimer etc. M_i , M_j are monomer molecules and $M_i \cdot$, $M_j \cdot$ are free radicals.

The formation of free radicals in the glow discharge results from (a) opening of double or triple bond (b) hydrogen abstraction, (c) cleavage of C-C bond and (d) opening of ring in ring compounds. The free radical formation may be related to the change in pressure observed in static conditions [99-101].

Millard [77] has suggested two approaches to explain the plasma polymerization. The first approach is that the monomer gets adsorbed on the substrate and subsequent

bombardment of the monomer by active species and radiation produced in the plasma result in polymerization on the substrate. The second one is that free radicals or ionic species are produced in the gas phase and that these may interact among themselves and with the monomer to produce active species of larger molecular weight called oligomers. The original species and oligomers diffuse onto the substrate and react further to form polymer. Ions or free radicals can be the active species taking part in the reaction and one may predominate over the other. Trapped free radicals observed in plasma polymerized films support the radical reaction in the polymerization process. Both the types, the radical polymerization and ionic polymerization are observed in the plasma polymerization of styrene [77].

A comprehensive mechanism for explaining plasma polymerization is not available. But it is certain that ions and free radicals play a decisive role in polymerization process which is supported by experiments.

1.3 Thickness Measurement of Thin Films

1.3.1 Film Thickness

The thickness of a film is a significant parameter for a specific application. For example, film thickness may affect the resistivity and transmittance. So the thickness of film must be measured to the best of its accuracy.

1.3.2 Thickness Measurement

To measure film thickness several methods have been adopted. The commonly used methods are briefly described below.

(i) Weighing

The film thickness can be found out by weighing the substrate before and after deposition of the film. If A is the area of the film, ρ_B the bulk density, m the mass of the deposited film and d the film thickness then,

$$dA\rho_B = m \quad (1.4)$$

$$\text{or } d = \frac{m}{A\rho_B} \quad (1.5)$$

The accuracy of weighing method is limited by the following factors.

1) Since the freshly deposited films sorb gases from the atmosphere the weight of the film will not be correct.

2) As the density of film differs from the bulk density the calculated thickness will not be the actual thickness of the film.

(ii) Stylus

In the stylus method the mechanical movement of a stylus as it traverses the film-substrate step is measured.

The vertical motion of the stylus relative to a reference plane is converted to an electrical signal, which is amplified and recorded on a rectilinear paper. Thus the profile graph produced represents a cross section of film step as well as substrate surface irregularities.

The limitations of this method are:

- 1) The diamond stylus may scratch a groove in soft films.
- 2) Substrate roughness may introduce noise.
- 3) Wavy substrates introduce slopes and curvatures.
- 4) A film-substrate step is required.

(iii) Multiple Beam Interferometry

This technique has been developed by Tolansky and his co-workers [102,103] for the thickness measurements of films. A beam which is reflected many times between two surfaces still has an intensity to affect the total interference. Then the intensity pattern is taken as the summation of a large number of beams, the intensity of each one of the beam will be slightly less than that of the previous one. Figure (1.6) shows schematic of multiple beam interferometry.

The two general methods of multiple beam interferometry are: (1) fringes of equal chromatic order (2) Fizeau fringes of equal thickness. Fringes of equal chromatic

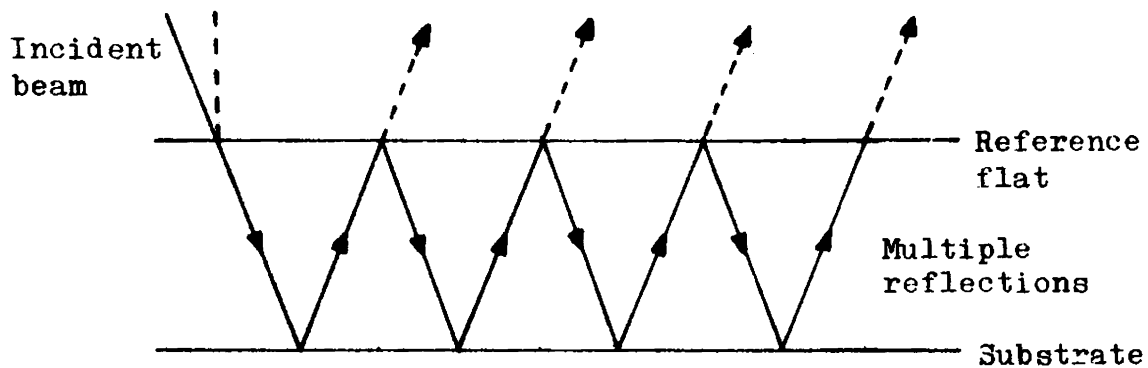


Fig.1.6 Schematic of multiple beam interferometry.

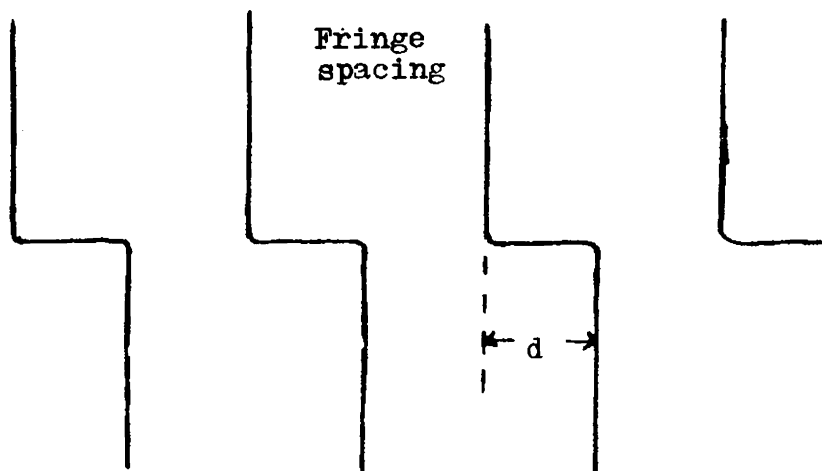


Fig.1.7 Fringe pattern produced by multiple beam interferometry across a film-substrate step.

order uses a white light source. Since this method is capable of higher resolving power it is applied for films thinner than a few hundred angstroms. Fizeau fringes of equal thickness uses a monochromatic light source. Apart from this the procedure is the same for both the methods. The second method has been used for measurement of film thickness in the present investigation and it is described here.

1.3.3 Fizeau Fringes of Equal Thickness

The fringe system was produced in the following way. Using suitable masks a sharp step was formed between the surface of the substrate and the surface of the film, while preparing the sample. Over the step a uniform opaque and high reflectivity coating was made. The reference plate was a semi-silvered glass plate. It was placed on the top of the step making a small angle with the substrate surface facing the two reflecting surfaces. This was then illuminated with collimated monochromatic light, mercury green ($\lambda = 5460 \text{ \AA}$), and the fringe system formed was viewed through a microscope. The fringe pattern and the interferometer arrangement are shown in figures (1.7) and (1.8) respectively.

The fringe spacing and fringe displacement were measured using a microscope.

The fringes are formed as a result of constructive interference of the beams. The distance between the maxima of successive fringes corresponds to $\lambda/2$ where λ is the

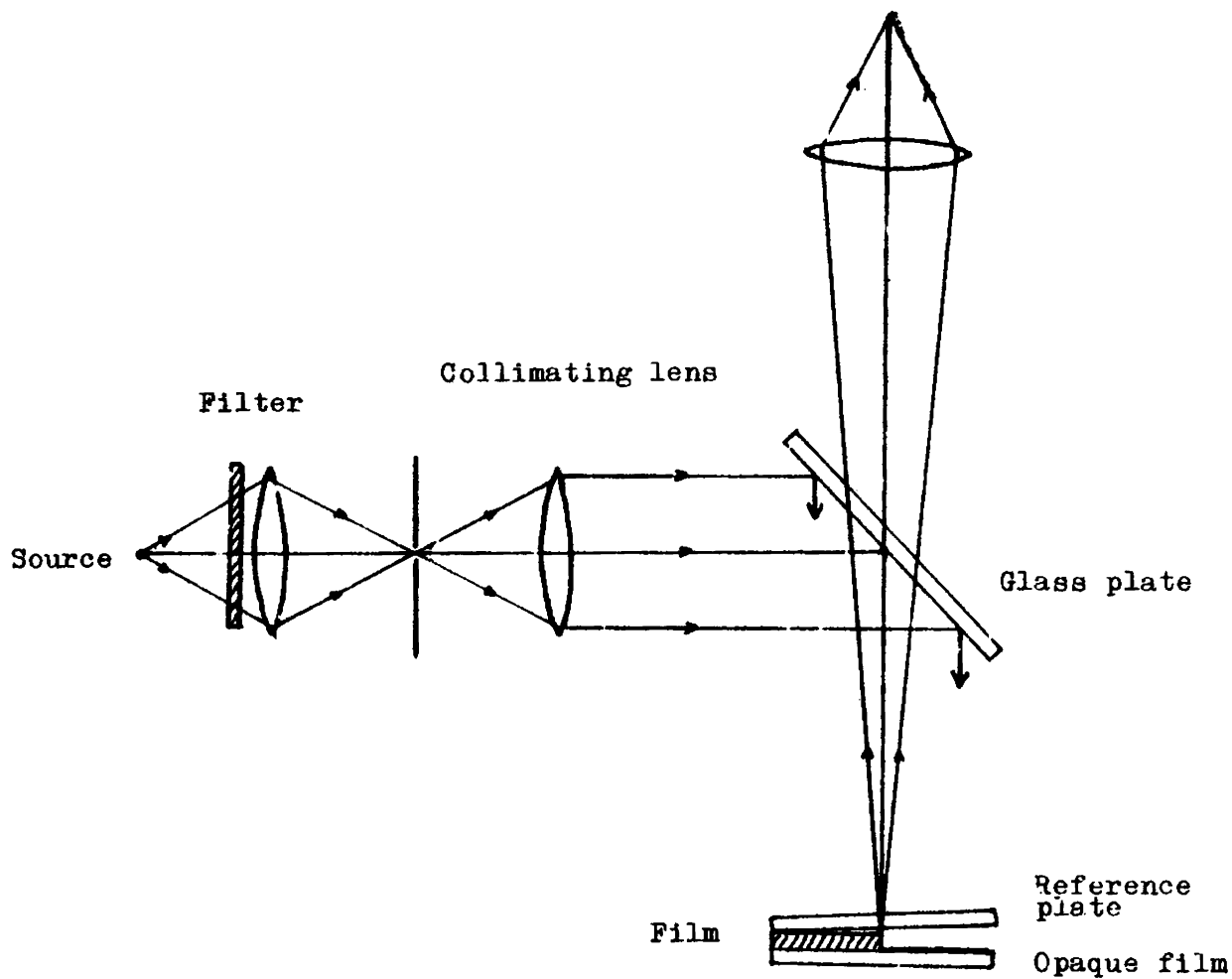


Fig.1.8 Interferometer arrangement for producing reflection Fizeau fringes of equal thickness.

wavelength of light used. The film thickness is then calculated as

$$d = \frac{\text{fringe displacement}}{\text{fringe spacing}} \frac{\lambda}{2} \quad (1.6)$$

For highly reflective surfaces fringe width is about $1/40^{\text{th}}$ of fringe separation.

1.4 Transport Properties of Insulating and Semiconducting Thin Films

The electrical properties of thin films are influenced by minute structural and chemical imperfections to a great extent. Because of these the electrical measurements are used as a sensitive tool to determine the characteristics of thin films.

The conventional conduction mechanisms applicable to inorganic insulators and semiconductors hold for polymer thin films also. The different conduction mechanisms are summarised below.

1.4.1 Ionic Conduction

Ionic conduction occurs due to the drift of ions (or vacancies) over a potential barrier from one site to another under the influence of an applied electric field [104]. The lattice defects present in films cause ionic conduction. Let E be the applied electric field, l the distance between two defect sites, e the charge on ion

(or vacancy), n the number of defects per unit volume, and $\bar{\nu}$ the probability that a defect will jump in one of the p directions then, for low applied fields ($Eel \ll kT$), the current density is given by

$$J = \frac{n\bar{\nu}Ee^2l^2}{kT} \quad (1.7)$$

where T is the temperature and k the Boltzmann's Constant. For larger fields ($Eel \approx kT$ for $E \approx 10^5$ V/cm) the defects can be assumed to have negligible chance of jumping in the backward direction and the current density is

$$J = ne l \bar{\nu}_E^+ \quad (1.8)$$

where $\bar{\nu}_E^+$ is the jump frequency in a direction in which the barrier lying in the field direction relative to a given equilibrium position is lowered by an amount $Eel/2$. If ϕ is the height of the potential barrier, the current density can be written as

$$J = J_0 \exp\left[- \left(\frac{\phi}{kT} - \frac{Eel}{2kT} \right) \right] \quad (1.9)$$

Experimentally it is difficult to distinguish between ionic and electronic conduction since in both cases the currents obtained have the same order of magnitude. It has been noted that the activation energy for ionic conduction is much larger than that for electronic conduction (normally < 1 eV). When ionic currents are dominant, there

will be polarization effects in a direct current field and the film resistivity will increase with time for a constant voltage. Also, there will be transport of material from one electrode to the other which can be observed by applying a reasonably high direct current field and looking for the mechanical or chemical change at the electrodes. The transit time for the ions will be large and it can be investigated by applying rectangular voltage pulses to the film and looking for delays in the current response.

Ionic currents in polymer thin films have been observed [105-107] and it is reported that the experimental data agrees with theoretical equation [106].

1.4.2 Electronic Conduction

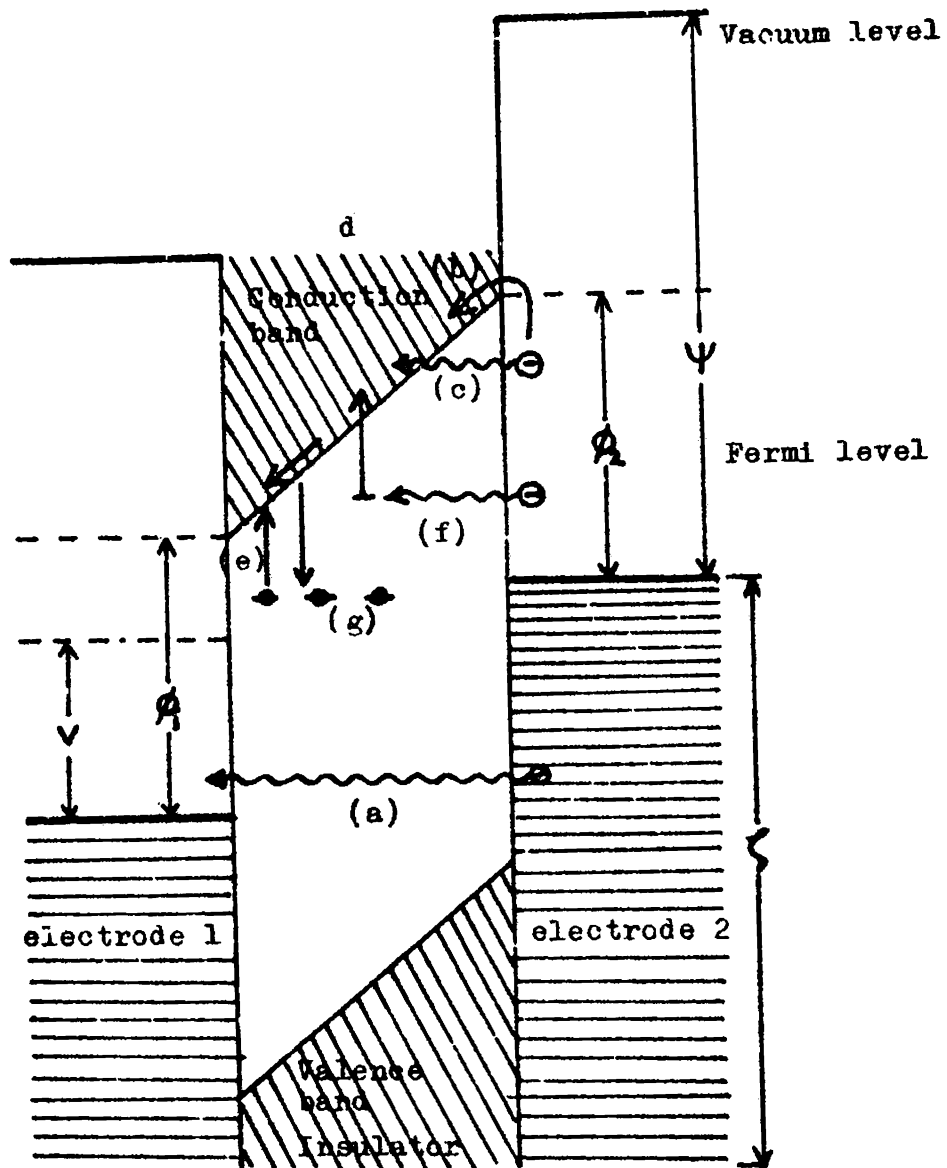
The band structure of an insulator gives a picture that the empty conduction band is separated from the fully occupied valence band by a forbidden energy gap of a few electron volts. For conduction to take place carriers may have either to be generated inside the insulator (bulk limited process) or injected from the metal electrode (injection limited process)[108]. The same is the case for semiconducting thin films also in which case the band gap is small compared to insulators [109-113].

The electronic conduction in an insulator or semiconductor film can be explained through several mechanisms in the metal-insulator-metal (MIM) structure [114]. They

are (a) Quantum mechanical tunneling of electrons from one metal electrode to the other (b) Injection of carriers into the conduction (valance) band of the insulator by thermionic or Schottky emission over the metal-insulator interface barrier (c) Tunneling of carriers through the insulator barrier gap at high applied fields (field or cold emission) (d) Scattering processes in the conduction band (e) Trapping of carriers in the large number of traps present in the film (f) Tunneling through traps (g) Hopping from trap to trap.

If at least one of the electrodes makes ohmic contact, then the current flow may be regulated by the prevailing space charge conditions. A schematic representation of the energy band diagram of MIM sandwich structure with positive voltage given to electrode 1 is shown in figure (1.9). The different conduction mechanisms are discussed below.

The electrical conduction through an insulator/semiconductor is dependent on the potential barrier at the electrode-insulator/semiconductor interface [115] and the electrons are emitted over the interface barrier which is generally termed as Schottky emission. The Richardson-Schottky formula for Schottky emission has been applied to tunnel structures by Simmons [116]. In a sandwich structure the thermionic currents in the forward and backward



- (a) Quantum mechanical tunnelling
- (b) Thermionic or Schottky emission
- (c) Field or cold emission
- (d) Scattering processes
- (e) Trapping of carriers
- (f) Tunnelling through traps
- (g) Hopping process from trap to trap

Fig.1.9 A schematic representation of the energy band diagram with positive voltage given to electrode 1.

directions are to be added. If ϕ_1 and ϕ_2 are the maximum barrier heights above the Fermi level of negatively and positively biased electrodes respectively, then the net current density is given by

$$J = AT^2(e^{-\phi_1/kT} - e^{-\phi_2/kT}) \quad (1.10)$$

Let V be the potential between the electrodes so that $\phi_2 = \phi_1 + eV$. Then,

$$J = AT^2 e^{-\phi_1/kT} (1 - e^{-eV/kT}) \quad (1.11)$$

where $A = 120 \frac{\text{A}}{\text{cm}^2 \text{K}^2}$ is the Richardson constant. If the barrier is symmetrical, then applying the image force correction [115], the Richardson-Schottky equation becomes

$$J = AT^2 \exp\left[- \frac{\phi - (14.4eV/\epsilon d)^{\frac{1}{2}}}{kT} \right] \quad (1.12)$$

where ϵ is the dielectric constant. For polymer films the value of Richardson constant is found to be lower by an order of magnitude [114]. For films with thickness greater than 40 \AA either Schottky or tunnel mechanism can predominate, depending upon the barrier height and the applied voltage.

The quantum mechanical tunnelling mechanism may be considered next. The penetration probability of an electron through a MIM structure depends on the applied voltage. The effects of temperature, image forces, dielectric constant and the effective electron mass on the

conduction band of the insulator, and the actual barrier shape have all been considered for the calculation of current flow through the metal-insulator/semiconductor-metal structure. The tunnel current is obtained by adding the current contribution from electrode 1 to electrode 2 and from electrode 2 to electrode 1. If electrode 2 is at a positive potential V with respect to electrode 1 then the net current density (at $T = 0$ K) is given by

$$J = J_0 \left\{ \bar{\phi} \exp(-B\bar{\phi}^{\frac{1}{2}}) - (\bar{\phi} + eV) \exp[-B(\bar{\phi} + eV)^{\frac{1}{2}}] \right\} \quad (1.13)$$

where

$$J_0 = e/2\pi\hbar(\beta\Delta d)^2$$

$\beta \approx 1$, a function of the barrier shape,

$\bar{\phi}$ - average barrier height,

$B = [4\pi\beta(\Delta d/\hbar)](2m_e)^{\frac{1}{2}}$ - constant, and

$\Delta d = d_1 - d_2$ - barrier width.

The expression for the current density given above is applicable to any shape of potential barrier, provided the average barrier height is known. For a rectangular barrier of height ϕ_0 with similar electrodes, at high fields and low temperatures the tunnel integral (eq. 1.13) yields the Fowler-Nordheim [117] equation.

$$J \propto F^2 \exp(-0.689 \phi_0^{3/2}/F) \quad (1.14)$$

where $F = V/d$. At low fields and high temperatures this equation becomes the Richardson-Schottky equation.

The space charges, image forces and traps present in the insulator/semiconductor have effects on the potential barrier. The presence of space charge will increase the potential barrier due to the film to a maximum at the mid-plane of the film. The image force, in particular for very thin films, will reduce the barrier height. The effect of traps is to delay the electrons crossing the barrier because of the trap life time. Also they limit the number of electrons that can pass through the barrier at a time.

Extensive measurements carried out on very thin films show that for films less than 100 \AA thick direct tunneling from one metal to the other metal takes place. This conclusion is based principally on the weak temperature dependence of the tunnel current. When the tunnelling is from the metal to the conduction band of the insulator the effect of trapping would give rise to a strongly temperature dependent current.

In practice the $\log I(\text{current})$ is plotted against $1/V$ which gives a straight line called the Fowler-Nordheim plot.

The thermal excitation of electrons from traps into the conduction band is the Poole-Frenkel effect [118-121]. Under the application of an electric field the potential

barrier of the trap is lowered which means that the probability of an electron being thermally excited out of the trap into the conduction band is increased. This conduction process is termed as internal field emission in the direction of the field [122]. The potential barrier reduction of trap under the application of an electric field is shown in figure (1.10). The conductivity equation is given by an expression of the form

$$\sigma = A \exp\left[-\phi + \frac{\phi_m}{2kT}\right] \quad (1.15)$$

where A is a constant. ϕ_m is the maximum value of potential barrier height when the field is applied and has a value:

$$\phi_m = -2(e^3 F / \epsilon)^{\frac{1}{2}}$$

In practice $\log I$ is plotted against $V^{\frac{1}{2}}$ which gives a straight line.

Space Charge Limited Conduction (SCLC)

When the applied field is large enough and when the electrode metal makes an ohmic contact to the insulator/semiconductor, injection of carriers into the insulator/semiconductor takes place [123,124]. When the injected carrier density is greater than the density of thermally free carriers, a cloud of charge carriers will be formed in the vicinity of the contacts. This space charge build up of injected carriers is due to the imbalance of both the

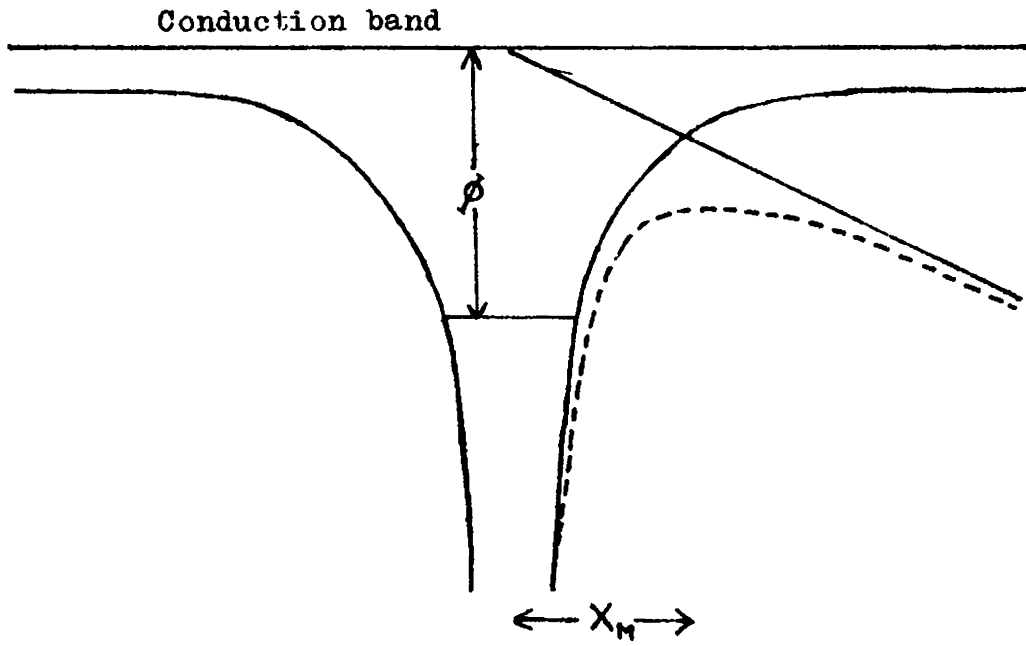


Fig.1.10 The lowering of the potential barrier (dashed line) for thermal excitation of trapped electrons into the conduction band.

types of carriers and it opposes the applied voltage and electron flow. To occur SCLC at least one electrode must make ohmic contact to the insulator/semiconductor [125,126]. In addition the insulator/semiconductor must be free from traps.

If the interface dipole energy barrier at a metal-insulator or metal-semiconductor contact is substantially smaller than the corresponding work function of metal-vacuum contact [127], space charge limited flow of electrons can occur even at room temperature. These electrons have to undergo collisions with phonons and impurities in the insulator/semiconductor. A more important effect comes from the localized traps present in the insulator/semiconductor which may capture the injected electrons, particularly at low temperatures at which they are stable [125,126]. The hole injection into the valence band of the insulator/semiconductor is equally well important because of the duality between electrons and holes. Figure (1.11) shows electron injecting metal insulator contact with localized trap levels.

In the case of a MIM system both electrodes can inject space charges into the insulator. If both the electrodes inject the same type of charge carriers, then it is a one carrier SCL conduction and if both holes and electrons are injected by the electrodes it is known as two carrier SCL conduction [128]. In the present investigation

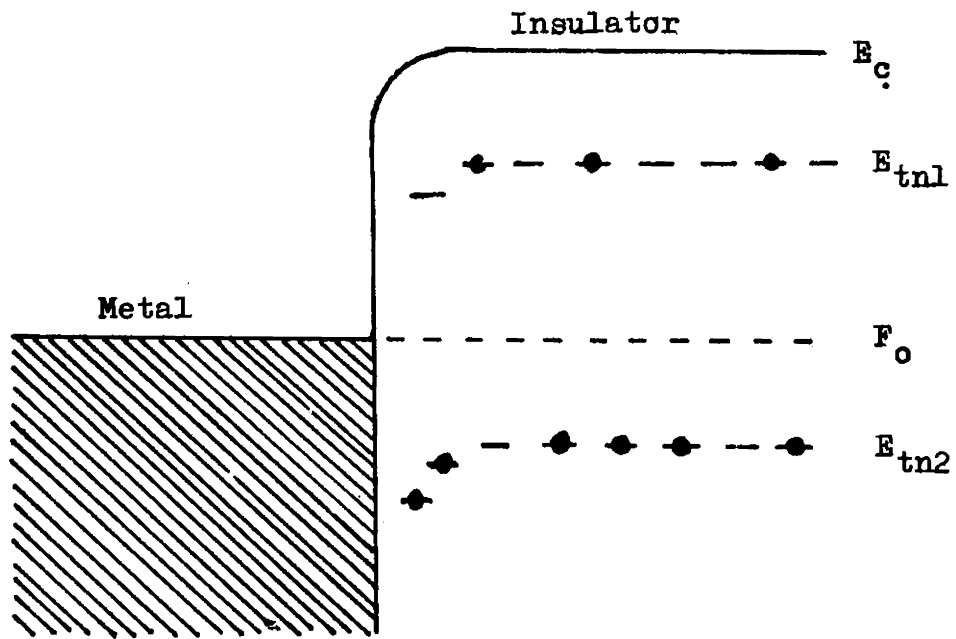


Fig.1.11 Schematic energy band diagram for electron injecting metal-insulator contact including traps (Solid circle indicates trap occupancy by an electron).

similar electrodes have been used for conductivity studies. Hence the one carrier SCLC is discussed here.

(i) Perfect Insulator

The perfect insulator can be considered as trap free with a negligible density of free carriers in thermal equilibrium, analogous to the thermionic vacuum diode. All the injected electrons remain free in the conduction band and will contribute to space charge. The current density in such a situation is given by

$$J \simeq \epsilon\mu \frac{V^2}{d^3} \quad (1.16)$$

where μ is the electron mobility.

If thermally free carriers are present in the insulator/semiconductor with concentration n_0 , at low fields the current-voltage behaviour obeys Ohm's law:

$$J = en_0\mu(V/d) \quad (1.17)$$

As the field is increased the injected free electron concentration n_i becomes comparable to that of thermally generated carrier concentration and a cross over from Ohm's law to trap free square law takes place [129], which is the onset of space charge limited current injection. This cross over voltage V_x is

$$V_x \simeq en_0 d^2 / \epsilon$$

Beyond this cross over voltage the injected electrons dominate over thermally free electrons.

(ii) Insulator with Traps

The traps will capture and immobilize the electrons which have been injected into the insulator. In this case the thermodynamic Fermi level E_{F_0} is important in determining the thermal equilibrium concentration n_0 of the electrons given by

$$n_0 = N_c \exp[(E_{F_0} - E_c)/kT] \quad (1.19)$$

where N_c is the effective density of states in the conduction band and E_c is the bottom energy level of the conduction band.

In the case of steady state injection, E_{F_0} will change to a quasi Fermi level E_F , where the concentration of filled electron traps is

$$n_{t,0} = \frac{N_t}{1 + (1/g)(N/n_0)} \quad (1.20)$$

where g is the degeneracy factor, $g \simeq 2$, N_t is the trap density and $N = N_c \exp[(E_t - E_c)/kT]$.

If the traps are shallow meaning that they lie above the Fermi level i.e., $(E_t - E_F)/kT > 1$ then a constant η defined as the ratio of free electrons in the conduction band to the total number of electrons, which is independent of injection,

is given by

$$\Theta = \frac{n}{n_t} = \frac{N}{gN_t} = \frac{N_c}{gN_t} \exp\left(\frac{E_t - E_c}{kT}\right) \quad (1.21)$$

If $\Theta \ll 1$, then the shallow trap density will affect the SCL injection current. The net current density in the system is given by

$$J \simeq \Theta \epsilon \mu V^2 / d^3 \quad (1.22)$$

The cross over voltage V_x from Ohm's law to shallow trap square law is

$$V_x \simeq \frac{e n_0 d^2}{\Theta \epsilon} \quad (1.23)$$

If the traps lie below the Fermi level they are characterized as deep traps. During electron injection the quasi Fermi level will move up and trap occupancies are like wise increased by the upward motion. In this case the cross over voltage V_x coincides with the trap filled limit voltage V_{TFL} given by

$$V_{TFL} = \frac{e(N_t - n_{t,0})d^2}{\epsilon}$$

This trap filled limit voltage V_{TFL} measures that fraction of the total concentration of traps which are empty in thermal equilibrium.

The current-voltage characteristics of a system with single set of trap density on a log-log scale give a

family of curves containing a triangle called Lampert's triangle (Fig.1.12). The triangle is bounded by Ohm's law, trap free square law and trap filled limit law (TFL) regions.

The space charge limited conduction observed in the present investigation is presented in chapter 7.

1.5 Transport Phenomena in Polymeric Materials

According to the division of organic substances into semiconductors and insulators with regard to their characteristic conductivity substances with conductivity in the range $10^2 - 10^{-12} \text{ ohm}^{-1} \text{ cm}^{-1}$ are treated as semiconductors and insulating substances have conductivity in the range $10^{-12} - 10^{-14} \text{ ohm}^{-1} \text{ cm}^{-1}$ to $10^{-16} - 10^{-19} \text{ ohm}^{-1} \text{ cm}^{-1}$ at 20°C [130]. The conduction mechanism in polymeric materials is explained by hopping conduction, tunnelling and band mechanism [130,131].

In the hopping model, conduction occurs by the activated jumps of carriers from regions of polyconjugation to other polyconjugation regions overcoming the region of nonconjugation [132-134]. In substances with low carrier mobility [$0.005 - 0.01 \text{ cm}^2/(\text{V. Sec.})$] where Hall effect is not measurable, hopping is the most predominant mechanism of conduction, though the concentration of carriers may be as high as $10^{12} - 10^{18} \text{ cm}^{-3}$ [133].

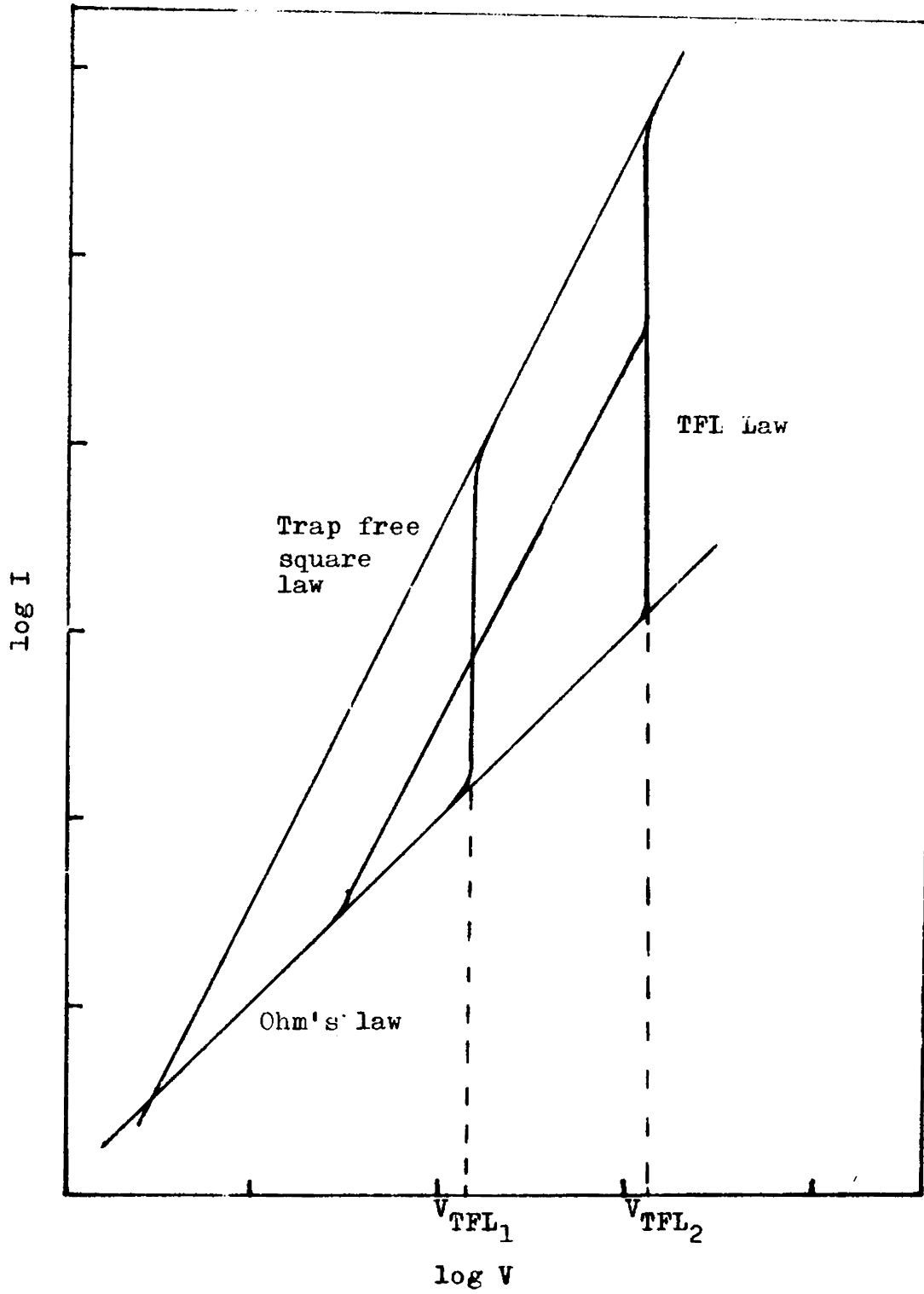


Fig.1.12 Lampert's triangle.

In the tunnel mechanism, for polymers with free radicals or for polyconjugated polymers the activation energy of conductance must be low. It must tend to zero with the increase in conjugation in the macromolecule, but in actual case it does not attain the value zero, the reason being the presence of intercrystallite defects [135].

The band model consists of a great many closely lying-energy levels in the crystals, with many levels formed due to the perturbation of atomic or molecular levels [131]. The energy levels of a molecular solid is given in figure (1.13). The energy levels are rather narrow because of smallness of intermolecular interactions across the long Van der Waal spacings. In the band mechanism of conduction transitory ions, especially deep lying anions, polarons which are delocalized electrons or holes lying in the conduction band, electrons or holes which are free in the conduction band of high level crystal states, excitons which are tightly associated bipolar entities, excimers which are intermolecularly coupled excited states etc. play active roles. The deep lying transitory anions conduct by a tunnelling or hopping process.

The electronic conduction of some polymeric solids is found to be enhanced due to strong and concerted mixing of intermolecular orbitals of molecules which have

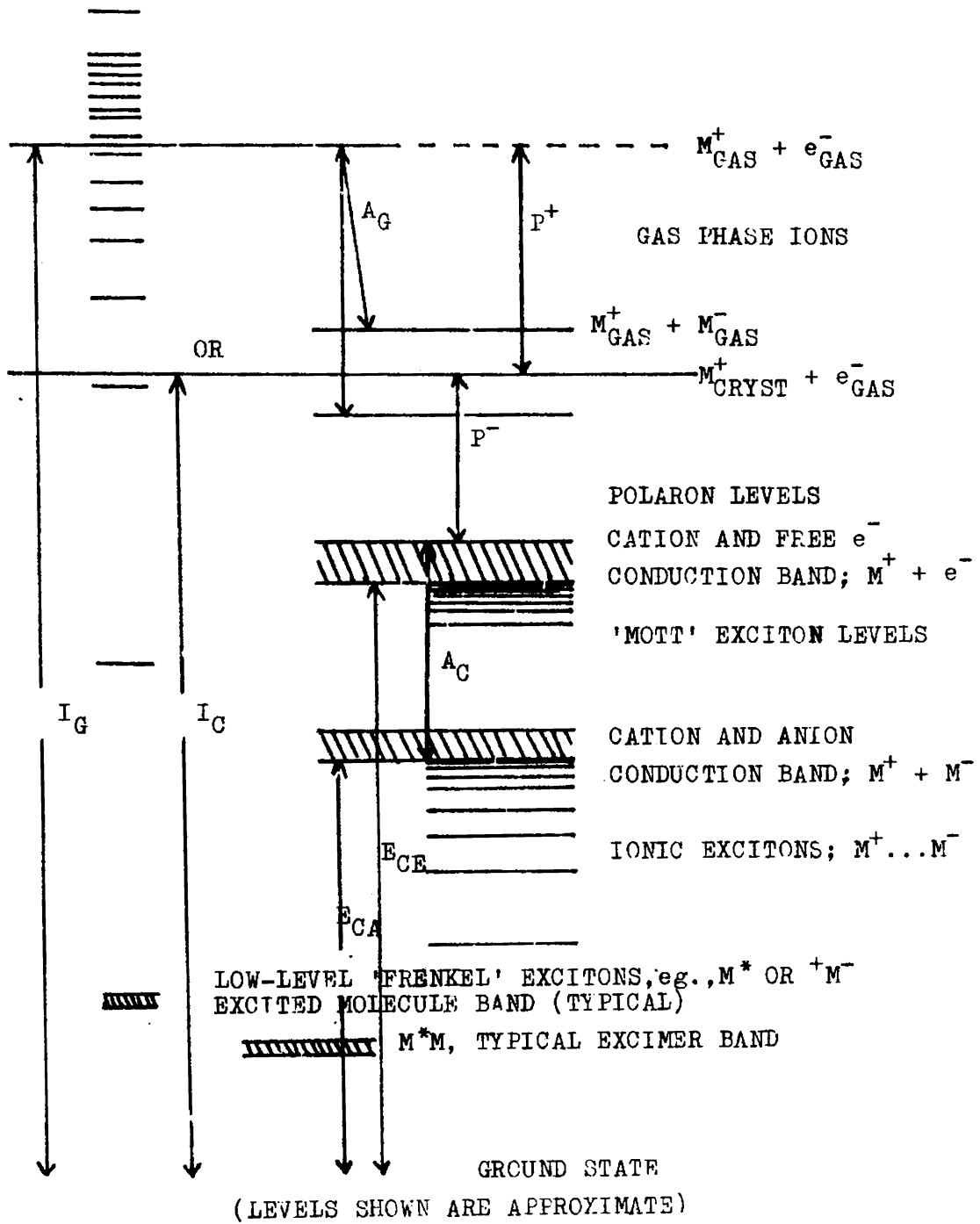


Fig.1.13 Energy levels in a molecular solid.

strongly delocalized electronic orbitals. The orbital overlap is activated by (a) coulombic effects which involve donor-accepter mechanism and (b) exchange effects which involve the intermixing of separate molecular states with the effect of which the energy bands get broadened. The donor-accepter mechanism increases conductivity. This can be proved by comparing the conduction of macromolecular solids before and after doping with suitable donors or accepters. Examples are poly (vinylanthracene) doped with iodine [136,137], polytetrafluoroethylene doped with sodium [130]. Evidences are also available for the exchange effects in polymeric solids. By the application of pressure the overlapping of the molecular orbitals can be increased and this may result in the increased mobility of the carriers in the solid [132] and thus increases the conductivity to a very great extent [138,139]. The high conductivity in potassium graphite, where the potassium atoms being sandwiched between graphite atoms is a typical example of exchange effect.

Considering the intramolecular aspects of polymeric solids, it is noted that all semiconducting solids have in their structure conjugated single and multiple bonds. Conjugated is meant for the alternation in a series of single and double and rarely triple bonds.

Two types of conjugation are introduced and they are ekaconjugation and rubiconjugation [130,138]. In a long polyene chain limited or broken sequences of electronic delocalization are caused by the attached side groups. In the simple case of an unsubstituted polyene with an even number of carbon atoms, quantum mechanical effects induce broken sequences of electronic delocalization and such a situation is called rubiconjugation. Polyphenylenes, polybenzimidazoles are rubiconjugated polymers. In ekaconjugated materials the molecular defects leading to the interruption of electron delocalization along the polyene chain are either absent or suppressed and extensive quantum mechanical linkage of the π orbitals of the entire chain or large regions of it can occur [130,138]. Examples for ekaconjugated polymers are polythalocyanines, graphite etc. Theoretical as well as experimental evidences support the existence of the two types of conjugation [131]. It can be stated in general terms that rubiconjugated polymers exhibit very low electrical conductivity ($\sim 10^{-12}$ ohm $^{-1}$ cm $^{-1}$ or less), low unpaired spin concentration (less than 10^{18} spins/gm) and have normal chemical reactivity. The ekaconjugated polymers have high electrical conductivity ($\sim 10^{-9}$ ohm $^{-1}$ cm $^{-1}$ or above) high concentration of unpaired electron spins (10^{18} - 10^{21} spins/gm) and are chemically rather inert.

CHAPTER TWO

PREPARATION AND CHARACTERIZATION OF SILVER SULPHIDE AND FERRIC HYDROXIDE THIN FILMS

2.1 Introduction

Compound semiconductor thin films are of great importance in the semiconductor device technology. Even though thin films of compound semiconductors can be prepared by different methods such as thermal evaporation of the compound [12,16] sputtering of the material [140] by various means etc., the films obtained by these methods show deviation in their stoichiometry. To prepare stoichiometric compound thin films three temperature method [141,142] and flash evaporation [143,144] are commonly used. However these preparation methods under high vacuum require much sophisticated equipments. It has been observed that semiconductor films of certain compounds such as sulphides and oxides can be prepared by initiating a chemical reaction at a liquid-vapour interface [145] in the chemical deposition technique [4]. Also this technique has been found suitable to produce large area films of uniform composition [31].

The chemical deposition technique extends its feasibility in controlling the thickness of the film by limiting the time of reaction at the interface, since the

building up of the layers from the monolayer formation is time dependent [35]. However care has to be taken to avoid fogging and cracking of the films during deposition as suggested by Blodgett and Langmuir [34]. Compound semiconductor films of cadmium sulphide [4] and zinc oxide [146] have been prepared by the interfacial chemical reaction of a liquid and a gas. Uniform films of fairly large area can be prepared by this method and it has the advantage of controlling the film thickness to a certain extent by limiting the reaction time with less elaborate procedure.

2.2 Preparation of Silver Sulphide Films

Silver sulphide is a I-VI group semiconductor of brownish black colour with a melting point 1098K [147]. Bulk silver sulphide has got two phases, an alpha-phase above 450K and a beta phase below 450K [148]. Benneaze et al. [149] have studied the electronic properties of α - Ag_2S controlling its stoichiometry and reported that the properties are highly dependent on the stoichiometry as suggested by Junod et al. [150]. Transport studies on silver sulphide at very high temperature have shown that this material has got a phase transformation near 900K and the conduction mechanism is n-type in both phases [151].

Studies on thin silver sulphide films have been carried out by various authors to investigate the optical

absorption of epitaxial films [152] and polycrystalline films [153]. However these films have been prepared by the vacuum evaporation of the compound. Cehan et al.[154] have chemically deposited silver sulphide films and studied their conductivity at various frequencies. Dielectric breakdown studies of silver sulphide films sandwiched between gold and silver electrodes have been reported by Sharma and Thomas [155].

The thermal evaporation of silver sulphide from a single source may result in a non-stoichiometric film whereas a chemical reaction at a liquid-gas interface in a very clean and controlled environment is capable of producing thin films of uniform thickness and structural and compositional homogeneity. The present method adopts a chemical reaction to be initiated at an interface of silver nitrate solution and hydrogen sulphide gas in a controlled environment.

2.2.1 Experimental Arrangement

Silver sulphide films have been prepared by the interfacial chemical reaction of silver nitrate solution and hydrogen sulphide gas. The BDH analytical reagent grade silver nitrate was used in the analysis. One percent solution of silver nitrate was prepared in doubly distilled water. This solution was filtered and used in the preparation of the films. Microscopic glass slides were used

as the substrates. These glass substrates were initially cleaned with dilute HCl, a detergent teepole, distilled water, acetone and again distilled water to remove the greasy particles on the surface. Finally they were subjected to ultrasonic agitation in an ultrasonic cleaner.

Hydrogen sulphide solution was prepared by passing pure H_2S through distilled water taken in a dish to get a solution of reasonable concentration. The dish with H_2S solution was used to evolve H_2S gas for the chemical reaction. The cleaned substrate was kept in the dish containing pure silver nitrate solution. A lift arrangement using glass rod was used to lift the substrate without disturbing the solution. The silver nitrate solution was allowed to make contact with hydrogen sulphide gas for the chemical reaction to take place in an enclosure. The experimental set up is shown in figure (2.1).

2.2.2 Film Formation

The enclosure used was made of glass so that one could observe the film formation from outside. A brownish dark layer would be formed on the surface of the silver nitrate solution after one or two minutes. The film formed was of uniform type. The enclosure was removed and the substrate was lifted carefully without breaking the film. Then the substrate was dipped in distilled water to have the

- 1 - Silver nitrate solution
- 2 - Substrate
- 3 - Lifter
- 4 - Hydrogen sulphide solution
- 5 - Enclosure

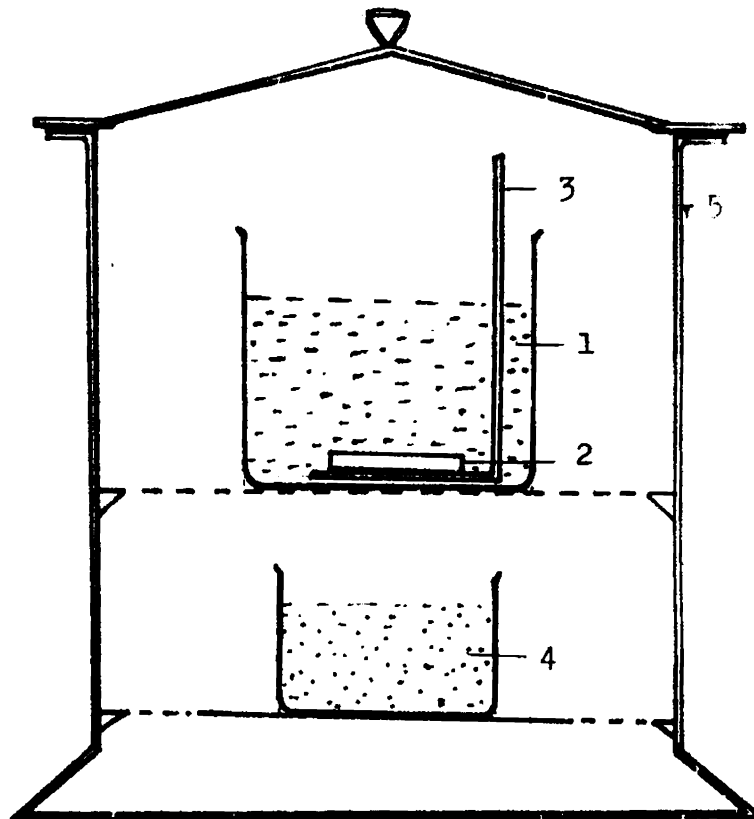


Fig.2.1 Experimental set up used for the chemical deposition of thin films.

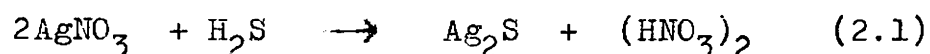
soluble impurities washed off. It was taken out and allowed to dry. The time of exposure of the silver nitrate solution to the hydrogen sulphide gas was found to be a parameter determining the thickness of the film formed. Films of different thicknesses have been prepared by varying the exposure time.

The concentration of the silver nitrate solution used need not be exactly 1%. But in very low concentrations of silver nitrate solution film growth has been found to be poor. Hydrogen sulphide concentration must also be reasonably high for good results. If the concentration of any of the reagents is low, exposure time must be increased. By varying the exposure time films with thicknesses in the range 400 Å to 2500 Å have been prepared for the present investigation.

2.3 Characterization of Silver Sulphide Films

2.3.1 Chemical Reaction

Silver nitrate and hydrogen sulphide react to form silver sulphide.



Nitric acid which is the other product of the reaction will get dissolved in water.

2.3.2 Nature of Film

Silver sulphide film has been found to be brownish black in colour. No effect on the colour and appearance of the film has been observed due to heat treatment. Silver sulphide is the most insoluble salt of silver.

The type of conductivity of the prepared silver sulphide has been determined by the hot probe method [156]. A thick film has been chosen for the purpose. A microvoltmeter is set to the most sensitive range and one of the multimeter probe has been heated for a few seconds. Then both probes of the microvoltmeter have been made to touch the film. The hot probe voltage has been found to be positive with respect to the cold probe indicating electron flow in the film. Hence it has been concluded that silver sulphide is n-type in nature.

2.4 Preparation of Ferric Hydroxide Films

Not much work has been done on the electrical and other related properties of oxides and hydroxides of iron. However Muckerjee [157] has carried out electric conductivity studies on ferric oxide in the temperature range 200K to 1000K and Bosman [158] has reported that thermally activated hopping is the conduction mechanism in $\alpha\text{-Fe}_2\text{O}_3$. It has been reported in the literature that there exists a non-linear relationship between the logarithm of conductivity and

reciprocal of temperature in the case of pure alpha ferric oxide [159]. In the thin film form no work on the electrical properties of ferric hydroxide has been found to be reported. Hence in the present investigation an attempt has been made to prepare and characterize ferric hydroxide films using a chemical deposition technique.

2.4.1 Experimental Set Up

The experimental set up used for the preparation of ferric hydroxide film was similar to the one employed for silver sulphide films (Fig.2.1). In this case ferrous sulphate solution and ammonia gas were used as the reagents. Both were of BDH analytical reagent grade. The ferrous sulphate solution was prepared by dissolving ferrous sulphate in doubly distilled water and filtering and making it a 1% solution. The ammonia gas atmosphere was formed inside the container by placing a dish containing approximately 100 ml water into which 5 or 6 drops of ammonia solution were added.

2.4.2 Film Formation

Due to the chemical reaction between the ferrous sulphate solution and the ammonia gas a film of ferrous hydroxide was formed on the surface of the ferrous sulphate solution. It was taken out carefully without breaking. The film was dipped in distilled water to get the soluble impurities washed off and then it was allowed to dry.

The thickness of the film was found to increase as the exposure time of the ferrous sulphate solution to ammonia atmosphere was increased. But on longer exposure a precipitate formation in the ferrous sulphate solution was observed. So the film thickness could not be increased beyond a limit. It was noted that for thick films there seemed to have a tendency to peel off from the substrate. So exposure time was limited. In the present study films of thickness in the range 180 Å to 1200 Å have been employed. In addition the concentration of ammonia should not be high in which case the OH^- ion concentration cannot rise above a very low value [160]; hence film could not be formed.

Ferric hydroxide film was formed on exposing ferrous hydroxide film to air. The change was taking place in the enclosure itself because of the presence of air in it and when it was taken out the change could take place speedily.

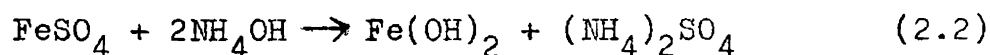
2.4.3 Ferric Oxide Film

It has been observed that ferric oxide is formed when ferric hydroxide is heated in air at 723K. In the present study ferric hydroxide film has been heated at 723K for one hour. These ferric oxide films have also been used for the conductivity studies.

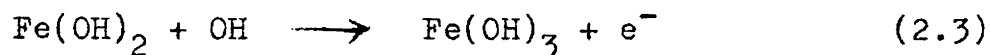
2.5 Characterization of Ferric Hydroxide Films

2.5.1 Chemical Reaction

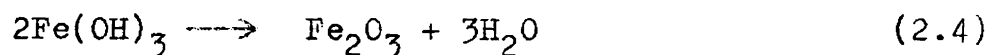
Ferrous sulphate and ammonium hydroxide will react to form ferrous hydroxide through the following chemical reaction:



The ferrous hydroxide oxidizes to ferric hydroxide on exposure to air. This oxidation process gives rise to the change of colour of ferrous hydroxide from light green to deep brown of ferric hydroxide. Shively and Weyl [161] have reported that in this oxidation process intermediate colours are observed before reaching the final deep brown colour. The formation of ferric hydroxide is given as:



On heating the ferric hydroxide film at 723K in air it decomposes as below:



The final product ferric oxide is reddish brown in colour.

2.5.2 X-Ray Investigation

The ferric hydroxide film on the glass substrate has been peeled off and used for X-ray diffraction study. The X-ray powder photograph of the film has been taken and

(CuK α , $\lambda = 1.3838 \text{ \AA}$) is shown in figure (2.2). It has been found that only a diffuse halo characteristic of amorphous structure is formed in the photograph. Hence it has been concluded that the film is amorphous in nature.

2.5.3 Estimation of Fe³⁺

Colourimetric estimation of Fe³⁺ in Fe₂O₃ has been carried out using a spectrophotometer. The colourimetric estimation has been done using thiocyanate method and the details are given below.

Standard solution of Fe³⁺ was prepared by dissolving 0.864 gm of ferricammonium sulphate in water and adding 10 ml of concentrated HCl and diluting to 1 litre in a standard flask. Twenty percent potassium thiocyanate solution and 4N nitric acid were prepared for the estimation.

Estimation

A known amount of Fe₂O₃ was dissolved in 500 ml of water containing 5 ml concentrated HCl.

From this 2 ml of the solution was taken in 50 ml standard flask. Five ml of potassium thiocyanate solution and 2 ml of 4N nitric acid were added to it. Red coloured solution was obtained. The transmission of the solution was read in the colourimeter.

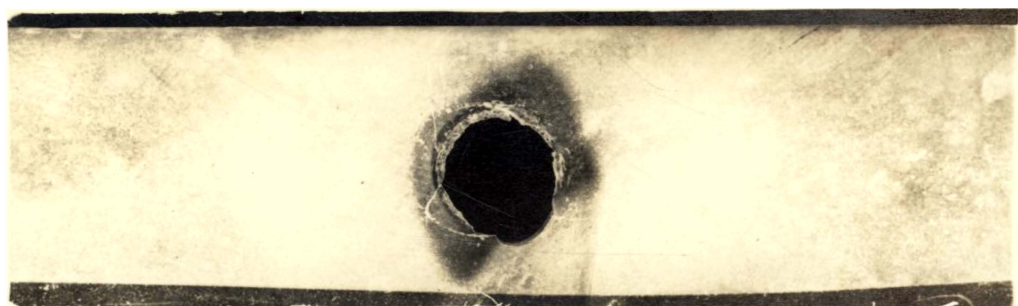


Fig. 2.3 X-Ray photograph of $\text{Fe}(\text{OH})_3$ film.

From the standard solution 0.1, 0.2, 0.3....0.5 ml were taken in different 50 ml standard flasks and potassium thiocyanate and nitric acid were added as in the above case. The transmission in each case was noted. The readings are tabulated below.

Vol.of standard solution in ml (V)	Percentage transmission (T)	Absorbance (A = -log T)
0.1	94	1.97
0.2	86	1.93
0.3	78	1.89
0.4	70.5	1.85
0.5	65.5	1.82
Vol.of unknown solution		
2 ml	86.5	1.93

A graph was plotted between absorbance and volume of the Fe^{3+} solution (Fig.2.3). The volume of unknown solution equivalent to that of standard solution was found out from the graph. The percentage of Fe^{3+} was then calculated and is given below:

1 ml of standard solution contains $\frac{111.7 \times 0.864}{964.43 \times 1000}$ gm of Fe^{3+}

2 ml of unknown solution ~~is~~ 0.2 ml of standard solution

Fe^{3+} in 500 ml of unknown solution = $\frac{111.7 \times 0.864 \times 0.2 \times 500}{964.43 \times 1000 \times 2} = 5 \text{ mg}$

Amount of Fe_2O_3 taken = 8.6 mg

Percentage Fe^{3+} = $\frac{5 \times 100}{8.6} = 58.2\%$

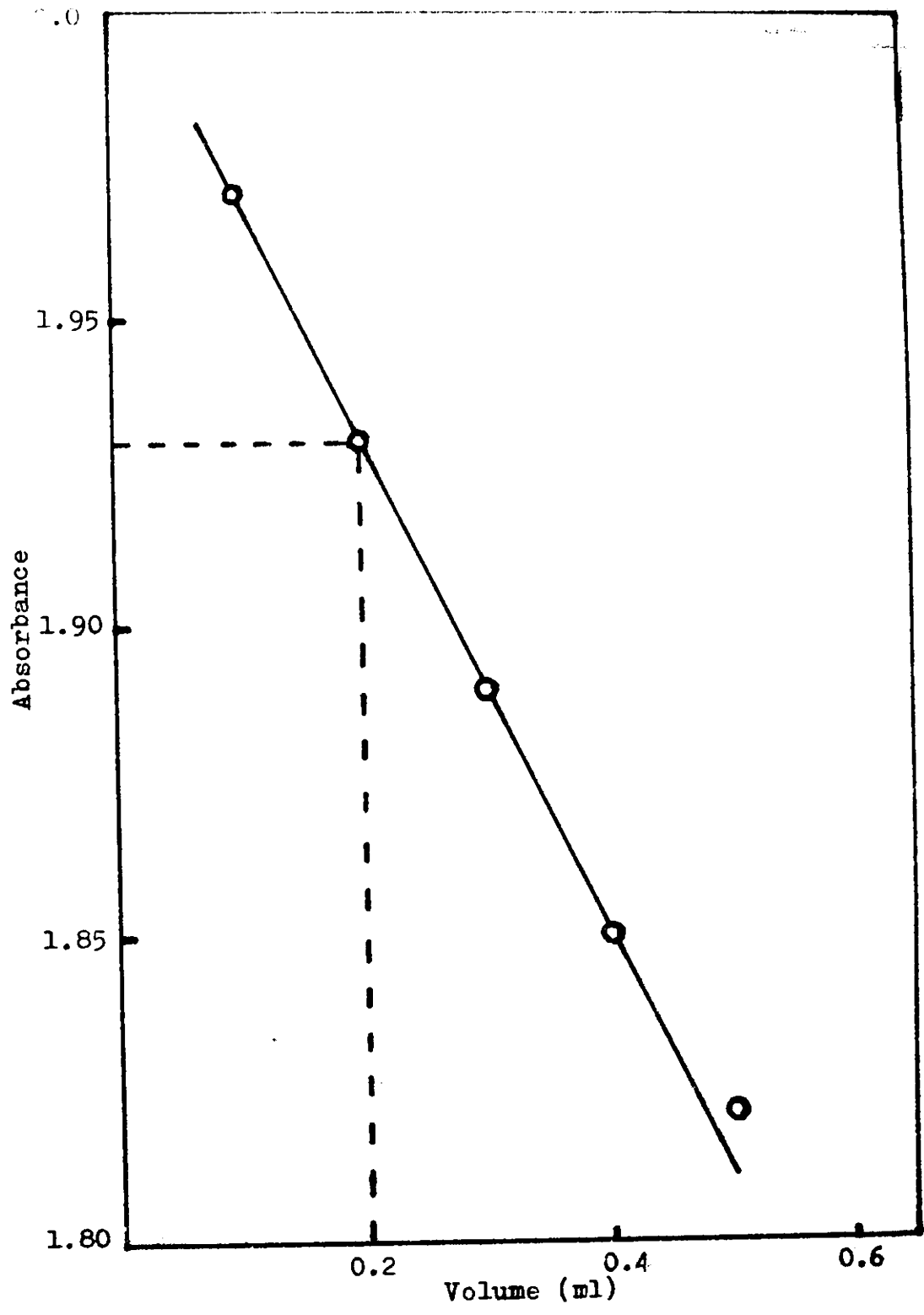


Fig.2.3 Absorbance-volume plot of Fe^{3+} solution.

ie, Fe_2O_3 contains only 58.2% of Fe^{3+} ion. In actual case the percentage of Fe^{3+} in Fe_2O_3 must be 69.9%. The lack of Fe^{3+} ion in the specimen has been attributed to the fact that ferrous sulphate has been used in the investigation. It has been observed that the percentage of Fe^{3+} ion in all the cases is the same.

CHAPTER THREE

ELECTRICAL CHARACTERIZATION OF SILVER SULPHIDE FILMS

3.1 Introduction

Surface conductivity of semiconductors is very sensitive to surface contaminants, methods of preparation, contacts, and induced localized charges. The surface transport phenomena play an important role in the conduction mechanism of semiconducting films of about 1000 \AA thickness and have a carrier concentration upto $\sim 10^{18} / \text{cm}^3$. The average mobility of the carriers decreases with decreasing film thickness. This decrease is partly ascribed to the size effect and partly to the increase in the density of structural defects in thin films.

When carrier transport takes place through the sample, the carriers undergo considerable scattering by the boundary surfaces, in addition to the bulk scattering in the sample. This scattering will reduce the effective carrier mobility to below that of the bulk value and this gives rise to conductivity size effects [162]. Let an extrinsic n-type semiconductor have a thickness d which is comparable to the mean free path of the carriers l . The band edges are assumed to be flat, and the electron

density n is uniform throughout the sample which is equal to that of the bulk value n_B . Let τ_s be the relaxation time due to surface scattering and τ_B that due to bulk scattering. Then the average relaxation time τ_F for electrons in the film is given by

$$\frac{1}{\tau_F} = \frac{1}{\tau_s} + \frac{1}{\tau_B} \quad (3.1)$$

The mean free path of the electron is given by

$$l = \mu_B \frac{h}{e} \left(\frac{3}{8\pi n_B} \right)^{1/3} \quad (3.2)$$

Where μ_B is the mobility of the carriers in the bulk, e is a unit electronic charge, and h is the Planck's constant. The average electron mobility in the film μ_F is given by an expression of the form

$$\mu_F = \frac{\mu_B}{1 + l/\gamma} \quad (3.3)$$

where $\gamma = d/l$; d is the film thickness. It is clear from equation (3.3) that the average mobility of the carriers decreases with decreasing film thickness and it approaches the bulk value for $\gamma \gg 1$. The equation is valid for thick films when the band edges are assumed to be flat. For very thin films the thickness d must be small compared

to the effective Debye length L_D . For an intrinsic semiconductor it is given by

$$L_D = \left[\frac{4\pi\epsilon kT}{e^2(n_B + p_B)} \right]^{\frac{1}{2}} \quad (3.4)$$

where ϵ is the Static dielectric constant. p_B is the density of positive carriers and n_B that of negative carriers. k is the Boltzmann's constant and T the temperature in absolute unit.

The expression for the conductivity of the film in the flat band approximation is obtained by introducing a boundary condition. The boundary condition is that all carriers incident at angles less than a critical value θ_0 to the surface are diffusely scattered. The carriers are specularly scattered for all incident angles greater than θ_0 [The specularity parameter (p) is a measure of the size effect deviation from the bulk behaviour. For perfect specular scattering (ie., $p = 1$) it is zero and for perfect diffuse scattering (ie., $p = 0$) it is maximum].

The film conductivity expression is given by

$$\sigma_F = en_B\mu_B \left(1 - \frac{3}{8} \frac{1}{\gamma} \sin^4 \theta_0 \right) \quad (\gamma \gg 1) \quad (3.5)$$

and

$$\sigma_F = en_B\mu_B \left[\frac{3}{2} \cos \theta_0 \left(1 - \frac{\cos^2 \theta_0}{3} \right) \right] \quad (\gamma \ll 1) \quad (3.6)$$

When the thickness of the semiconductor film is comparable with or smaller than both the mean free path and the effective de Broglie wave length of the carriers, quantum size effects appear in them [163]. As a result of the quantization of the transverse component of the quasi-momentum and, due to the finite thickness of the film the electron states obtain quasi-discrete energy values in the film. Because of the quantization, the bottom of the conduction band and the top of the valence band are separated by an energy value ΔE given by the uncertainty principle

$$\Delta E \sim \frac{h^2}{8m^*d^2}$$

where m^* is the effective mass of the electron.

The transport properties of many compound semiconductor thin films have been reported. Some of them are PbS [164], CdS [165,166], Ag_2Se [167], Ag_2Te [168].

The transport properties in most cases are dominated by microstructure, impurities and structural imperfections.

Investigations have been carried out on the electrical properties of the semiconductor, silver sulphide [169-172].

Solid silver sulphide exhibits two types of electrical conductivity which are partly ionic and partly electronic [173]. The ionic conductivity occurs below a temperature of 450K. It changes largely with temperature. At temperatures above 450K the conductivity is mainly electronic. It depends only slightly on temperature. Measurements of electrical conductivity at high temperatures (700K to 1500K) have also been carried out and the conclusion arrived at is that electronic conductivity occurs at high temperatures [174]. It has also been suggested that electronic processes are dominated by the influence of disorder in the cation sublattice [174].

3.2 Structure Fabrication and Resistance Measurements

3.2.1 Structure Fabrication

A suitable structure has been fabricated for electrical measurements of the silver sulphide films. Aluminium electrode films have been evaporated over the silver sulphide film with suitable masks in a high vacuum coating unit so that the electrode spacing is as required. The thickness of the electrode film was about 1500^oA in all cases. Well cleaned fine copper foil has been placed over the aluminium electrode and over that well cleaned copper strips have been fixed tightly to have good electrical contact with the film. Silver

conducting paint has been applied at the interfaces of film-copper foil and copper foil-copper strip. The connecting leads have been taken from the copper strips. The arrangement is given in figure 3.1.

3.2.2 Vacuum Cell and Measurement Set Up

The vacuum cell for the measurements has been fabricated using corning glass. The cell has got provisions for making external connections and thermocouple lead connections through vacuum tight couplings. A schematic diagram of such a set up is shown in figure 3.2.

Keeping the film with the connections given inside the vacuum cell, the cell has been evacuated using a rotary pump. The vacuum inside the cell has been measured using a Pirani gauge connected to the vacuum line. The electrical measurements have been carried out in a vacuum of the order of 10^{-2} torr.

The system has been heated externally using a heating mantle wound over the cell. This provides isochronal heating. The temperature of the system has been measured using a Chromel-alumel thermocouple set inside the vacuum cell.

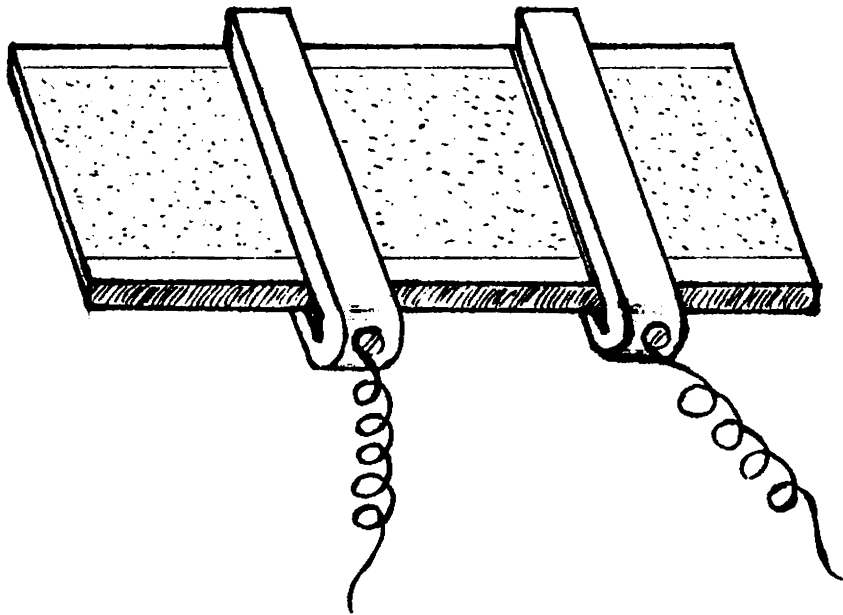


Fig.3.1 Silver sulphide film with contacts given.

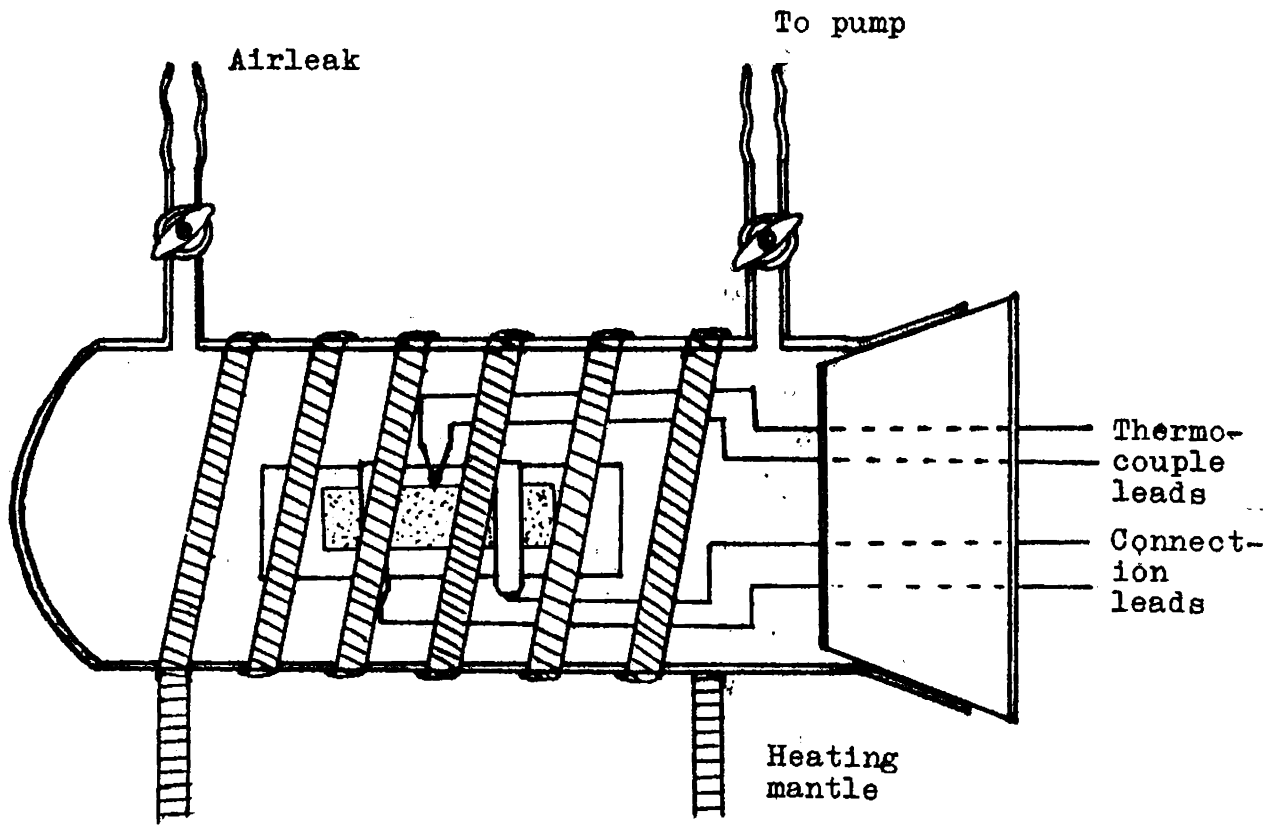


Fig.3.2 Vacuum cell with film system inside.

The entire set up has been kept inside a perfectly earthed copper box to give proper electrical shielding.

3.2.3 Resistance Measurements

The resistance measurements have been carried out using a million megohmmeter and a Philips multimeter. The million megohmmeter has been used in high resistance region. Prior to measurements the films have been annealed at 373K for 30 minutes in vacuum. After annealing it has been allowed to cool in vacuum to room temperature. Resistance measurements have been carried out in the temperature range room temperature to 473K for the heating and cooling processes. This has been repeated for three heating-cooling cycles for films of different thickness in the range 400 \AA to 2500 \AA , and of different surface area (2.5 cm x 1 cm, 2.5 cm x 0.8 cm, 2.5 cm x 0.7 cm).

3.3 Results

The electrical resistance of the film has been found to decrease with increase of temperature. For all the films measured, the resistance-temperature curve shows two conduction regions in between which there is a transition region. A linear decrease in resistance has

been observed in the first conduction region. In the second conduction region the resistance has been found to be almost independent of temperature. The transition from the first conduction region to the second is not sharp but it is in a range of about 25°C . In the transition process the resistance has been found to decrease for more than about two decades. The transition from the first region to the second region is observed in the heating process. In the cooling process reverse transition from the second region to the first has been observed. In the reverse transition process the region of transition temperature has been found to be a little displaced, to the low temperature region even though the range is the same. In the heating process the first conduction region extends upto about 433K and the second region starts from about 455K and in between is the transition range. Figure (3.3) shows the resistance-temperature curve for a film of 450 \AA thickness. The nature of the resistance-temperature curve remains the same for different heating-cooling cycles. The resistance-temperature characteristics for a film of thickness 2150 \AA are given in figure (3.4). The variation of resistivity with inverse of temperature has been plotted for the films and are shown in figures (3.5) and (3.6).

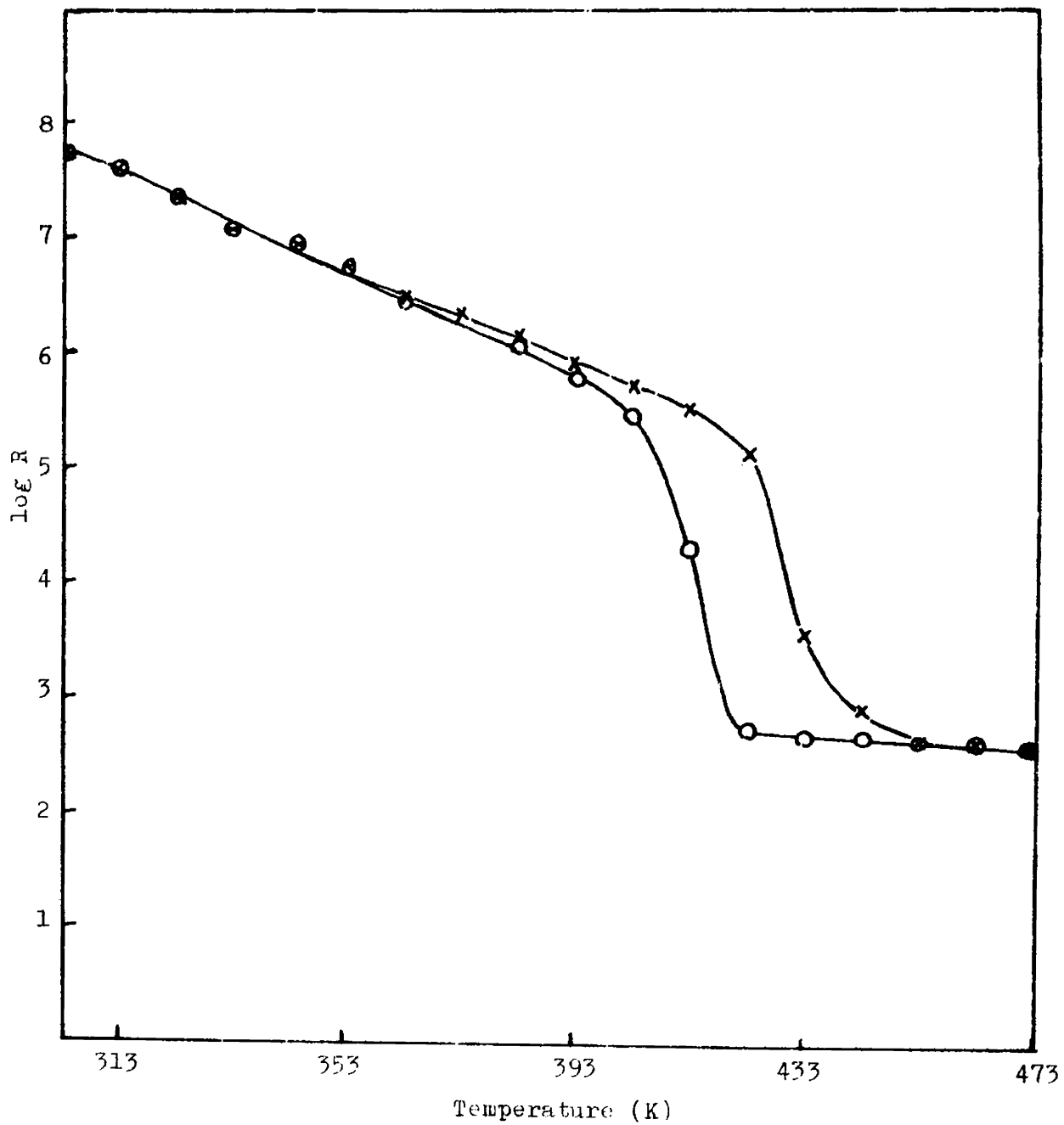


Fig.3.3 Resistance-temperature characteristics of Ag_2S film
 ($d = 450 \text{ \AA}$); xxx - Heating ; ooo - Cooling.

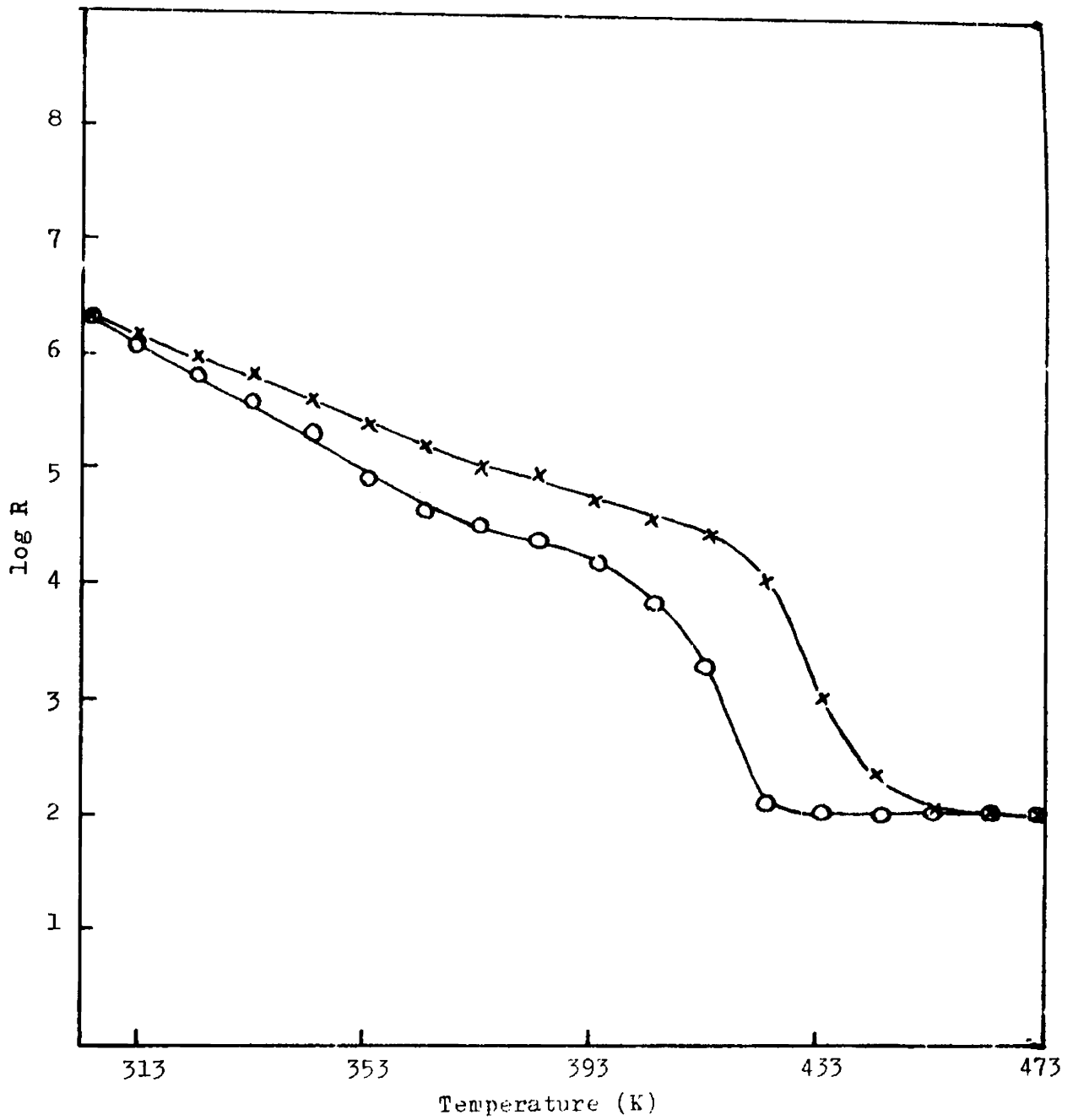


Fig.3.4 Resistance-temperature characteristics of Ag_2S film ($d = 2150 \text{ \AA}$); xxx - Heating; ooo - Cooling.

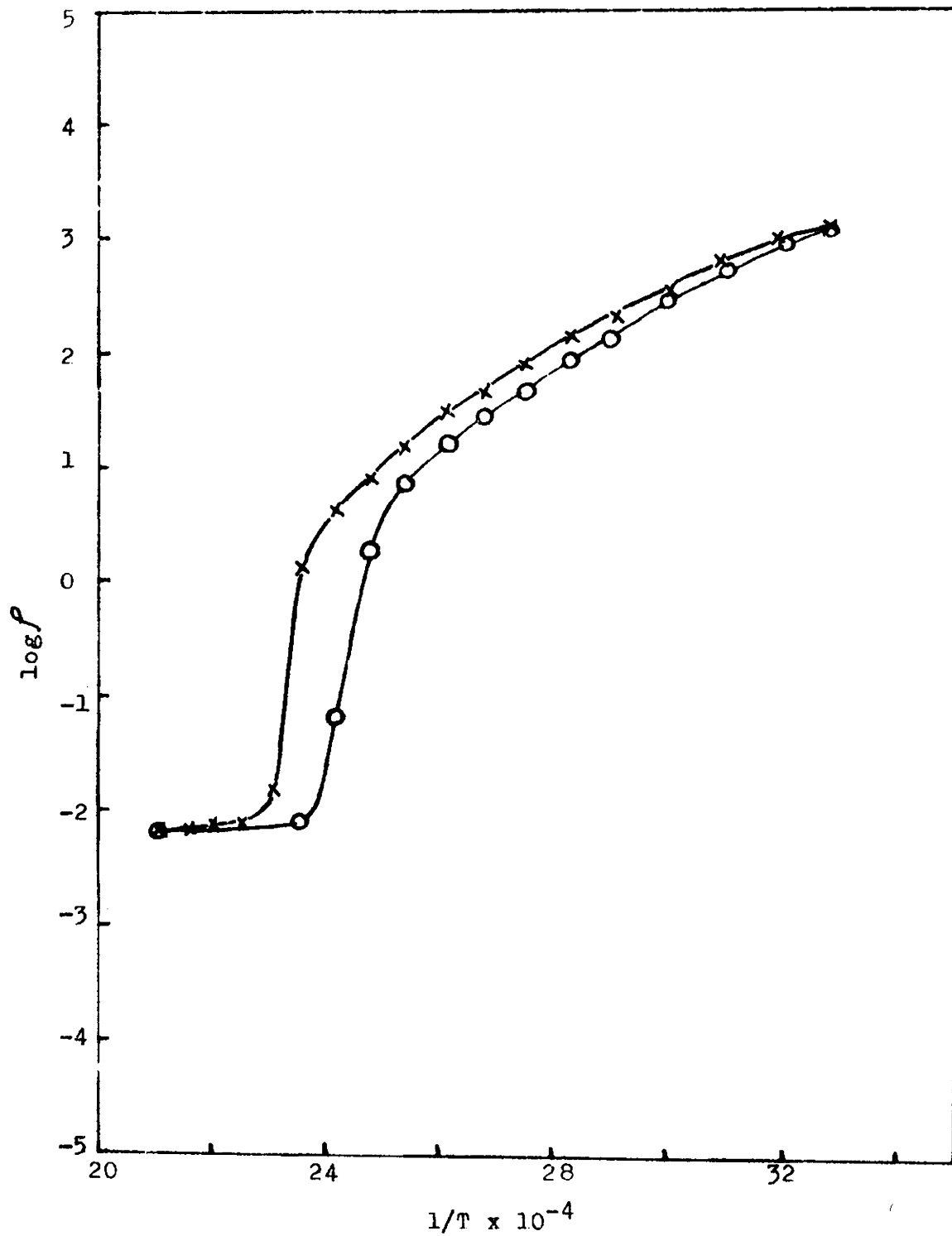


Fig.3.5 Resistivity-^oreciprocal temperature characteristics
 (d = 450 Å).

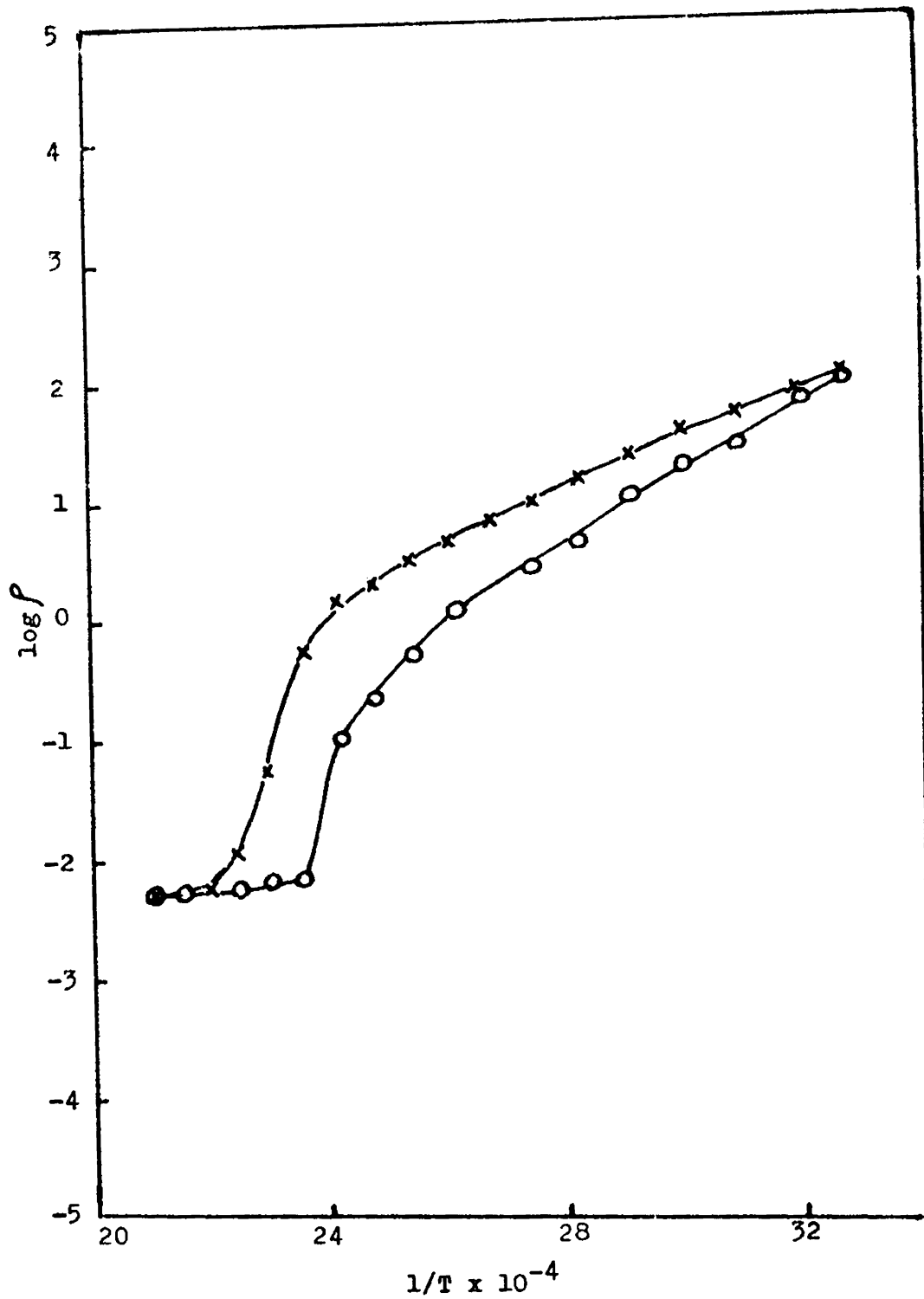


Fig.3.6 Resistivity-reciprocal temperature characteristics.
 ($d = 2150 \text{ \AA}$).

The activation energy ΔE in the two conduction regions for films of different thickness has been calculated using the formula

$$\rho = \rho_0 \exp- \Delta E/kT \quad (3.7)$$

where ρ is the resistivity of the film, ρ_0 a constant, k Boltzmann's constant and T the absolute temperature. The activation energy values in the two conduction regions for films of different thicknesses are given in the table (3.1)

Table 3.1

Film thickness ρ (A)	Activation Energy (eV)	
	Region I	Region II
450	0.661	0.0380
610	0.630	0.0330
1450	0.601	0.0118
2150	0.630	0.0102

The temperature coefficient of resistance in the temperature range 303K to 473K has been determined for films of varying thickness. The variation of temperature coefficient

of resistance with temperature for two different thicknesses are given in figures (3.7) and (3.8). The temperature coefficient of resistance has been found to decrease with increase of temperature. The temperature coefficient of resistance has also been found to vary with film thickness in the first conduction region. It decreases with increase of film thickness and with increase of temperature. In the second conduction region the temperature coefficient has been found to be independent of thickness. In figure (3.9) the temperature coefficient of resistance versus film thickness in the first conduction region at temperatures 353K and 383K, and in figure (3.10) that in the second conduction region at temperatures 460K and 473K are shown.

3.4 Discussion

Sulphides of most metals are semiconducting in nature. The nature of resistance-temperature characteristics observed in silver sulphide films is similar to that reported earlier [175,176]. Silver sulphide exists in two forms, one at temperatures less than 450K which is called β -silver sulphide and the second form at temperatures above 450K, called α -silver sulphide [169-173,175,176]. The electrical conduction in both these forms of silver

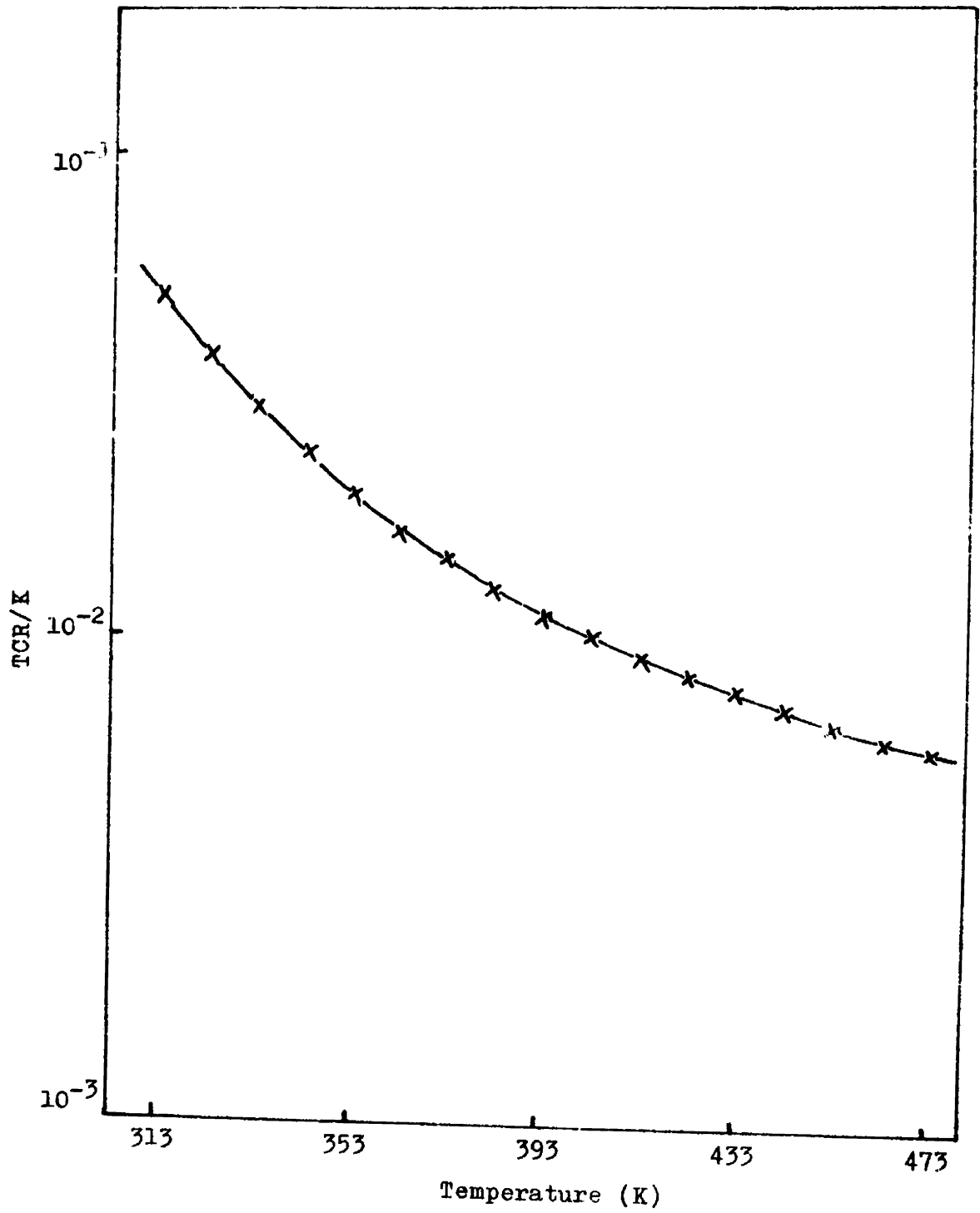


Fig.3.7 Temperature coefficient of resistance versus temperature plot ($d = 450 \text{ \AA}$).

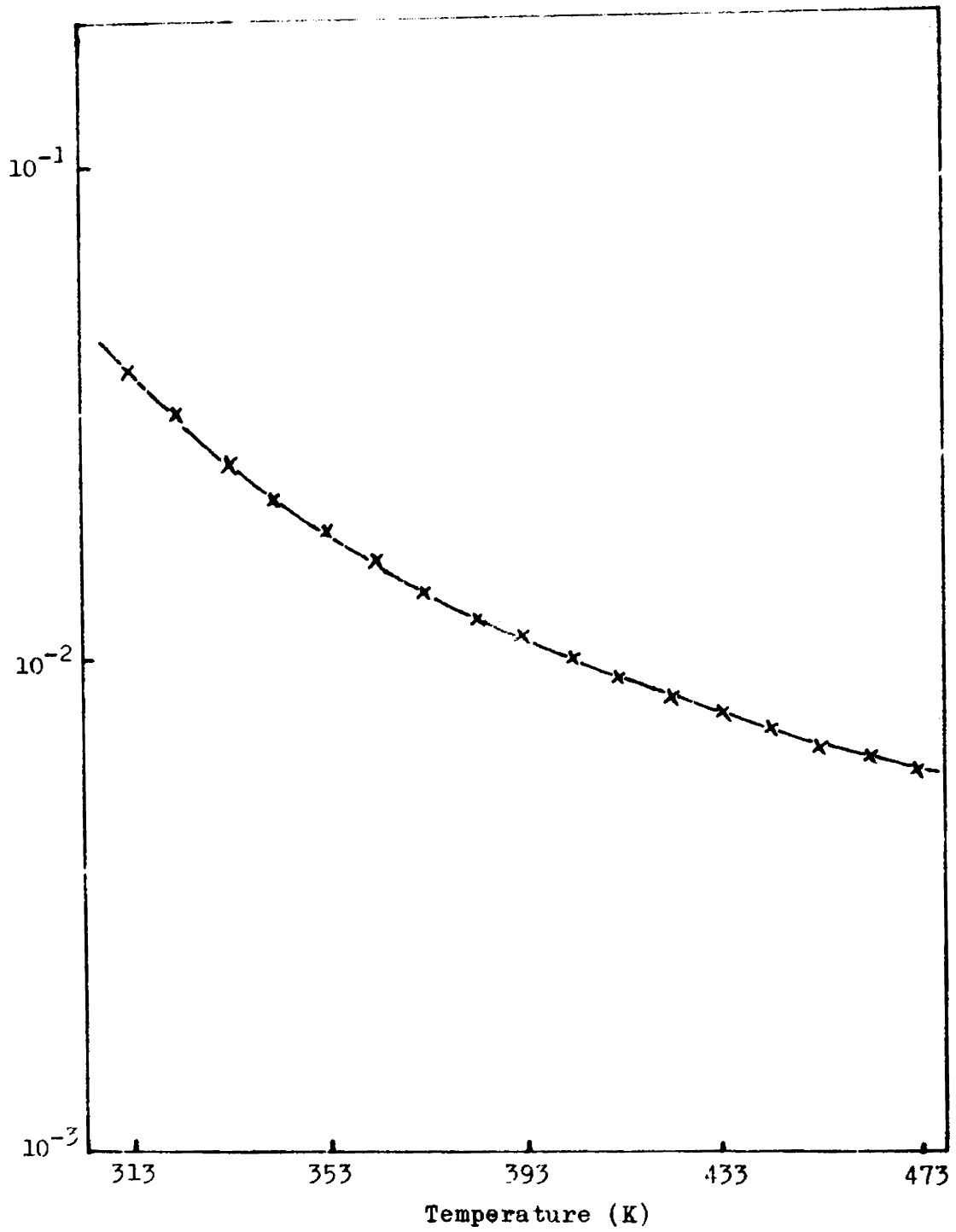


Fig.3.8 Temperature coefficient of resistance versus temperature plot ($d = 2150 \text{ \AA}$).

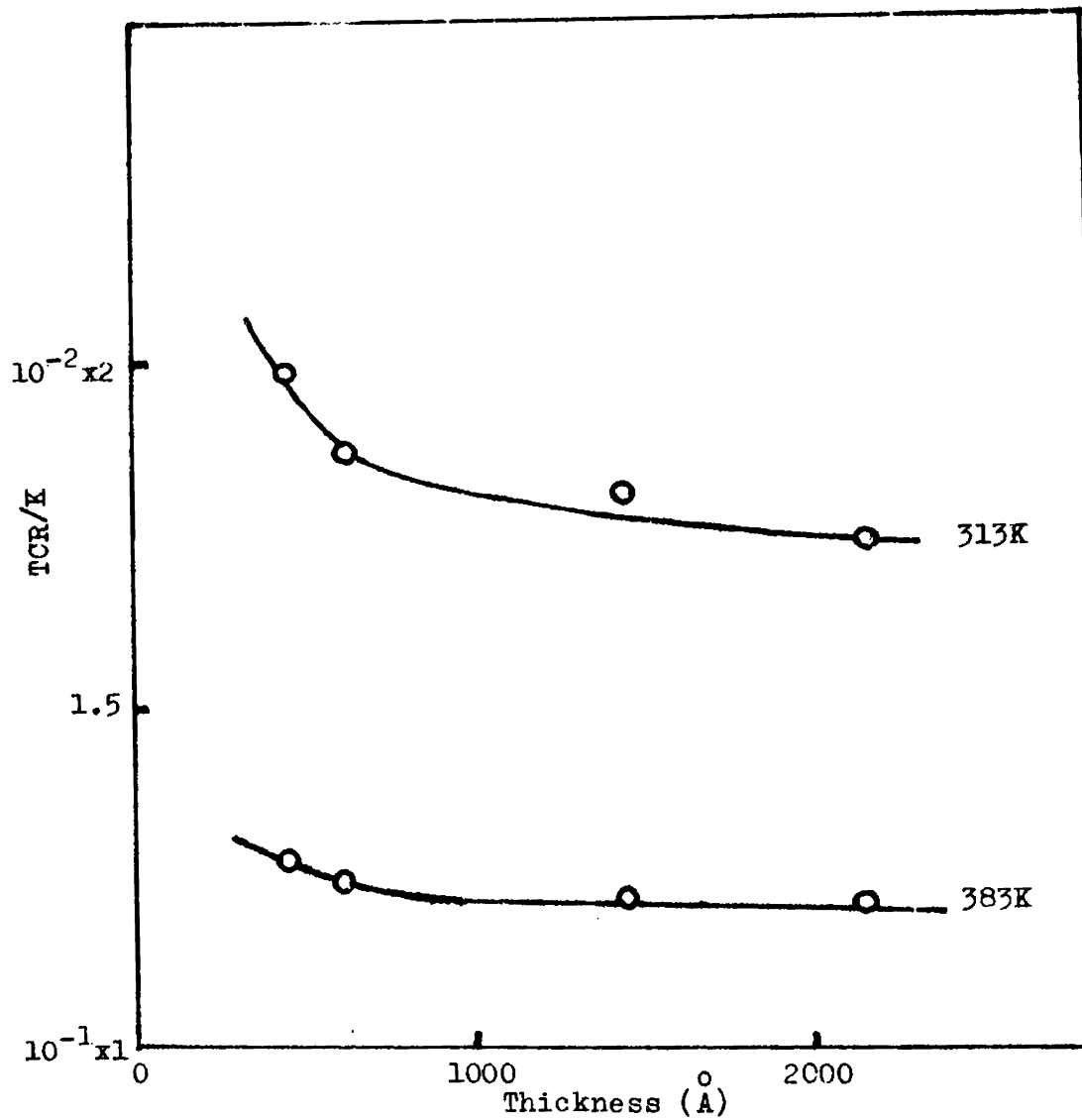


Fig.3.9 Temperature coefficient of resistance versus film thickness for Ag_2S films (at two temperatures) in the first conduction region.

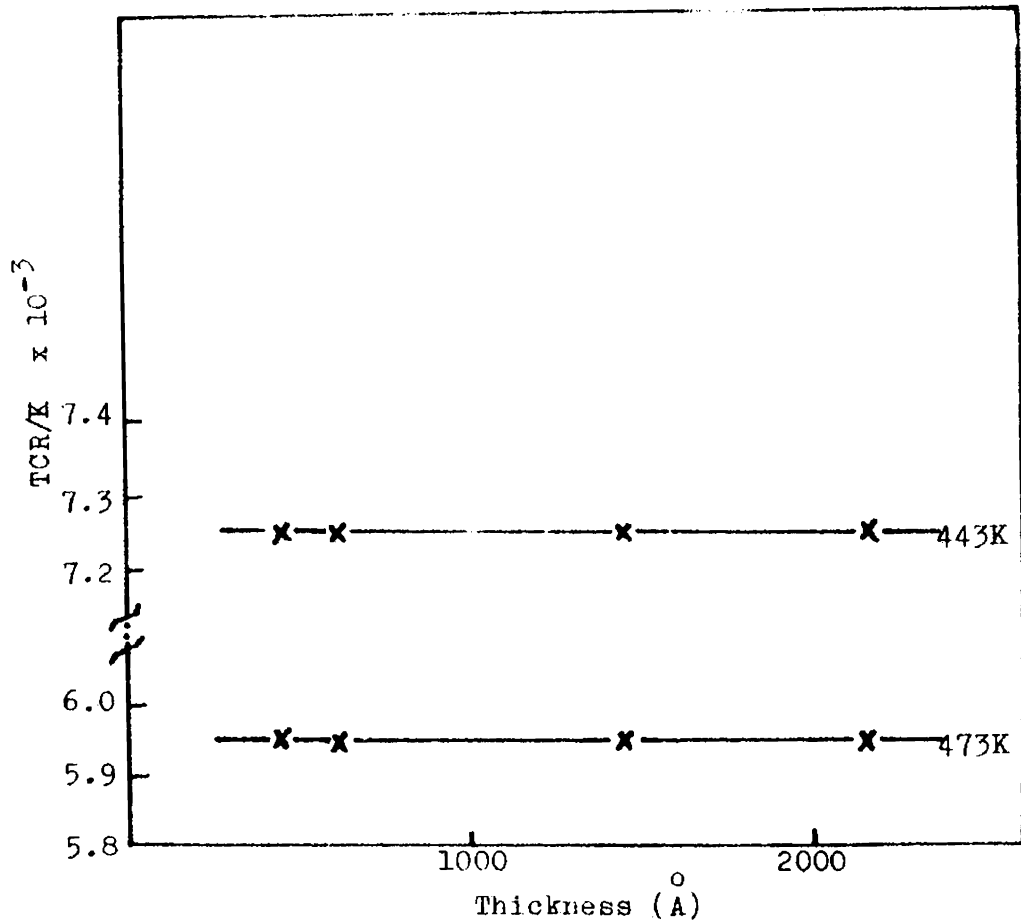


Fig.3.10 Temperature coefficient of resistance versus film thickness for Ag_2S films (at two temperatures) in the second conduction region.

sulphide is reported to be different [173,176]. Ionic conduction exists for β -Ag₂S, below 450K and in the α -phase, above 450K silver sulphide shows electronic conduction. At 450K it has been observed that transition from β -phase to α -phase or from ionic to electronic conduction occurs very rapidly [175-177]. Ichimescu et al. have observed a sudden transition for epitaxial layers of silver sulphide and transition for polycrystal layers extends over a temperature range of 20°C [175,176].

In the present study the silver sulphide films show decrease of resistance with increase of temperature upto about 430K which is taken as the upper limit of the first conduction region. After the limit of the first conduction region a transition occurs in a temperature range of about 25°C. It has been found that during the transition resistance of the film undergoes a sudden drop from the semiconductor range to the metallic range. Thereafter the resistance remains almost independent of temperature. The almost temperature independent region is the second conduction region. The activation energy for the first conduction region has been determined to be 0.633 eV comparable to that obtained by previous workers [173,175]. The conduction in this region is mainly ionic. The

transition observed in the present case is not too rapid at a particular temperature but it is in a temperature range which is the same as that for polycrystalline silver sulphide films [175]. The variation in the polycrystallinity also contributes to the electrical conduction. Cehan et al. [178] have observed such a variation in AC conductivity with thickness for chemically deposited silver sulphide films and found that it is predominant at thicknesses less than 900 Å. It has also been observed in the present case that the change of conductivity with temperature is more predominant at less thicknesses.

In the second region the conduction is found to be almost temperature independent. In this region the conduction is electronic. The transition is not sharp itself means that the film is polycrystalline in nature. The activation energy calculated in the electronic conduction region is found to be slightly dependent on film thickness. In the α -phase the electrical conduction is in metallic range. It has been reported that the I-V characteristics of silver sulphide show a rapid rise of electrical conduction with temperature in the β -phase and, a discontinuous increase of conduction by order of magnitude is observed when the transition to α -phase occurs at 450K [177]. This supports the two types

of conduction. The homogeneous behaviour in a wide temperature range is attributed to the stoichiometry of the system [179]. The change of the transition temperature region to the lower temperature region observed in the cooling process suggests that the reverse transition, i.e., from the electronic to ionic conduction occurs at a slight different temperature than the first transition.

The variation of temperature coefficient of resistance with temperature has been found to be similar for the thin and thick films. This uniform behaviour of temperature coefficient for all films reveals that all the films are of same stoichiometry. The thickness dependence of the temperature coefficient of resistance observed for films with thickness less than 1000 \AA below the transition region supports ionic conduction in the system. Thus the ionic conduction is found to be temperature dependent and thickness dependent. The temperature dependence of the ionic current has been found to be decreasing with increase of film thickness whereas its thickness dependence has been found to be decreasing with increase of thickness and increase of temperature. The thickness independent and almost

temperature independent nature of conduction in the second region confirms the electronic conduction.

It can be concluded from the observations that silver sulphide films prepared by the chemical method exhibit mainly two types of conduction, the ionic conduction and electronic conduction.

CHAPTER FOUR

ELECTRICAL CHARACTERIZATION OF FERRIC HYDROXIDE AND FERRIC OXIDE THIN FILMS

4.1 Structure Fabrication and Resistance Measurements

4.1.1 Structure Fabrication

The electrical measurements of the ferric hydroxide and ferric oxide (prepared as given in chapter two) have been carried out after fabricating suitable structures. The area of the film taken was $0.5 \times 2.5 \text{ cm}^2$. Electrode films were prepared by the evaporation of silver from a molybdenum boat in a vacuum better than 10^{-5} torr in a high vacuum coating unit. The electrode spacing was of 0.5 cm. The thickness of the electrode film was maintained the same in all cases. To provide electrical connections to the film cleaned thin copper foil strips were placed over the silver electrodes and over that cleaned copper blocks were screwed tightly without disturbing the film. To make good electrical contact silver conducting paint was used between electrode film and copper foil and between copper foil and copper block.

4.1.2 Measurement Set Up

The electrical measurements of the ferric hydroxide and ferric oxide films were carried out by keeping the film in a perfectly shielded copper box, having provisions for making external connections.

The system was heated externally with a heater kept close to the substrate. The temperature was varied by adjusting the current through the heater element by means of a dimmerstat. The temperature was measured using a chromel-alumel thermocouple placed in contact with the substrate. The film system with the heating arrangement is shown in figure (4.1).

4.1.3 Resistance Measurements

The resistance measurements were carried out using the million megohmmeter with a test voltage of 10V. The measurements were taken for both the unannealed and annealed ~~films~~ keeping them in air. The temperature of the film was varied from room temperature (303K) to 473K in three heating and cooling cycles and the resistances were measured at different temperature intervals and for films of varying thicknesses.

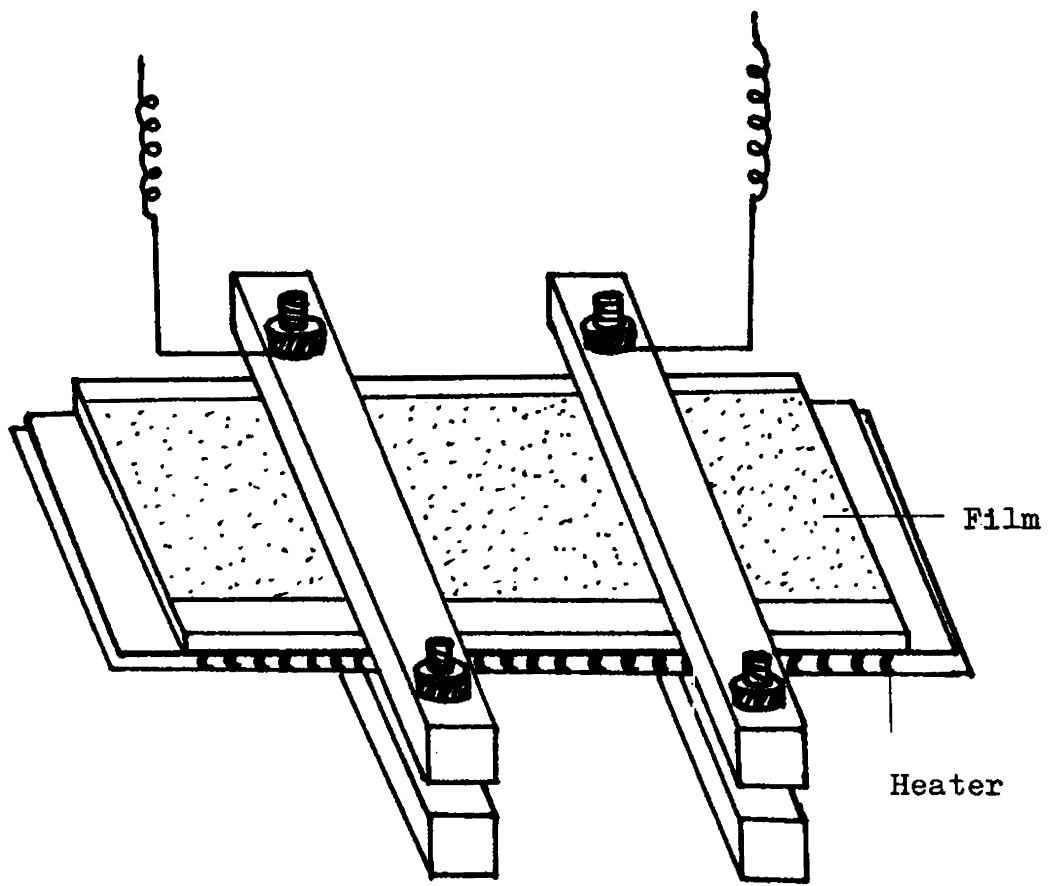


Fig.4.1 Ferric hydroxide film with contacts and heater arrangement.

4.2 Results

4.2.1 Unannealed Films

The nature of variation of resistance has been found to be the same for all the films irrespective of thickness. On first heating the resistance has been found to increase upto about 363-373K. This increase has been found to occur rapidly. After this rapid increase of resistance it has been found to decrease with increase of temperature upto 473K. In the cooling process from 473K the resistance increases upto about 313K and then decreases upto room temperature. On subsequent heatings and coolings more or less the above cooling path has been followed. Figure (4.2) shows the resistance-temperature curve for a film of thickness 340 Å. It has been found that the graph consists of two distinct branches.

The heating-cooling cycles follow more or less the same path especially for thin films. For thick films a little change between the heating and cooling paths has been observed. As the thickness of the film increases, the variation of resistances with temperature decreases. The resistance versus temperature curve for a film of thickness 1480 Å is shown in figure (4.3).

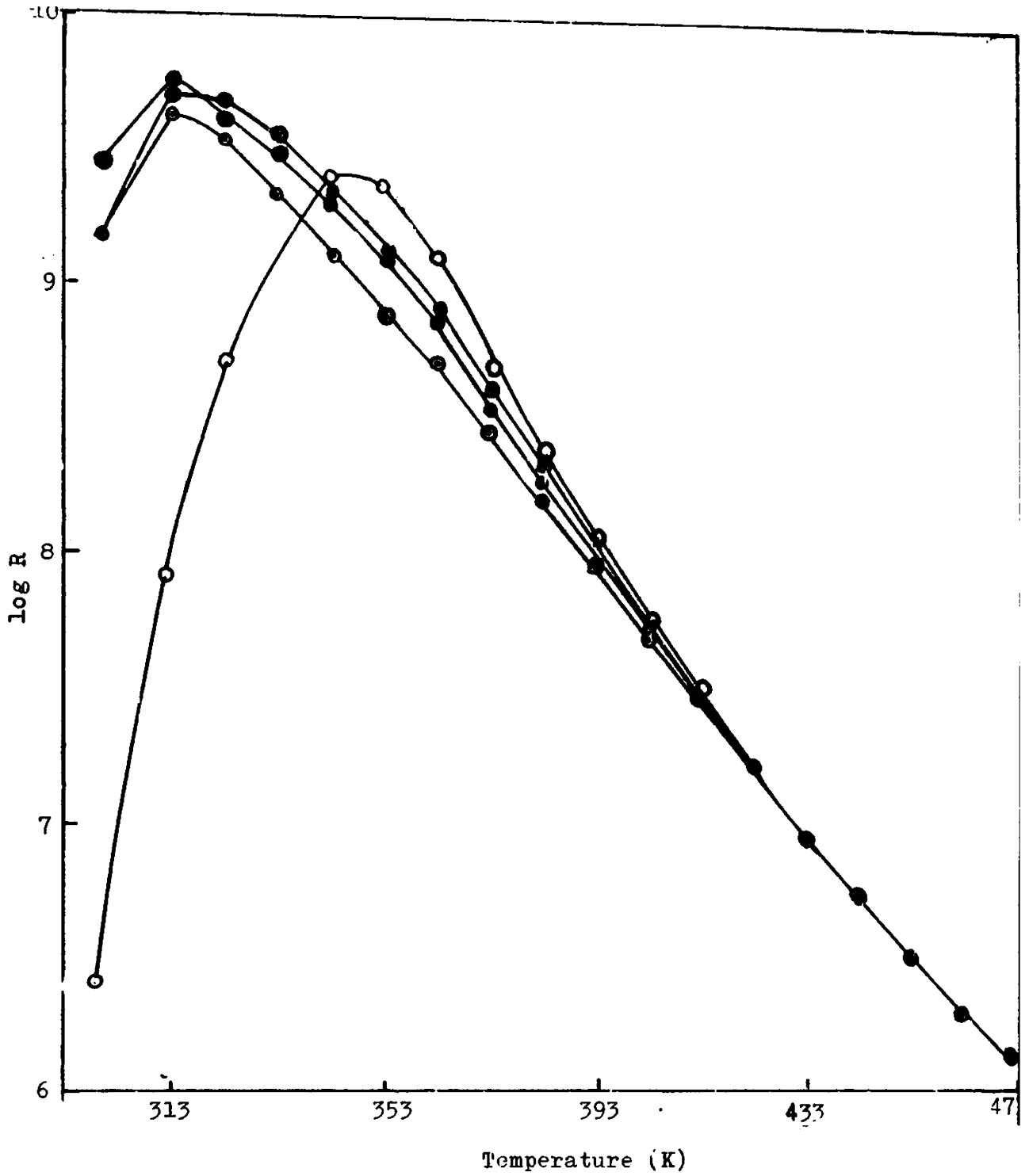


Fig.4.2 Resistance-temperature characteristics of ferric hydroxide film ($d = 340 \text{ \AA}$). ooo - first heating, ●●● - first cooling, ooo - second heating, ●●● - second cooling.

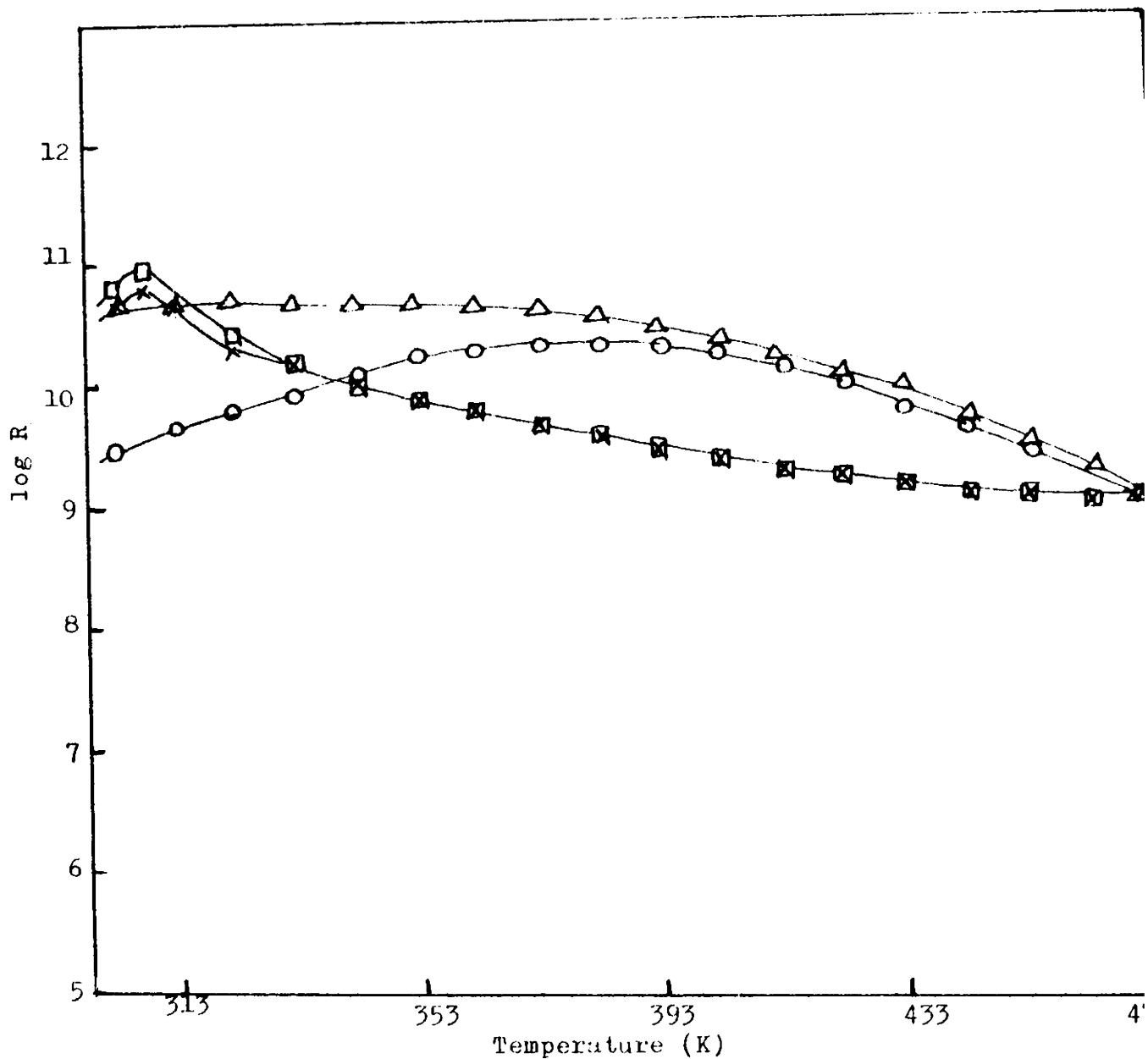


Fig.4.3 Resistance-temperature characteristics of ferric hydroxide film ($d = 1480 \text{ \AA}$). ○○○ - first heating, ××× - first cooling, △△△ - second heating, □□□ - second cooling.

4.2.2 Annealed Films

For films which have been annealed at 723K the nature of resistance-temperature curves has some similarity in the low temperature regions. The resistance-temperature curve for a film of 630 Å thickness is shown in figure (4.4). The resistance first increases with increase of temperature upto about 333K. From 333K the resistance remains almost constant with further increase of temperature upto about 413K and then decreases upto 473K. On cooling, there is not a pronounced increment. A reasonable increase can be observed only from about 363K upto 313K and then there is decrease of resistance. In all the subsequent heating-cooling cycles it has been observed that the almost temperature independent region is between 313K and 413K for heatings and from 473K to 363K for coolings.

The dependence of resistivity on the reciprocal of temperature for a film of 340 Å thickness is shown in figure (4.5). The plot consists of two distinct branches, each of which is approximately linear. The activation energy has been calculated using the formula

$$P = P_0 \exp -\frac{\Delta E}{kT} \quad (4.1)$$

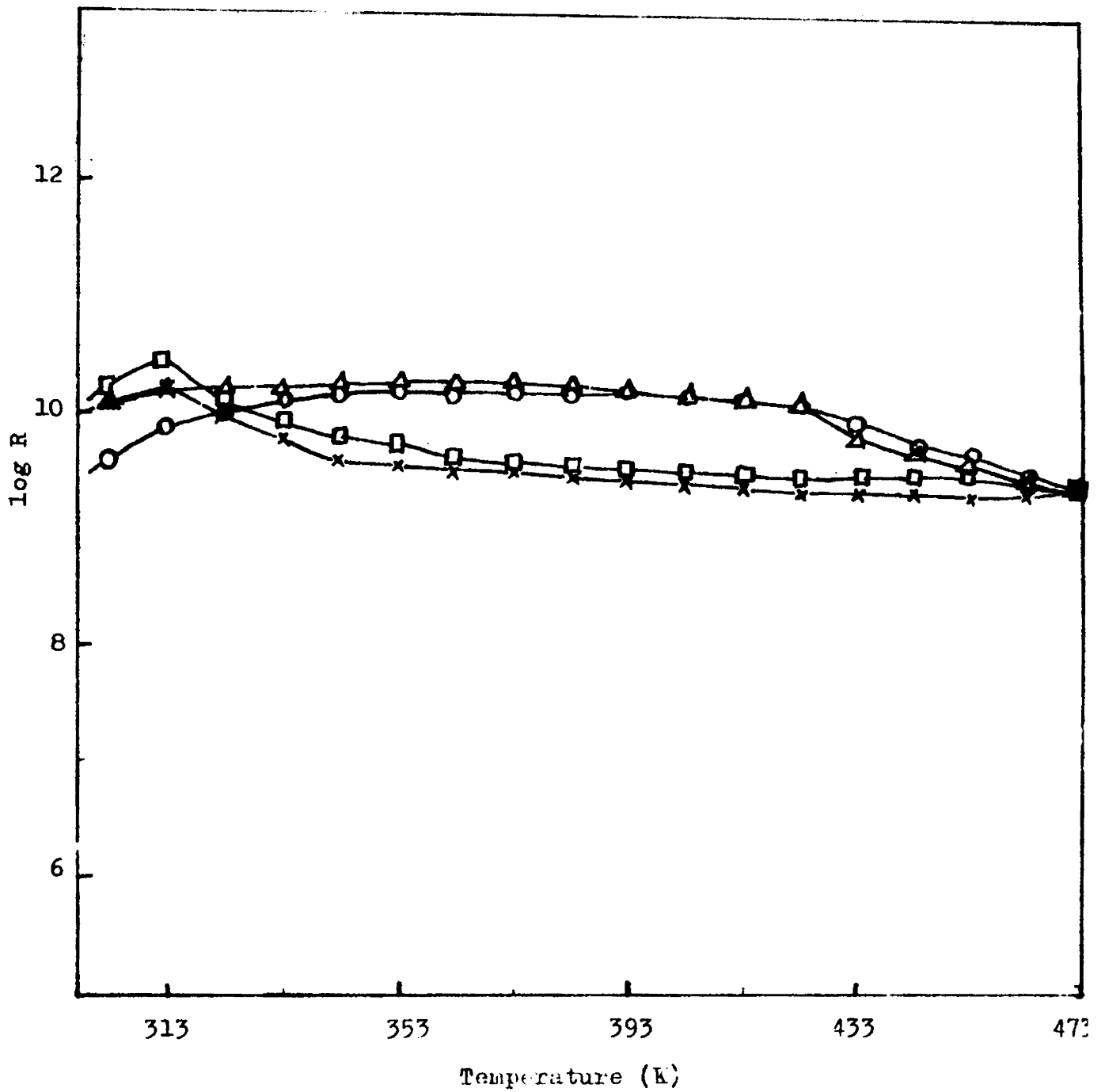


Fig.4.4 Resistance-temperature characteristics for film annealed at 723K for 1 hour ($d = 630 \text{ \AA}$). ooo - first heating, xxx - first cooling, $\Delta\Delta\Delta$ - second heating, $\square\square\square$ - second cooling.

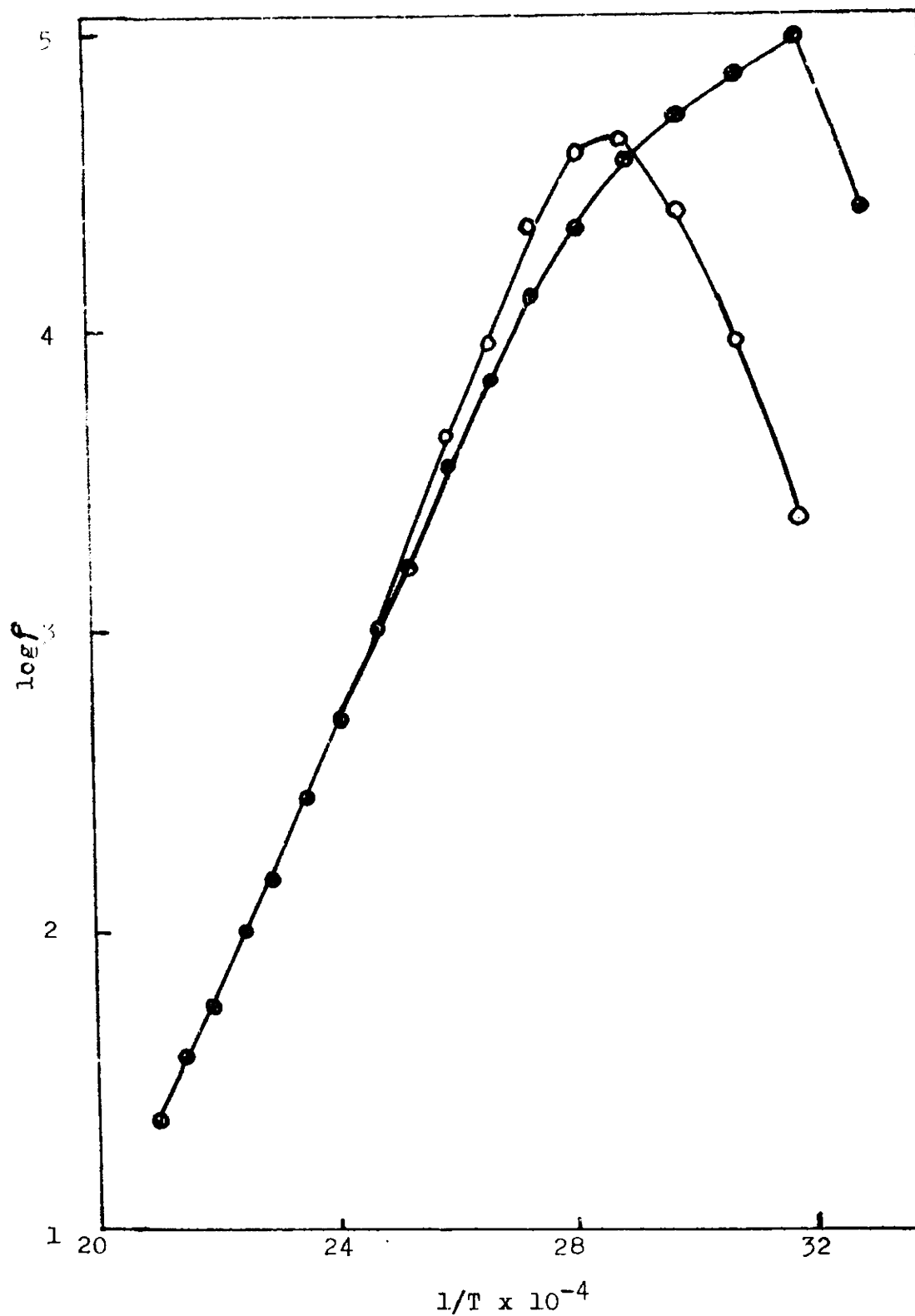


Fig.4.5 Resistivity-reciprocal temperature characteristics
($d = 340 \text{ \AA}$).

In the high temperature region the value of ΔE obtained is 0.36 eV and in the low temperature region it has been found to be very low.

The activation energy ΔE of the film has been found to decrease with the increase of film thickness. The activation energy versus film thickness plot is given in figure (4.6).

4.3 Discussion

The electrical resistance of semiconducting films depends on a number of factors such as the presence of impurities, defects, temperature, humidity, applied voltage etc. The conductivity increases with rise of temperature due to the higher concentration of carriers, which depends in a large measure on the presence of impurities. At very low temperatures the impurities are only weakly ionized. But, even at room temperature all the impurity atoms are thermally ionized. So in order to increase the conductivity of semiconductors a negligible amount of impurities is sufficient. The presence of impurities and vacancies mainly determines the low temperature conductivity. The energy to drift a defect is lower than that needed to

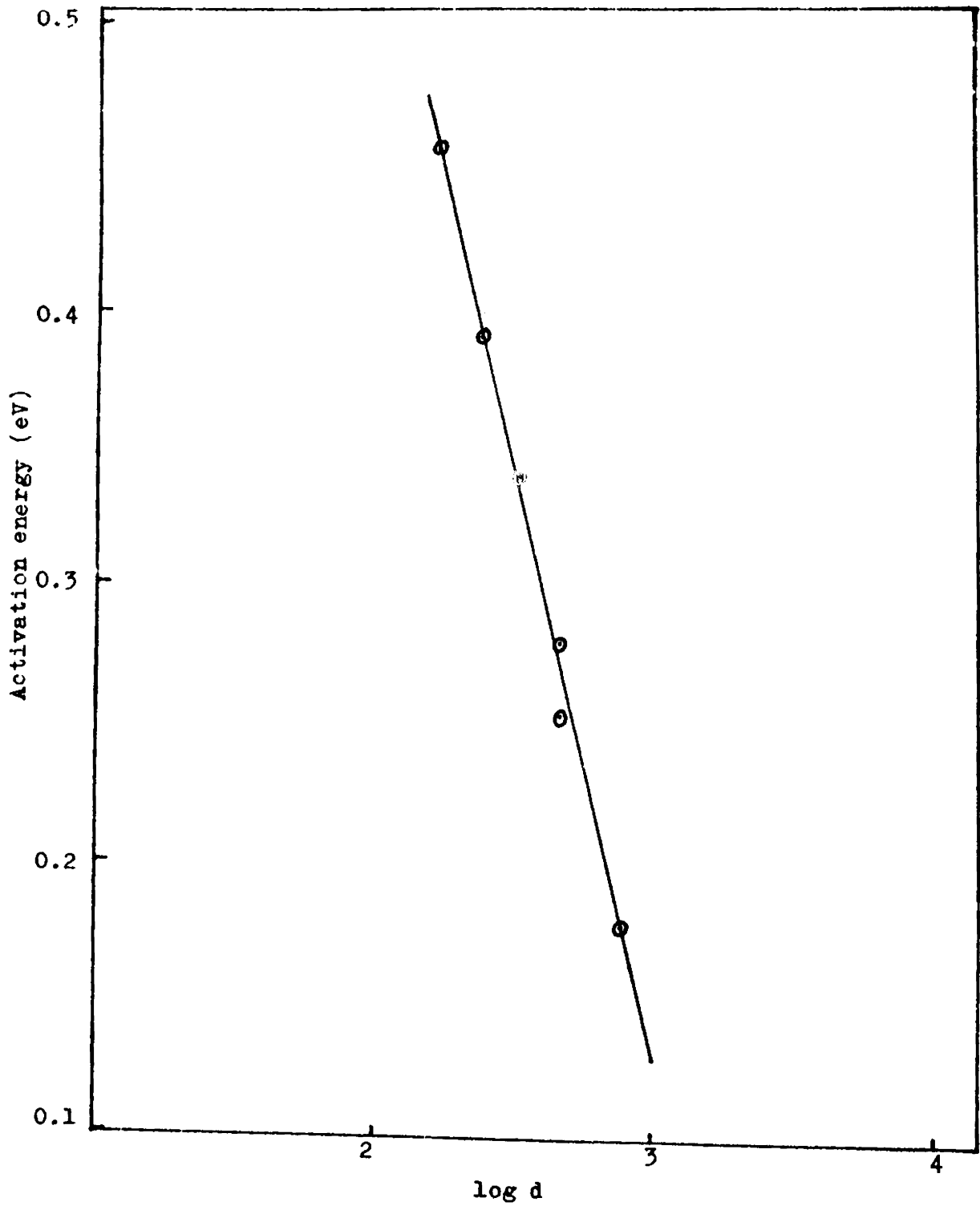


Fig.4.6 Activation energy versus film thickness plot.

form a defect. So the intrinsic defects mainly conduct at high temperatures. The upper limit of the low temperature conduction for a given compound is upto the temperature at which intrinsic defect concentration becomes equal to the impurity concentration.

In the present case it has been found that the resistance of all the unannealed films shows a rapid increase in the resistance during the first heating of the film system. This increase in resistance with temperature is attributed to the removal of the moisture content in the film system [180]. Also the moisture content in freshly prepared ferric hydroxide is high since they have been prepared by the chemical method and since they have been dipped in distilled water to remove the soluble impurities. The resistance increase is only upto about 373K which again supports the concept of the removal of moisture. However, the resistance begins to decrease when a considerable portion of moisture has been removed. In the cooling process as well as in all subsequent heating-cooling cycles, the resistance monotonically increases upto 308-313K. In this region impurities may be the controlling factor determining the conductivity. Also the non-stoichiometry of the film may be another factor [181,182]. The activation

energy calculated has been found to be very low in the low temperature region, the reason being that the carriers may be hopping to a more distant centre [183]. The second region extends from 313K to 473K where the heating and cooling curves are almost linear, especially in the case of very thin films. Conduction in this region is apparently dominated by intrinsic defects. At high temperatures a certain number of ions will get released from their normal positions and will be free to cause an increase in conductivity [184,185]. Since the heating is done in ambient air, the specimen chemisorbs oxygen, which gets ionized and the electrons thus liberated tend to enhance the conductivity. In the cooling process the recombination may be assumed to dominate over ionization resulting in a decrease in conductivity upto the point where impurity conduction starts.

The activation energy determined from the linear portion of $\log \rho$ versus $1/T \times 10^{-4}$ plot shows a dependence on thickness. Higher values of activation energy for thin films and smaller values for thick films have been observed, i.e., the activation energy decreases with increase of film thickness. This may be due to the possibility of impurity charge carriers giving rise to various energy levels in

the band gap and various defects which are not removed by heating as pointed out by Goswami et al. in their study of MnTe films [186].

In the case of annealed films the variation of resistance with temperature is not as much significant as in the case of unannealed films. The resistance has been found to be almost temperature independent in a wide temperature range. The annealed films must have completely changed to ferric oxide, which has a reddish brown colour. This may be the reason for the observed change in the resistance-temperature curve of these films from that of the curves of ferric hydroxide films. Since the films have been annealed at 723K for one hour, while heating upto 473K, the contribution to the resistance values from the removal of defects and imperfections by annealing will be negligible. The results are in agreement with those of Acket and Volger [187] in Fe_2O_3 indicating that the conduction below 400K is complicated.

CHAPTER FIVE

PREPARATION AND CHARACTERIZATION OF GLOW DISCHARGE POLYMERIZED PARA-TOLUIDINE THIN FILMS

5.1 Introduction

Polymer thin films of various organic compounds have been given attention from a technological point of view in microelectronics as well as an interest in their anti-corrosive nature, electric and dielectric properties, physical and chemical properties, and surface phenomena. The semiconducting and insulating properties of the polymer films are being much appreciated in technological fields. Different methods, such as glow discharge, electron bombardment, photolysis etc. have been proposed to produce polymer thin films. Among them, the glow discharge polymerization is a widely accepted and preferred method, on account of the desirable qualities of the films produced such as good adhesion to the substrate, excellent electrical, mechanical and chemical properties and their pin hole free nature [188]. Polymer films of many organo and organometallic materials have been prepared by the glow discharge method. The films produced by this method are found to be useful as thin film insulators and capacitors because of their good dielectric properties [49,70,6,189].

The glow discharge polymerization consists of DC as well as AC glow discharge methods. Different kinds of modifications for the glow discharge method have been reported in order to improve the film properties and to develop their applications. When DC field is used the polymer films form principally on the electrode acting as the cathode. AC discharges with internal electrodes and electrodeless discharges are used [78,93,8]. The details of the different polymerization methods are given in chapter one. In the present study polymer thin films were produced by electrodeless glow discharge method. The power source used in polymerization process is a radio-frequency oscillator. It oscillates at a frequency of about 4.5 MHz. The power was coupled to the discharge tube by capacitive coupling. The monomer taken was para-toluidine. The details of the radio-frequency oscillator, vacuum set up and the procedure employed for depositing the polymer films are discussed below.

5.2 The Electrodeless Glow Discharge Set Up

5.2.1 Radio-Frequency Oscillator

The radio-frequency oscillator with the required RF power was constructed and the valves used were 807 tetrodes

in a parallel push pull configuration (Figure 5.1). The centre tapped tuning coil L_1 tuned with $C_1 = 200$ pf was symmetrically wound with 16 turns of 20 standard wire gauge enamelled copper wire at 12 turns per inch over the tertiary winding L_3 of 18 standard wire gauge enamelled copper wire wound over a $1\frac{1}{4}$ inch glass ferret at 12 turns per inch. L_3 consists of 72 turns. The feedback tuning coil L_2 consists of 4 turns of 26 standard wire gauge enamelled copper wire. Grid leak biasing was obtained with the parallel construction of 22K resistor and 47 pf capacitor. The 10K 10W wire wound resistor feeding the screen grid of the tubes was adequately bypassed. Variable capacitor C_2 was used to have the tertiary winding connected to the load. The frequency of the oscillator was around 4.5 MHz. The power output was adjusted using the variable capacitor C_2 . The power was fed to the polymerizing system using two copper foils which acted as the capacitor plates.

5.2.2 Vacuum System

A vacuum system was designed for the polymerization purpose and it was fabricated using corning glass. It was fixed on a sturdy stand mounted on a table. The system is capable of attaining a vacuum of 10^{-2} torr. The schematic diagram of the set up is shown in figure (5.2).

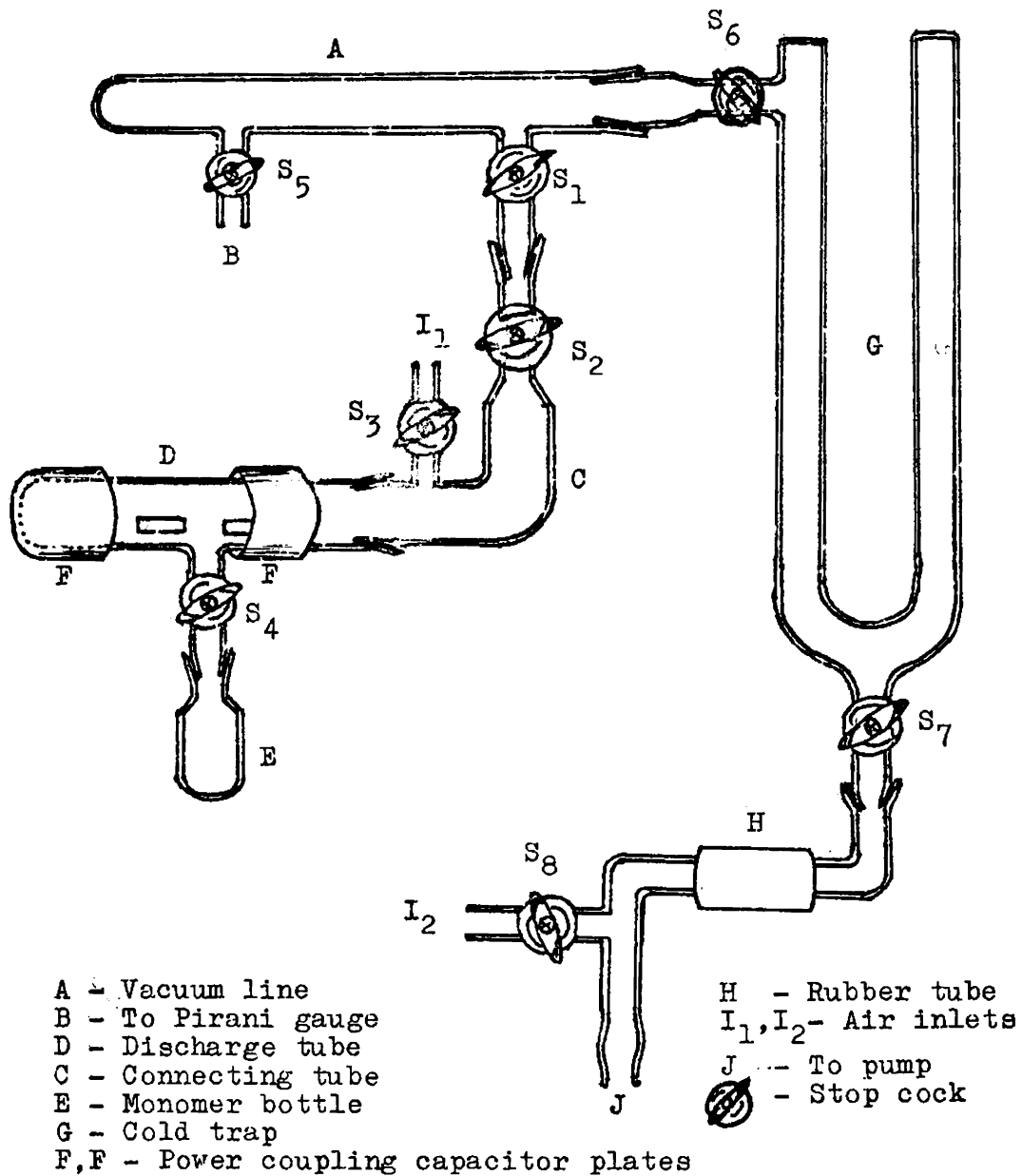


Fig.5.2 Schematic diagram of the electrodeless discharge set up.

The vacuum set up consists of a vacuum line A to which the discharge tube D is connected through a connecting tube C. E is a small bottle to take the monomer and it is connected to the discharge tube. The stop-cock S_4 on the side tube of the discharge tube controls the rate of flow of the monomer vapour into the plasma zone. The power from the oscillator is fed to the plasma zone through two capacitor plates F, F which are wrapped over the discharge tube. An air-inlet I_1 is provided on the connecting tube C by which air leak can be given into the discharge tube alone by closing stop-cock S_2 and opening S_3 . G is a double walled tube acting as cold trap connected to the vacuum line to get the impurities condensed. The stop-cock S_6 is provided between the vacuum line and the cold trap. H is a rubber tube via which the rotary pump is connected to the system. Another air-inlet I_2 is given in the vacuum line through the stop-cock S_8 . The Pirani gauge which is used to measure the vacuum is connected to the vacuum line at B. The different parts of the set up are connected through vacuum tight joints. The substrate is placed in the vicinity of the external electrodes.

5.3 Polymer Film Deposition

To deposit the polymer films the cleaned substrate

was properly placed inside the discharge tube and it was connected to the vacuum line. The monomer was taken in the small bottle provided, and it was connected to the side tube of the discharge tube. After closing the air-inlet I_2 the vacuum system was evacuated to about 10^{-2} torr. Then the air-inlet I_1 and the stop-cock S_4 were closed. The discharge tube was then evacuated by opening the stop-cock S_2 . The power feeding capacitor plates were connected to the discharge tube. After reaching a vacuum of 10^{-2} torr the power source was switched on and the power was adjusted to a reasonable value with the help of the variable condenser C_2 . Then an intense glow appeared in the discharge tube. The monomer was then heated and the vapour was admitted into the discharge tube at a slow and constant rate by opening the stop-cock S_4 . The monomer flow rate was adjusted such that the pressure in the system was about 0.5 torr. The monomer gets polymerized and deposited on the substrate and also on the sides of the discharge tube. The film thickness can be controlled by limiting the time of flow of the monomer vapour. High rate of flow of the monomer vapour may result in deposition of partially polymerized material. Hence it was avoided. After depositing the film the stop-cock S_4 was closed. After a few minutes the stop-cock S_2 was closed and then the RF source was switched off. Air leak was given

to the discharge tube and it was taken out. Finally the pump was also switched off. The photograph of the discharge set up is shown in figure (5.3).

In this type of set up polymerization as well as the film deposition take place simultaneously. It has been reported that the polymerization takes place in the gas phase [97]. Radical reaction in the gas phase has been found to be predominantly occurring at discharge frequencies higher than a few MHz [84,190] and ionic polymerization predominates at lower frequencies [81,191,192]. The possibility of both the types of polymerization cannot be excluded since it has not been established quantitatively that one or the other mechanism is exclusively responsible for polymerization.

5.4 Characterization

5.4.1 Physical Studies

The colour of the deposited polymer film has been found to be dark brown while the monomer is almost colourless. The monomer has been found to melt at 318K whereas the polymer is stable upto 673K. On heat treatment above 573K the colour gets changed to darker brown. A similar phenomenon

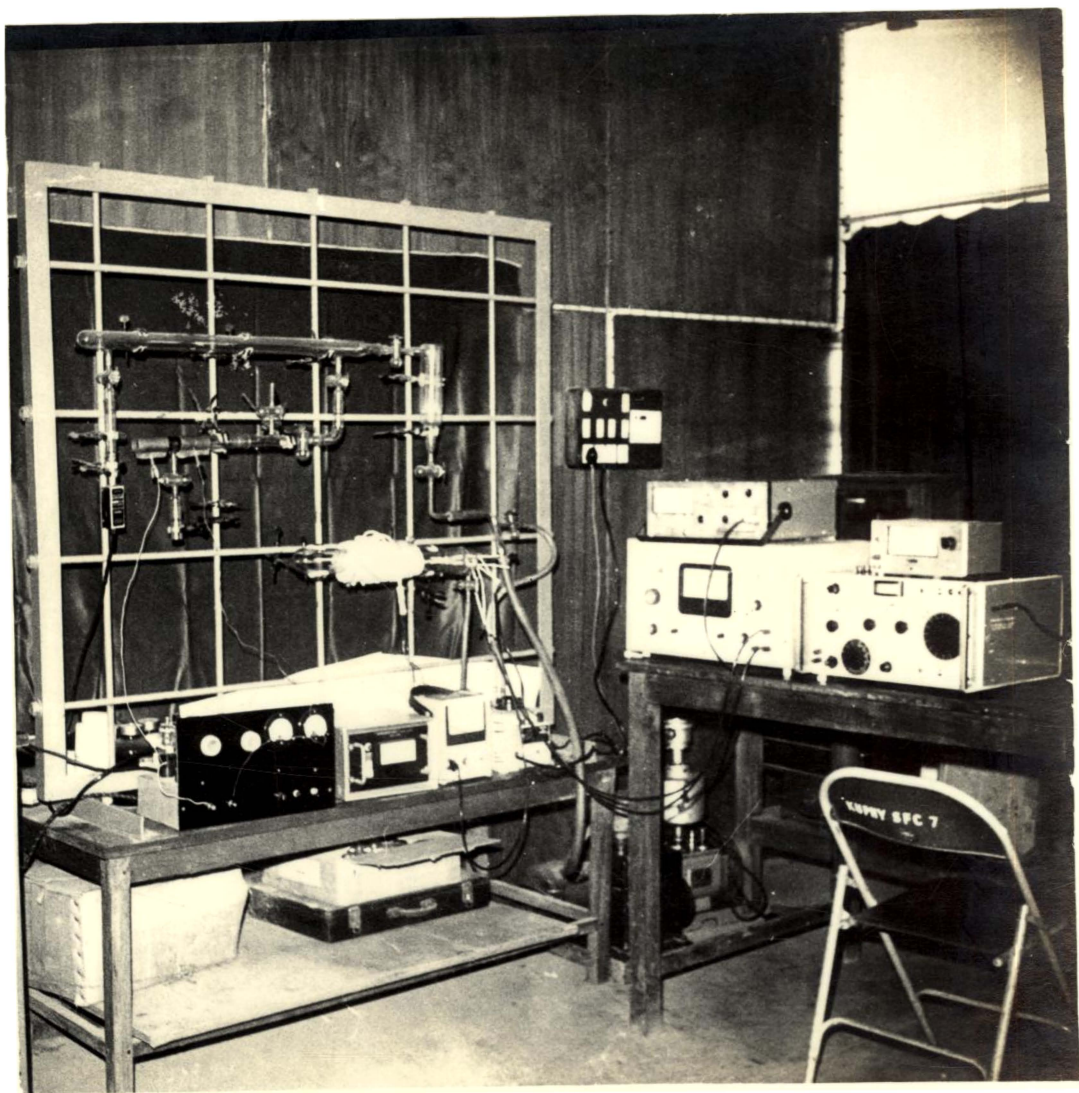


Fig. 5.3 Electrodeless glow discharge set up together with the electrical measurement arrangements.

has also been observed in the polymerization process when the power coupled has been increased, as a result of which a good amount of heat is produced in the plasma region. Also the films produced in the high power condition have a tendency to peel off from the substrate. However, the films deposited at a reasonable power have a very good adhesion to the substrate which is a very good property of the films. Also such films are found to be stable for a long time.

Another property of the polymer films of para-toluidine obtained in the electrodeless glow discharge method is their insolubility in organic as well as inorganic solvents which suggests the presence of cross linking. The monomer para-toluidine dissolves in chloroform, acetone etc. which also differentiates the polymer from the monomer. Because of the insolubility of the polymer, it is not possible to determine its molecular weight.

5.4.2 Infrared Studies

The infrared spectra of the monomer and the polymer have been recorded using Beckman infrared spectrophotometer (Figure 5.4) in the range 4000 cm^{-1} - 600 cm^{-1} . The infrared spectra of the monomer and polymer are shown

in figure (5.5). The IR spectrum of the monomer contains all the bands reported earlier [193-196]. The two bands at 3420 and 3340 cm^{-1} represent the asymmetric and symmetric NH modes. Instead of these two bands there is only one band at 3370 cm^{-1} , in the polymer spectrum. This represents the NH band of a secondary amine. In the monomer spectrum there are three lines at 3020, 2920 and 2860 cm^{-1} in the order of decreasing intensity indicating the presence of a $-\text{CH}_3-$ group in the molecule. In the polymer spectrum there is one strong line at 2920 cm^{-1} and a weak line at 2860 cm^{-1} . This seems to indicate the presence of a $-\text{CH}_2-$ group instead of the $-\text{CH}_3-$ group in the molecule. The CN band at 1270 cm^{-1} which is one of the strongest bands in the monomer spectrum, is reduced to a weak broad band centered round 1270 cm^{-1} in the polymer spectrum. The bands due to the phenyl ring and bands indicative of disubstitution are present unchanged in the spectra of para-toluidine and glow discharge polymerized para-toluidine. There is also an additional band at 2200 cm^{-1} in the polymer spectrum.

From the observed changes in the infrared spectrum of the polymer from that of the monomer it is concluded that in the polymer the $-\text{CH}_3-$ group is replaced by the $-\text{CH}_2-$ group and the $-\text{NH}_2-$ group by $-\text{NH}-$. Thus the structure

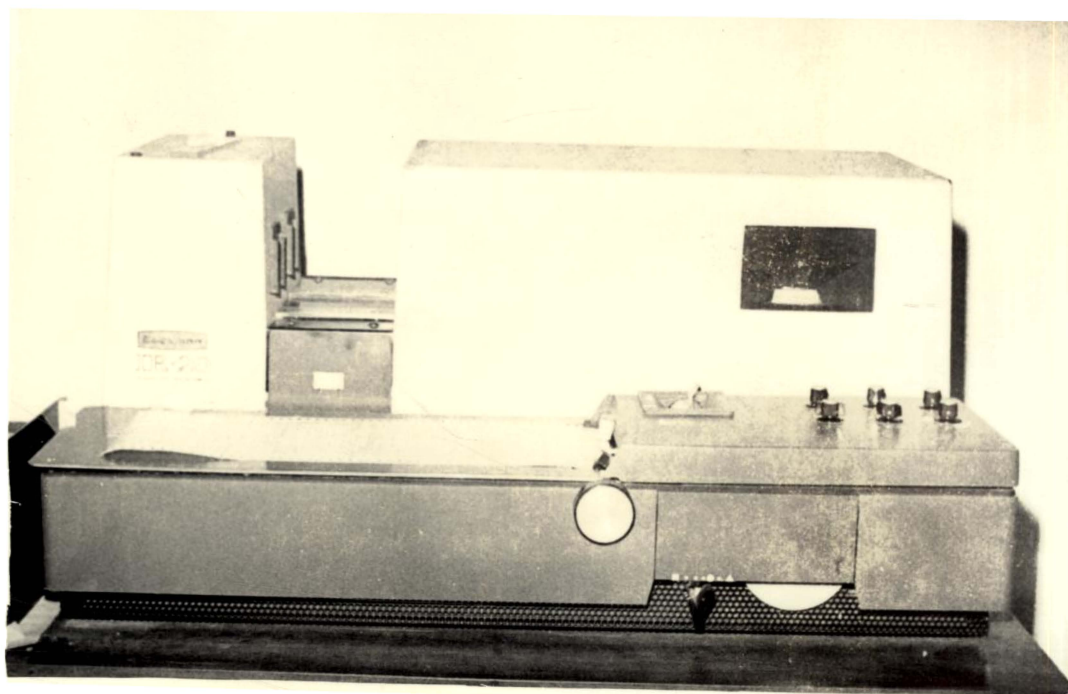


Fig.5.4 Beckman infrared spectrophotometer

fabricated for the purpose. The prepared polymer films show good adhesion to substrates and they are found to be insoluble in organic as well as in inorganic solvents. From the infrared studies of the polymer and parent monomer the possible structure of the polymer and the polymerization mechanism have been proposed.

CHAPTER SIX

DIELECTRIC STUDIES ON GLOW DISCHARGE POLYMERIZED PARA-TOIUIDINE THIN FILMS

6.1 Introduction

The dielectric behaviour of material provides information regarding the orientational and translational arrangements of dipoles and mobile charges present in the system in response to an applied electric field [199]. The two types of dipole moments present in materials are permanent dipole moments and induced dipole moments. The displacement of charges can give rise to polarization. The time dependence of the charging or discharging current in response to a sinusoidal field of given frequency is the essential feature of the dielectric response. The total permittivity (ϵ) of a dielectric consists of four components (in the absence of electrode effects discussed later) viz., (1) extrinsic contribution (ϵ_{ex}), (2) electronic polarizability contribution (ϵ_e), (3) ionic polarizability contribution (ϵ_n) caused by the vibration of nuclei, and (4) the contribution of the deformation of ions (ϵ_d) ie,

$$\epsilon = f(\epsilon_{ex}, \epsilon_e, \epsilon_n, \epsilon_d)$$

Generally the extrinsic contribution to the permittivity is very small since the permittivity is an intrinsic property of the constituent ions in the dielectric. The electronic contribution mainly occurs when there is a high concentration of conduction electrons and also when the ion concentration is low and nondeformable. The ionic polarizability contribution dominates in deformable fully ionic compounds for infrared and beyond frequencies. The ionic deformation contribution occurs when the ions are deformable as in oxides since oxygen ion is very deformable. Dielectric properties of thin films are due to interfacial effects and also due to effects arising from the material bulk properties. The dielectric polarization and dielectric losses in the films are briefly dealt with here.

6.2 Dielectric Polarization

A large number of polarization mechanisms are possible in thin films, irrespective of whether the films are polycrystalline or amorphous. These polarization mechanisms in general can be classified into two, viz., those due to the presence of interfaces and those which are characteristic of the material itself. The polarization mechanisms which are characteristic of the material do not

owe their existence in anyway to the interfaces. The interface effect is mainly due to the presence of concentration modifications at electrodes and at interfaces, which may occur within the film. However, in the bulk dielectric studies, these interface effects are neglected, but these may dominate in thin film structures [200].

The polarization behaviour characteristic of the material can be considered to be due to its bulk property. These include dipole and dipole-like polarization effects which result when dipolar molecules and ions are capable of occupying several closely spaced positions in a given region. Polarization mechanism arising from imperfections such as an effective dipole resulting from a cation vacancy pair is another bulk mechanism. Electronic mechanism which gives rise to effective polarization can also be categorized in this group. In thin films, the predominant electronic mechanism includes effective polarization involving internal electronic carriers such as electron transport by hopping or percolation.

At a given point in a thin film the flux density D , the macroscopic electric field E and the polarization P can be related by [201,202)

$$\epsilon_0 E = D - P \quad (6.1)$$

where ϵ_0 is the permittivity of free space. The above equation is valid only for mechanisms arising from the bulk. If the macroscopic charge density is ρ , then the interface effects can be discussed using Poisson's equation

$$\frac{\partial D}{\partial x} = \rho \quad (6.2)$$

In a static field, the static polarization will be proportional to the macroscopic field E.

In the case of thin films, for a static field, the electric flux configuration is static and only a particle current can be detected flowing in them. In this situation no information can be obtained on polarization effects from electrical measurements. Hence to probe the dielectric properties of thin films, it is necessary to study currents passing through the film in dynamic conditions. For this, the common thin film configuration employed is metal-dielectric-metal structures.

6.2.1 Interfacial Polarization

Interfacial effects, which contribute to the dielectric properties of thin film structures, arise due to the modifications near the interfaces, in the concentration of various charged species present in thin films.

Even in the absence of any DC current there can be space charge regions and built in potentials at the interfaces of the films [203-206] and these lead the analysis to more complications. In considering the AC dependence, the term involving bulk polarization is neglected. However, the particle current includes contributions from various mobile charges.

If the mobile carriers in a system are ions, the large densities required for a contribution to the effective dielectric properties can be detected by the material transport in the film in DC current [207]. This is valid irrespective of the nature of the contacts to the film, either ohmic or blocking.

In certain wide band gap dielectric thin film materials the low frequency dielectric constant is greater by several orders of magnitude than the high frequency values. This can be interpreted in terms of an effect attributable to the mobile ions and defects having their concentrations perturbed at electrode interfaces [206-209]. Thin films of ionic materials also show similar effects [210].

For many thin film materials, the possibility of band bending at the interfaces is very high. This can occur

even at zero bias [203,206,208,211-214]. If the material is amorphous there will be certain empty or filled states in the gap of the material, near the interfaces to equate the Fermi level. In an analysis of the polarization effects the existence of the concentration modifications in the region of band bending less than kT can be ignored, assuming the space charge to grow only at its edge.

The charge carriers of more interest is assumed to be electrons, the source of which is a donor level below the conduction band edge. The Fermi level is assumed to lie above the donor states. Hence a wide gap thin film material can be represented with a model which has a very few mobile electrons, but which can develop a substantial space charge region at the interfaces.

6.2.2 Polarization due to Bulk

Dielectric polarization arising from the characteristic of the thin film material is termed as polarization due to bulk. These contributions can be from permanent dipoles or from the dipole-like phenomenon for which the simple bistable configuration is applicable. Polarization in thin films arising from point defects, impurities, vacancies and even due to two centre electron hopping [209]

can be taken as bulk polarization. The polarization caused by the distortion of the spacial configuration of tightly bound electrons is also a bulk effect. The polarization can be varied by a changing field.

6.3 Dielectric Losses

Dielectric losses occur when the electric polarization in a material does not follow the varying electric field [215]. The dielectric loss is a bulk property and does not depend on the film thickness. But depending upon the defect pattern in the film, relaxation occurs. Electronic, ionic, dipole, or interfacial polarizations will contribute their characteristic relaxation processes, for dielectric losses to occur. In certain cases dielectric losses are found to decrease with the aging of the material [216].

Frequency dependence of the dielectric relaxation has been observed in thin films for a varying frequency range, from a lower range of 0.1 Hz to higher frequencies of GHz. Temperature dependence of relaxation peaks shows a shift towards higher frequencies [217]. At higher temperatures above about 473K to 673K, in some capacitor materials the film electrode may diffuse into the insulator film significantly which may produce a rapidly rising

dielectric loss [218]. However, if the mobile charge carrier density in a dielectric material is significantly high, loss peaks are not observed even at the lowest frequencies [219,220].

Interpretation of the dielectric data is mainly carried out with the help of Cole-Cole diagram. The Cole-Cole diagram is a plot of the imaginary part of the permittivity at a particular frequency against the real part of the permittivity at the same frequency [221] resulting in a semicircular graph. However, according to Jonscher [199] the Cole-Cole diagram is not the meaningful representation. The meaningful representation of dielectric data is the frequency dependence of the real and imaginary parts of the dielectric permittivity, since the semicircular graph is valid only for homogeneous systems. In the case of inhomogeneous systems the expected semicircular graph is not observed [222].

6.4 Dielectric Properties of Polymeric Solids

Many of the polymeric materials are very good dielectrics. The dielectric properties of the polymers depend on their structure. Structures with permanent dipoles are known as polar polymers and those in which

there is not any permanent dipole are called non-polar polymers. For non-polar polymers the dielectric loss is low and it varies only slightly over a wide frequency range. Permanent dipole polymers have a moderate loss at room temperature.

In a polymer the chain section consisting of a large number of monomeric units (or segments) undergoes independent movements in addition to the smaller kinetic units which are side chains or individual atomic groups. Two types of dielectric losses exist in polymers [223-225]. The first type, called the dipole-segmental loss is due to the orientational rotation of the polar units when segmental movements are possible. The second type, called the dipole-group loss is due to the orientation of the polar groups themselves. In cross linked polymers, since the segmental mobility is low, the relaxation time of dipole segmental loss is increased.

Of the two types of dipole-group losses in polymers the first type, called the dipole-segmental loss occurs at high temperature (or low frequency). It is called as α -loss peak. The second type, called as the dipole-group loss occurs at low temperature (or high frequency). This is denoted by the letter β . Sometimes

a third loss peak called as the γ -loss peak occurs at very low temperatures. In the case of a polar polymer where the polar groups are capable of orientation independently in an electric field, two dipole-group loss maxima will occur on the loss angle ($\tan \delta$) versus temperature or $\tan \delta$ vs frequency curves. As the frequency is increased $\tan \delta$ maximum shifts towards higher temperatures.

The dielectric studies of plasma polymerized thin films of styrene [75,226], acrylonitrile [6], hexamethyldisiloxane [227], hydrocarbons and fluorocarbons [228] etc. have already been reported. The work done on the dielectric properties of glow discharge polymerized paratoluidine thin film is discussed below.

6.5 Structure Fabrication and Measurement Set Up

6.5.1 Structure Fabrication

Aluminium-polymer-aluminium structures have been used for the dielectric studies. The aluminium electrodes were pre-deposited on the glass substrate from a tungsten filament in a high vacuum coating unit. After the polymer deposition the aluminium electrodes were post-deposited. The effective area of the M-P-M structure was 0.16 cm^2 .

6.5.2 Measurement Set Up

The electrical connections were made to the system using 'U' shaped small copper strips of size $1\frac{1}{2}$ cms in length, 0.5 cm in width and 0.2 cm in thickness. Cleaned thin copper foil strip was placed on the electrode film and over that small copper strip was tightened with small screws from the other side of the substrate so that the flat portion of the copper strip was in good contact with the copper foil and hence, with the film. A thin layer of silver conducting paint was pasted at the interfaces of the electrode film, copper foil and the copper strip to make better contact. Figure (6.1) shows the M-P-M structure with the contacts given.

6.5.3 Dielectric Studies

The dielectric studies were carried out in a vacuum cell having provisions for making external connections. The film system with the connections given was placed in the cell and it was evacuated to a vacuum of 10^{-2} torr. The system was then annealed at 373K for 20 minutes and allowed to cool. The system was heated externally and the temperature was noted using a chromel-alumel thermocouple. The measurements were carried out in the temperature range 303K to 473K at a fixed frequency of 1 KHz using a LCR bridge.

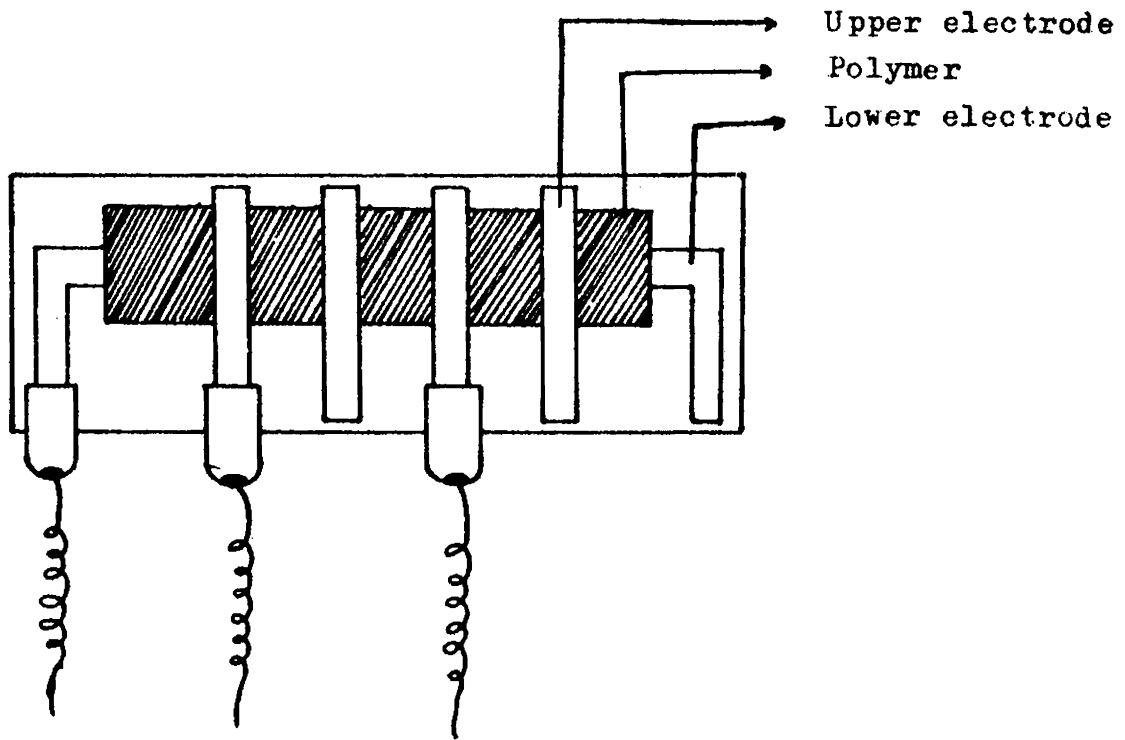


Fig.6.1 Al-P-Al Structure with contacts given.

6.6 Results

The variation of capacitance with film thickness is shown in figure (6.2). The capacitance decreases with increase of film thickness and at higher thicknesses not much variation of capacitance is observed. The film capacitance is found to increase with temperature appreciably only above 363K. Upto 363K the capacitance remains almost constant with increase of temperature. Figure (6.3) shows the capacitance versus temperature graph for a film of thickness 2400 Å. On cooling from 473K the capacitance-temperature curve retraces the same path.

Figure (6.4) shows the variation of dielectric constant with temperature for a film of thickness 3500 Å. The variation in the dielectric constant starts above 363K and above 423K it rises rapidly. The dielectric constant increases with increase of temperature above 363K upto 473K.

The observed variation in the dielectric loss factor $\tan \delta$ in the heating and cooling process is shown in figure (6.5). $\tan \delta$ is found to increase with increase of temperature and a loss peak is observed at above 423K. The cooling curve does not exactly follow the heating curve.

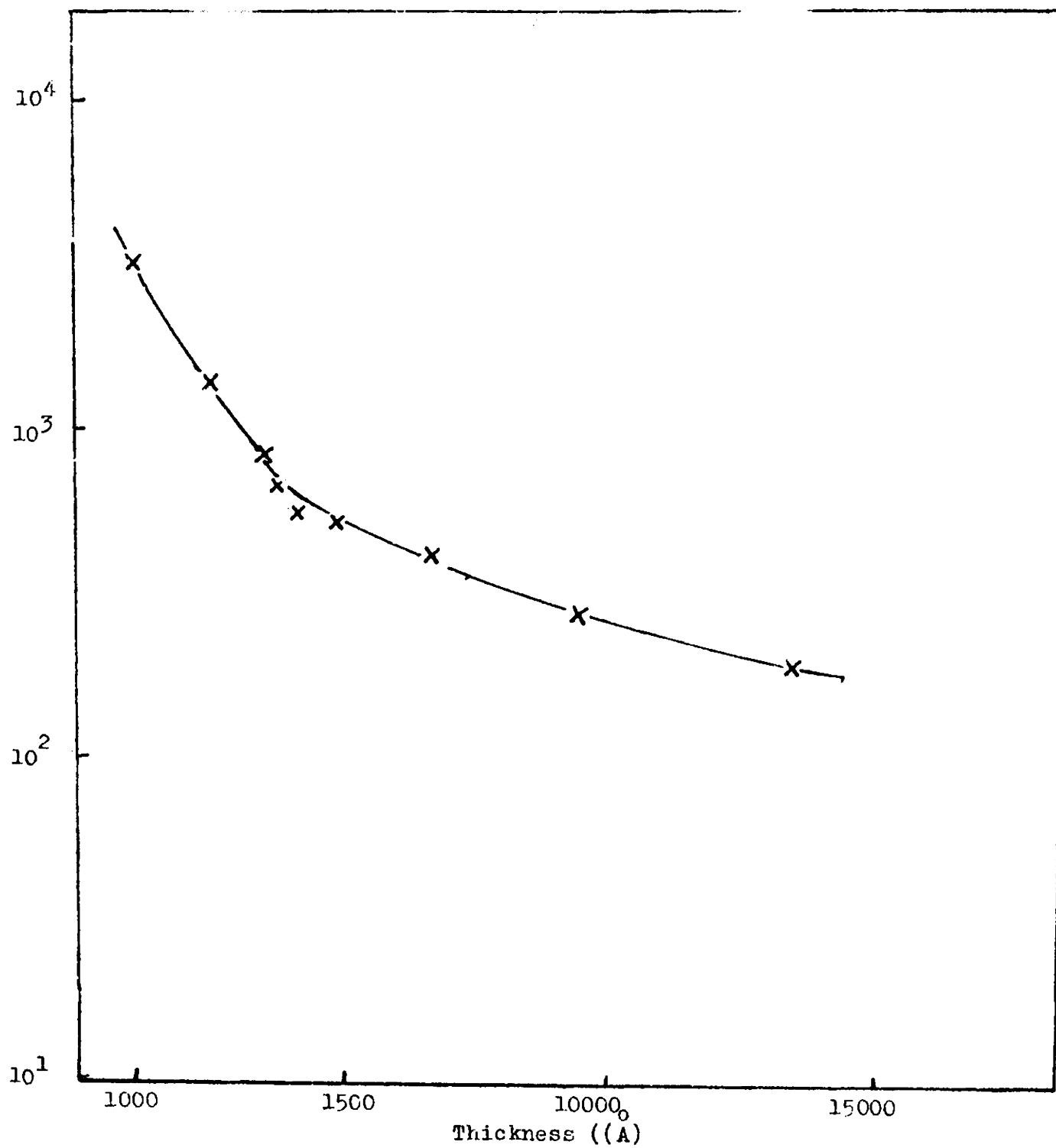


Fig.6.2 Capacitance versus film thickness plot.

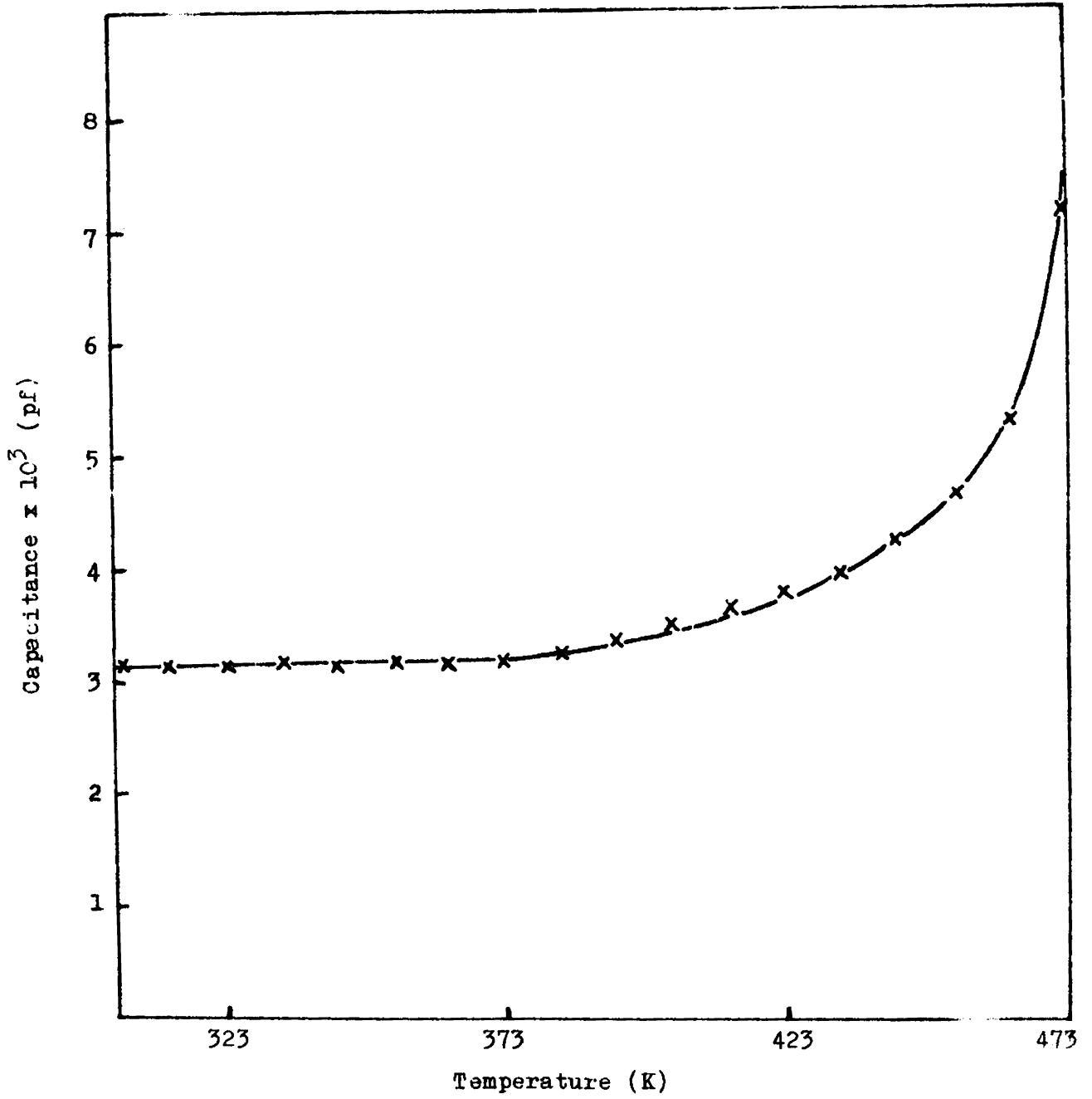


Fig.6.3 Capacitance-temperature plot ($d = 2400 \text{ \AA}$).

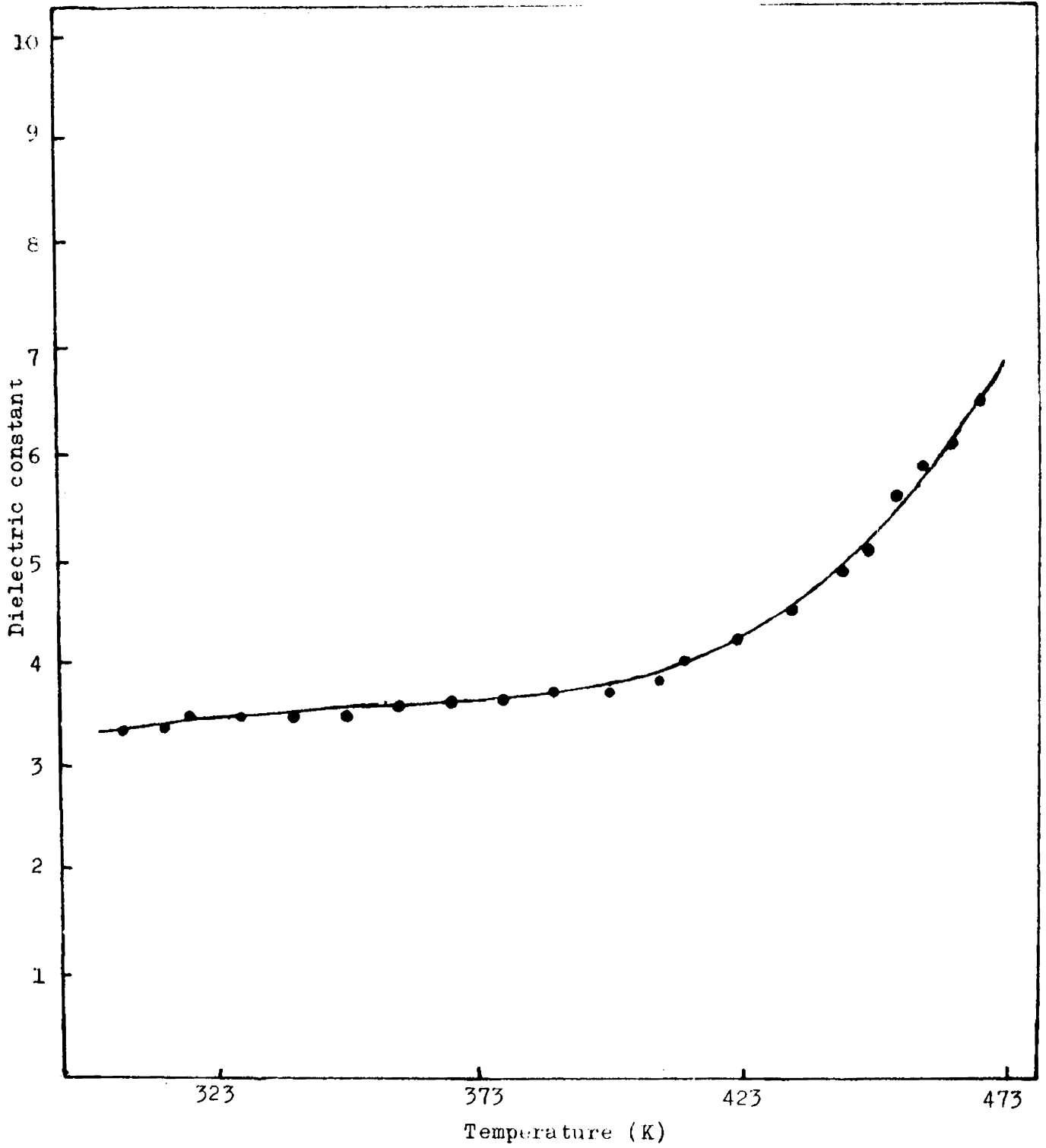


Fig.6.4 Dielectric constant-temperature characteristic ($d = 3500 \text{ \AA}$)

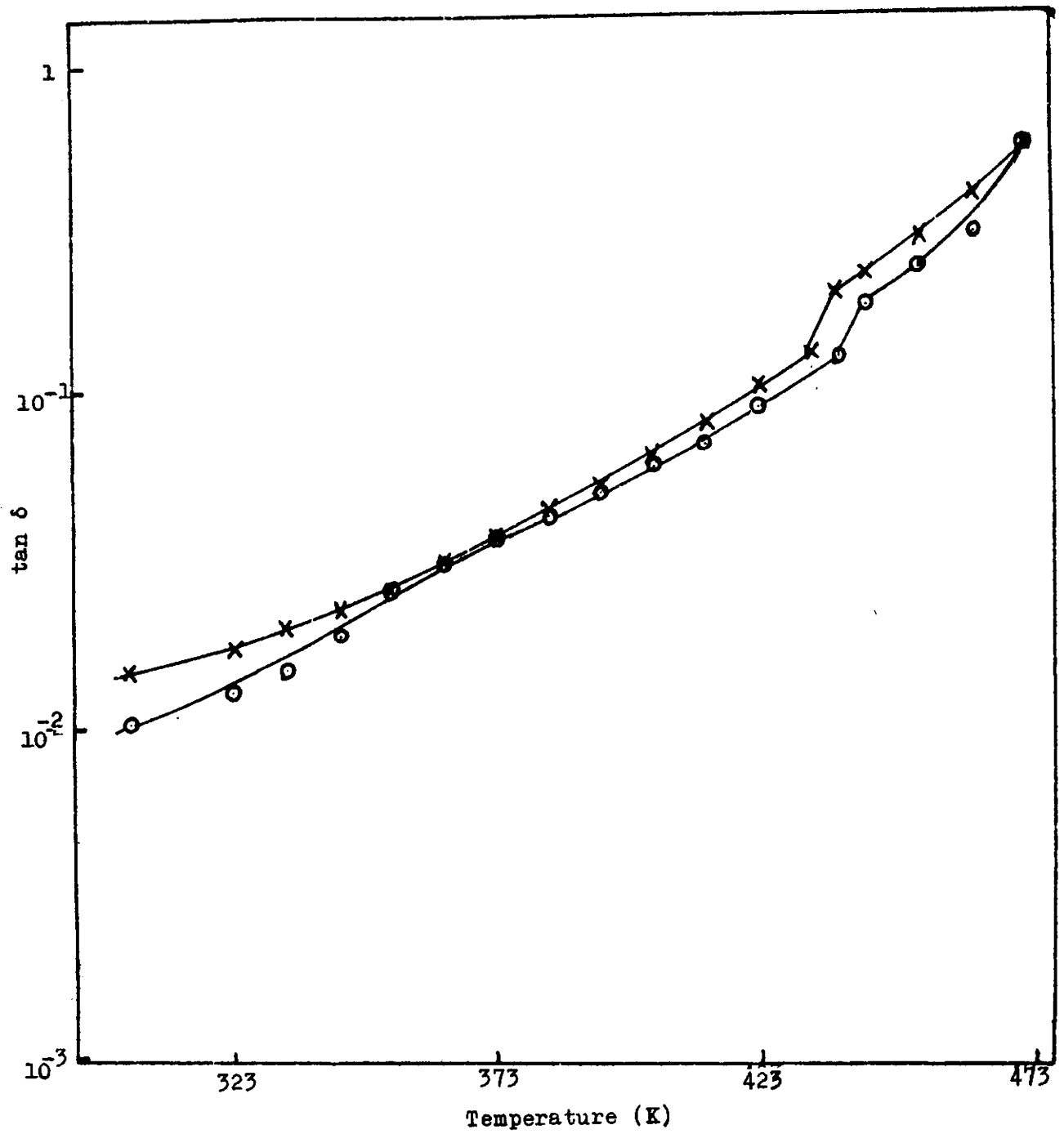


Fig.6.5 Dielectric loss-temperature characteristics.

6.7 Discussion

The thickness dependence of capacitance indicates that for thicknesses higher than 4000 Å there is not much dependence of the capacitance on the film thickness. Further in the range 1000 Å to 4000 Å of thickness, the capacitance shows a gradual decrease with thickness, the general characteristic of good dielectrics.

The dependence of the dielectric properties of polymers on the temperature is related to the nature, structure and size of the molecules and the molecular bond stability [229]. However, according to Harrop and Campbell [217], materials with dielectric constant between 2.5 and 11 will have comparable values of electronic and ionic polarizabilities and their temperature coefficient of capacitance (TCC) will be low. From the dielectric constant versus temperature curve of para-toluidine films it can be seen that the dielectric constant value suggests a combined electronic and ionic polarizabilities. At high temperatures partial removal of impurities, lattice defects etc. in the film takes place and this in turn increases the dielectric constant with increase of temperature. Also, at high temperatures the ionic contribution to the



dielectric material may be more [223] and it may increase the dielectric constant. The interfacial effects due to the electrodes as in the case of several compound semiconductors may be negligible, since the possibility of aluminium electrodes diffusing into the polymer is very small.

The $\tan \delta$ versus temperature curve shows a peak at high temperatures, which seems to be a characteristic of this polymer. Dipole-segmental losses at high temperatures may be due to the changes in crystallinity of the polymer [224]. This may also be the reason for the relaxation. The polar C-N bond connecting the polymeric units may interact with impurities in the low vacuum conditions which can change the dielectric loss, especially at high temperatures.

CHAPTER SEVEN

SPACE CHARGE LIMITED CONDUCTION IN POLYMER FILMS OF PARA-TOLUIDINE

7.1 Introduction

Polymer films are found to have high electrical resistivity and dielectric strength. Because of their peculiar properties, such as high molecular weight, material disorder etc. the electrical conduction in them is not well understood. The current conduction in insulator films is found to be valid for polymer thin films also. The DC current-voltage characteristics of some polymer films have been reported by different authors [49,106,230,231,232]. The current-voltage characteristics observed in electrodeless glow discharge polymerized para-toluidine films are discussed below.

7.2 Structure Fabrication and Measurement Set Up

7.2.1 Structure Fabrication

The electrical conduction through the polymer film of para-toluidine was investigated by analysing the current-voltage characteristics of the metal-polymer-metal (M-P-M) structures deposited on well cleaned glass

substrates. The metal used as electrode films was aluminium (99.999%) which was deposited by thermal evaporation from a tungsten filament in a high vacuum coating unit.

In order to fabricate the metal-polymer-metal systems of pre-decided area and shape, well defined masks of freshly cleaved mica sheet were used. The aluminium electrodes used had a thickness of about 1500 Å. After depositing the bottom aluminium electrode the polymer film was deposited over it using suitable masks. Then the top aluminium electrode was deposited so that the effective area of the aluminium-polymer-aluminium was 1.2cm x 1.2cm (Fig. 7.1).

7.2.2 Measurement Set Up

The electrical contacts were given to the system using 'U' shaped copper strips as described in chapter six. The electrical measurements were carried out after keeping the system in a vacuum cell which was evacuated to a vacuum of 10^{-2} torr. The vacuum cell was perfectly shielded. (It has got provisions for external connections).

7.2.3 Current-Voltage Measurements

For current-voltage (I-V) measurements a DC supply of 9V (dry cell) was used. The current through

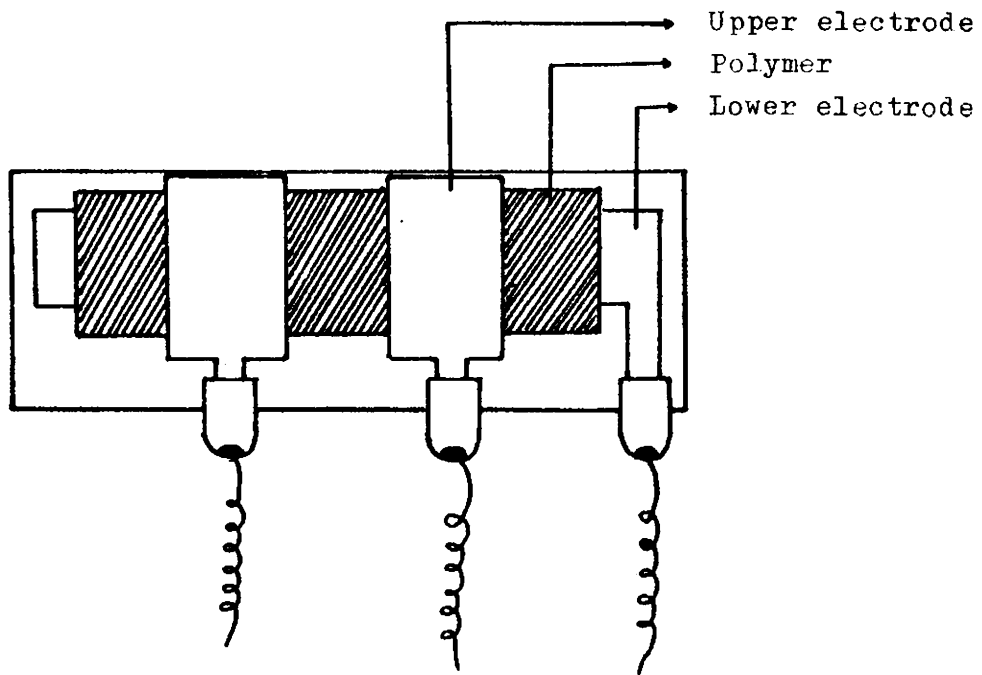


Fig.7.1 Al-P-Al Structure with contacts used for I-V characteristics studies.

the film was measured using an Electrometer. The voltage across the specimen was measured with a high impedance multimeter. The current-voltage characteristics of films of different thicknesses (500 Å to 3700 Å) were drawn.

7.3 Results

In the current-voltage characteristics of aluminium-polymer-aluminium (Al-P-Al) structures four types of conduction regions are observed. In the first conduction region the current through the film is found to be proportional to the applied voltage ($I \propto V$) satisfying the Ohm's law. The current-voltage (log-log scale) characteristic of a Al-P-Al system of polymer film of thickness 3590 Å is shown in figure (7.2). The ($I \propto V$) region is followed by another conduction region where the current is found to vary as the square of the voltage ($I \propto V^2$). In this region, which is called as the square law region the current shows an inverse cube dependence on the film thickness ($I \propto d^{-3}$). The log I versus film thickness in the square law region is shown in figure (7.3). Beyond the square law region lies a third region, where the current increases more or less steeply with the increase of voltage. The current in this region

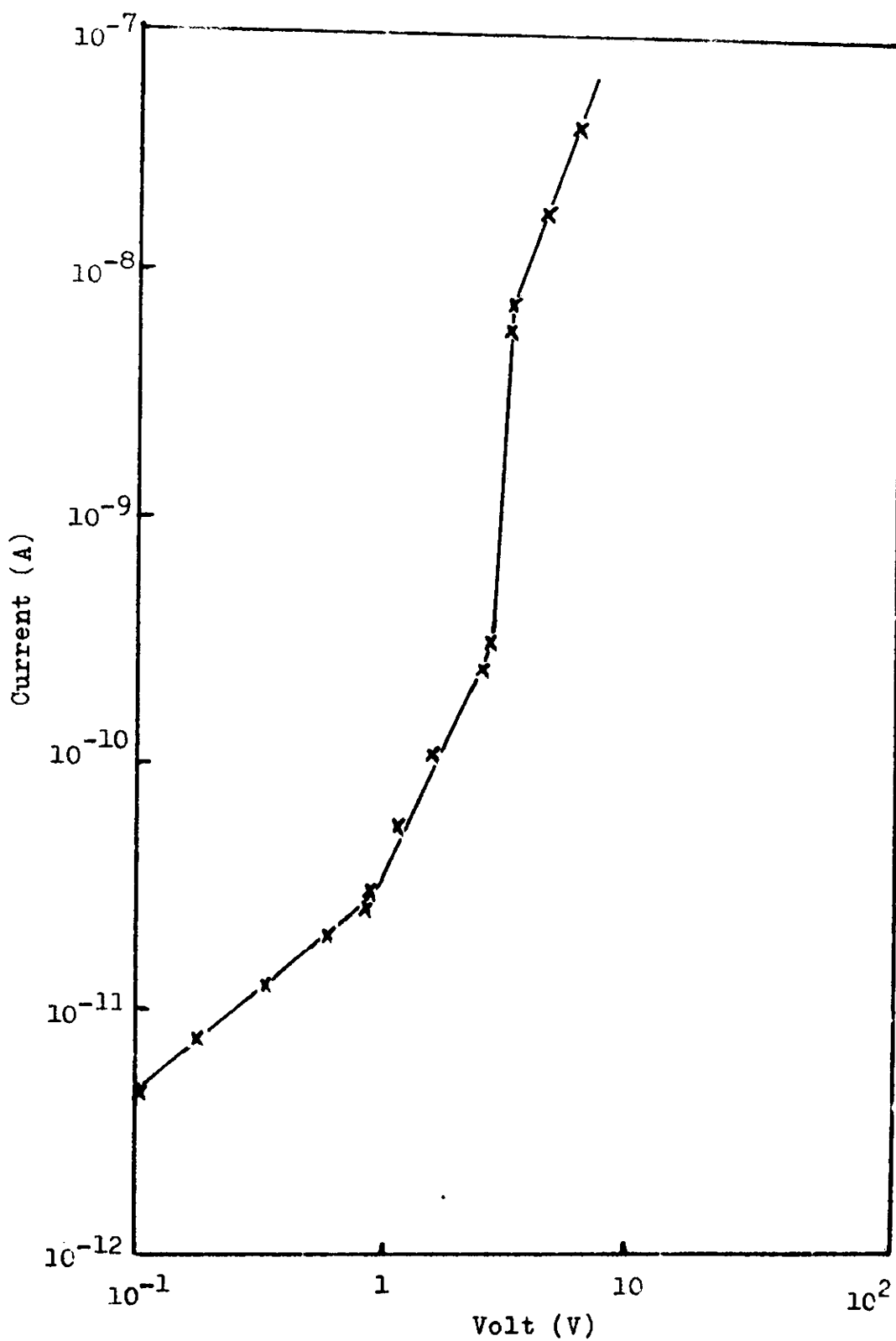


Fig.7.2 Current-voltage characteristics of polymerized p-toluidine film ($d = 3590 \text{ \AA}$).

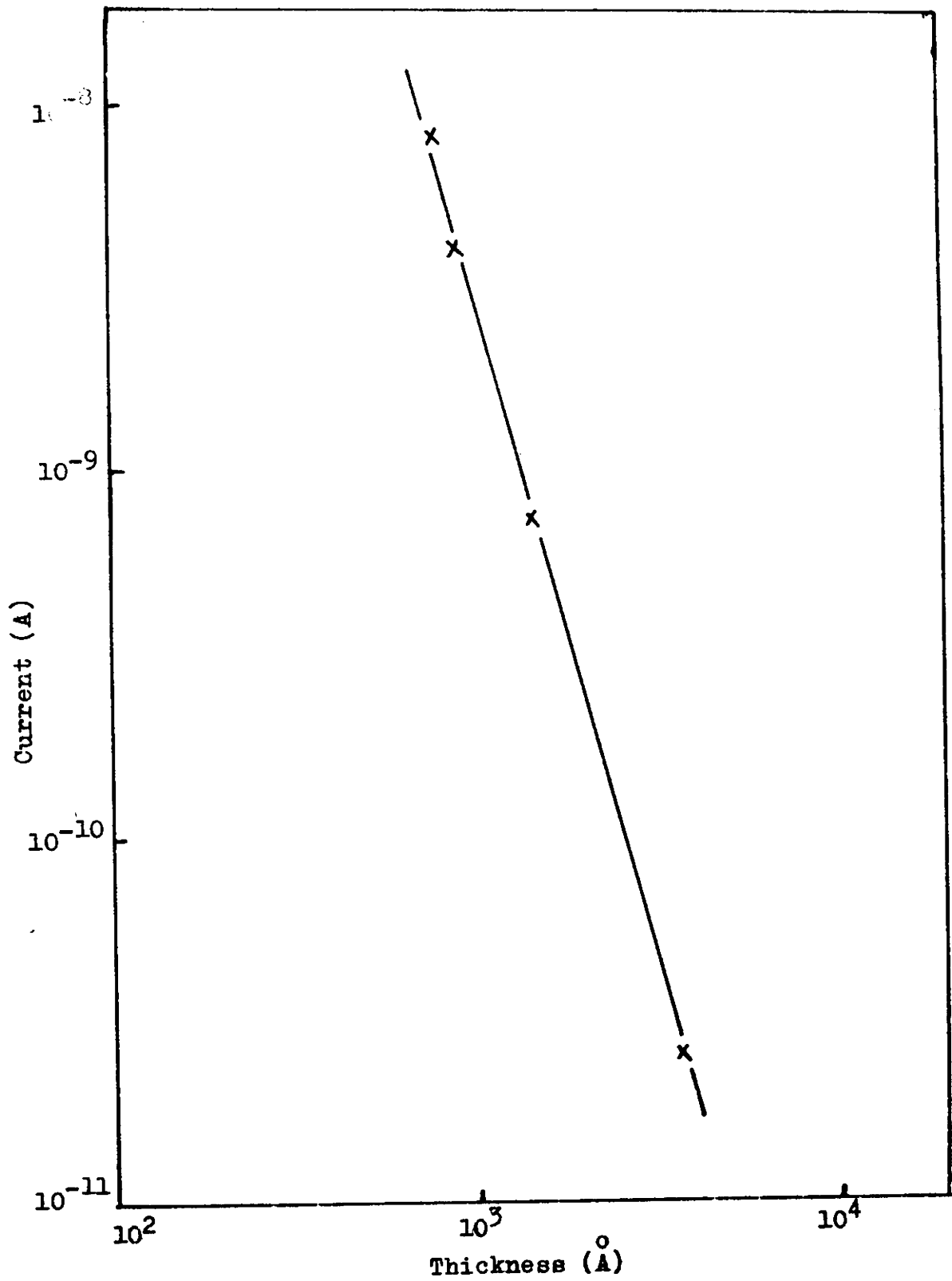


Fig.7.3 Current versus film thickness in the square law region.

is found to vary to some power 'n' of the voltage ($I \propto V^n$), n being 7 to 8. This region is followed by another conduction region where the current varies in a similar fashion as in square law region and the current is proportional to voltage as ($I \propto V^{2.5}$).

The current-voltage characteristic of a film of thickness 790 Å is shown in figure (7.4). In this case only three conduction regions are observed.

The transition from one conduction region to another is exactly located by extrapolating the curve in different regions. By finding the different transition voltages, the trap density, the carrier concentration and the energy of trap level can be determined.

7.4 Discussion

The current-voltage characteristics of the films (Figures 7.2 and 7.4) show an ohmic region at low voltages which is characterised by the ($I \propto V$) nature. The square law region, followed by the steep increase in current suggests that space charge limited conduction is predominant in the system. The thickness dependence of current in the square law region showing an inverse cube dependence (Figure 7.3) is a clear evidence of space charge limited

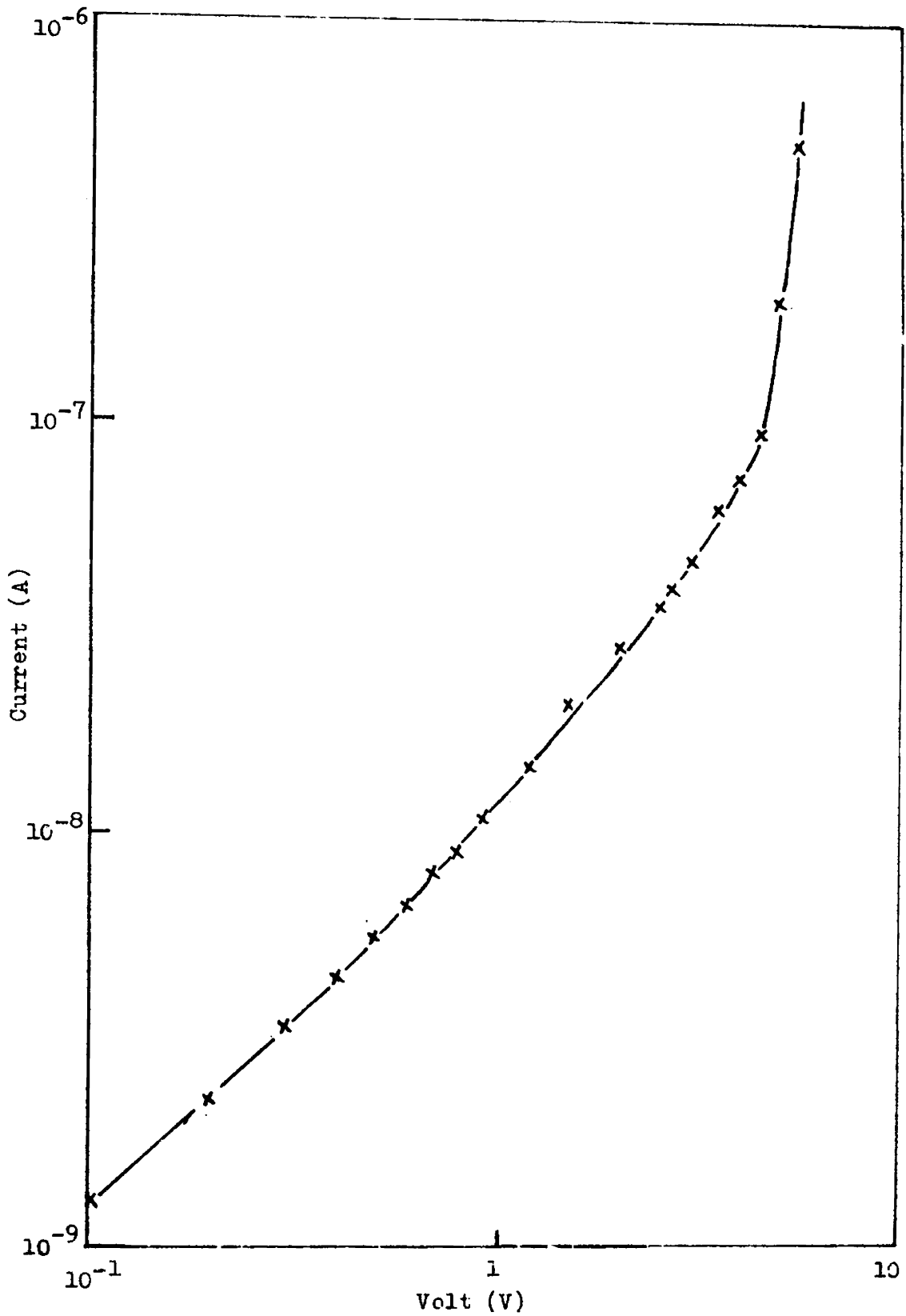


Fig.7.4 Current-voltage characteristics of polymerized p-toluidine film ($d = 790 \text{ \AA}$).

(SCL) conduction, since the SCL current density, according to Lampert [133] is

$$J \propto V^2/d^3 \quad (7.1)$$

The region where the sharp increase in current occurs can be taken as the trap filled limit (TFL) region. The square law region beyond the TFL region is the trap free square law region. This region is not observed in thin films of thicknesses less than 900 Å since breakdown occurs.

Knowing the cross over voltage from Ohm's law region to the square law region and from the square law region to the trap filled region, the trap density, density of carriers and the trap energy level are calculated. According to Lampert and Mark [124], for a thin film sandwiched between metal electrodes, the trap density N_t can be written in practical units as

$$N_t = \frac{1.1 \times 10^6 \epsilon V_{TFL}}{d^2} \text{ cm}^{-3} \quad (7.2)$$

where V_{TFL} is the trap filled limit voltage, d is the thickness of the insulator and ϵ is its dielectric constant. The dielectric constant of the polymer film has already

been reported [134]. The trap density is calculated for films of different thicknesses and the average value of N_t obtained is $6.17 \times 10^{16} \text{ cm}^{-3}$

The factor θ (ratio of the number of free electrons (n_0) in the conduction band and the total electron density ($n_0 + N_t$)) is found out experimentally as the ratio of the current (I_1) at the beginning and that (I_2) at the end of the TFL region [230]. The value of θ obtained in the present investigation is

$$\theta = I_1/I_2 = 3.5 \times 10^{-2}$$

The value of θ is used for determining the carrier concentration n_0 in the polymer film using the formula

$$n_0 = (\epsilon\epsilon_0\theta/ed^2)V_x \quad (7.3)$$

where ϵ_0 is the permittivity of free space, e is the electronic charge and V_x is the cross over voltage from the Ohm's law region to the square law region. The carrier concentration thus obtained is $n_0 = 4.7 \times 10^{15} \text{ cm}^{-3}$.

The trap energy level E_t is calculated using the formula [124]

$$E_t = kT \ln\left(\frac{N_c}{\theta g N_t}\right) \quad (7.4)$$

where k is the Boltzmann's Constant, T , the temperature, N_c , the density of states in the conduction band and g , the degeneracy factor. The value of N_c is taken as 10^{20} cm^{-3} . The calculated value of trap depth for films of different thicknesses is $E_t = 0.31 \text{ eV}$. This indicates that there exists an electron trap at 0.31 eV below the bottom edge of the conduction band in glow discharge polymerized para-toluidine films. This trap can be considered as shallow since it lies above the Fermi level of the material close to the conduction band.

Similar space charge limited conduction in polymer thin films and semiconductor films have been reported by other workers. This analysis of SCL conduction is an efficient tool to characterize the material and to determine the energy band picture with different localized trap levels of the material.

CHAPTER EIGHT
SUMMARY AND CONCLUSION

8.1 Summary

Silver sulphide films have been prepared by a chemical method in which silver nitrate solution and hydrogen sulphide gas are used as the reagents and the film is formed on the liquid-gas interface in an enclosure. The darkish brown silver sulphide thus formed is found to be n-type semiconductor at room temperature. The electrical resistance of the silver sulphide films in the temperature range 303K to 473K has been studied. It has been observed that there exist two conduction regions and in between them is a transition region. The resistance decreases with increase of temperature in the first conduction region and in this region the conduction mechanism is ionic. The value of activation energy determined in this region is found to be 0.633 eV. Silver sulphide exists in β -form in the ionic conduction region. In the second conduction region the resistance is found to be almost independent of temperature and conduction in this region is mainly electronic and silver sulphide exists in α -form in this region. The transition

from ionic to electronic conduction is found to occur in a temperature range of 25°C at about 450K. In the electronic conduction region the activation energy is found to be very low and it shows a thickness dependence. The temperature coefficient of resistance has been determined for the temperature range studied. The temperature coefficient is found to decrease with increase of temperature. Also it decreases with increase of film thickness in the first conduction region. In the second conduction region the temperature coefficient of resistance is found to be independent of film thickness.

Ferric hydroxide films have been prepared by the chemical method involving the chemical reaction between ferrous sulphate solution and ammonia gas. Ferrous hydroxide thus formed, easily oxidizes to ferric hydroxide and it has got a brown colour. X-ray diffraction study reveals that the film is amorphous in nature. On heating the film at 723K it decomposes to ferric oxide. The percentage of ferric ion in ferric oxide has been determined by colourimetric estimation and is found to be 58.2%. The conduction in ferric hydroxide and ferric oxide film has been studied in the temperature range from room temperature to 473K. At high temperatures the resistance of ferric hydroxide is

found to decrease with increase of temperature and the conduction is due to the intrinsic defects and the activation energy has been determined to be about 0.36 eV for a 340 Å^o thick film. On the other hand at low temperatures the activation energy is found to be very low and the conduction is attributed to the impurity charge carriers. The activation energy is found to decrease with increase of film thickness. The conduction in ferric oxide is found to be complicated.

The electrodeless glow discharge method is found to be a powerful technique for preparation of polymer thin films. These films are found to be good dielectrics because of their insulating nature. The glow discharge polymerized films are superior in all respects to the conventional polymers. These films are characterized by their pin-hole free nature, high field electrical properties, high thermal stability, good adhesion to the substrate and chemical inertness.

A set up has been fabricated to produce polymer films by electrodeless glow discharge method. A radio-frequency oscillator of required power has been constructed. It oscillates at a frequency of about 4.5 MHz and it has been used as the power source for polymerization. The

power from the oscillator is coupled to the discharge tube by capacitor coupling. Polymer films of para-toluidine have been successfully produced by the electrodeless glow discharge set up. The polymer films thus produced are brown in colour and they show good adhesion to glass and sodium chloride substrates. They are found to be chemically inert. These films show high thermal stability. The insolubility and high stability of the polymer films indicate the presence of cross links in them. From infra-red studies, the polymerization is found to take place through hydrogen abstraction. The probable structure of the polymer unit is thus deduced.

The dielectric properties of the polymer films sandwiched between aluminium electrodes have been studied. In the dielectric studies the variation of capacitance, dielectric constant and dielectric loss with temperature in the range 303K to 473K and the variation of capacitance with film thickness have been carried out at a fixed frequency of 1 KHz. The capacitance and dielectric constant are found to be almost unchanged upto 363K and then they start to increase with increase of temperature. After 413K they show a marked increase upto 473K. The dielectric loss is found to increase with increase of

temperature and a loss peak is observed at temperature above 423K. The relaxation peak observed at high temperature is attributed to the dipole-segmental loss occurring in the polymer film. The nature of dielectric constant value obtained for polymer films of para-toluidine suggests that the contribution to permittivity is from electronic and ionic polarizabilities. The capacitance of the film is found to decrease with increase of film thickness.

The DC conduction in polymer films is analysed by studying the current-voltage characteristics of aluminium-polymer-aluminium structures. At low applied fields the films show ohmic conduction and at high fields non-ohmic behaviour is observed. The current through the film is found to be proportional to the square of the voltage and the inverse cube of the film thickness, i.e., ($I \propto V^2/d^3$), suggesting space charge limited conduction. Beyond the space charge limited conduction region, the trap filled limit region and then the trap free square law region are observed. The parameters such as carrier concentration, density of traps and energy of trap level are determined. The carrier concentration is obtained as $n_0 = 4.7 \times 10^{15} \text{ cm}^{-3}$ and the trap density as $N_t = 6.17 \times 10^{16} \text{ cm}^{-3}$. The value obtained for trap energy level is, $E_t = 0.31 \text{ eV}$ which indicates that an electron

trap exists at 0.31 eV below the bottom edge of the conduction band. This trap can be considered as shallow since it lies above the Fermi level close to the conduction band.

8.2 Conclusion

The chemical method used to prepare silver sulphide and ferric hydroxide films is rather simple. The silver sulphide films thus prepared have properties similar to those of the films prepared by other standard methods. As no work has been found to be reported on ferric hydroxide films, the method adopted in the present investigation can be used for producing such films. Compound thin films of many materials can be prepared by this method with less elaborate procedure.

In the glow discharge plasma, ions and free radicals are produced which may initiate the polymerization and they recombine with monomeric units to form polymer films on the substrates. The intermolecular arrangements of the chemical bonds result in different polymer structures. The presence of crosslinks has been well established in glow discharge polymerized films

as the molecular fragments undergo high energy bombardment in the plasma. Both the ionic and radical polymerization mechanisms have been found to take place in polymerization process.

The polymerization of para-toluidine is found to take place by hydrogen abstraction and polymer units are linked by polar C-N bonds. The high stability and chemical inertness of the polymer films support the presence of cross linking.

The appearance of $\tan \delta$ peak at a particular temperature is due to dipole-segmental losses. The dielectric loss is found to be low for this polymer. The dielectric constant remains almost constant over a wide temperature region. The space charge limited conduction helps to characterize the material and to determine the energy band picture with different localized trap levels of the material.

On comparing the properties of the films with those of high quality films, it has been observed that the polymer films produced by the glow discharge have got desirable properties which qualify them in technological applications.

REFERENCES

- [1] M. Faraday, Philos. Trans. Roy. Soc. London, 147, 145 (1857)
- [2] R. Pohl and P. Pringsheim, Verhandl. Deut. Physik Ges., 14, 546 (1912)
- [3] Y. Tarui, H. Teshima, K. Okura and A. Minamiya, J. Electrochem. Soc., 110, 1167 (1963)
- [4] S.D. Sathaye and A.P.B. Sinha, Thin Solid Films, 37, 15 (1976)
- [5] A.K. Jonscher, in C.H.S. Dupuy and A. Cachard (eds.), "Physics of Non-Metallic Thin Films", Plenum Press, New York (1974)
- [6] T. Hirai and O. Nakada, Japan J. Appl. Phys., 7, 112 (1968)
- [7] S. Morita, T. Mizutani and M. Ieda, Japan J. Appl. Phys., 10, 1275 (1971)
- [8] M. Millard, in J.R. Hollahan and A.T. Bell (eds.), "Techniques and Applications of Plasma Chemistry", John Wiley and Sons, New York (1974)
- [9] Y. Segui and Bui Ai, Thin Solid Films, 50, 321 (1978)
- [10] H. Carchano and M. Valentin, Thin Solid Films, 30, 351 (1975)

- [11] K.L. Chopra, "Thin Film Phenomena", McGraw-Hill, New York, (1969) Ch.1.
- [12] L. Holland, "Vacuum Deposition of Thin Films", Chapman and Hall, London (1963)
- [13] R.W. Berry, P.M. Hall and M.T. Harris, "Thin Film Technology", Van Nostrand, New York (1963)
- [14] L.I. Maissel and R. Glang (eds.), "Hand Book of Thin Film Technology", McGraw-Hill, New York (1970)
- [15] D.S. Campbell, in J.C. Anderson (ed.), "The Use of Thin Films in Physical Investigations", Academic Press, London (1966)
- [16] D.S. Campbell, in C.H.S. Dupuy and A. Cachard (eds.), "Physics of Non-Metallic Thin Films", Plenum Press, New York (1976)
- [17] B.N. Chapman and J.C. Anderson (eds.), "Science and Technology of Surface Coatings", Academic Press, London (1974)
- [18] H. Schäfer, "Chemical Transport Reactions", Academic Press, New York (1964)
- [19] P.J. Jorgenson, J. Chem. Phys., 37, 874 (1962)
- [20] W.M. Feist, S.R. Steele and D.W. Readey, in G. Hass and R.F. Thun (eds.), "Physics of Thin Films", vol.5, Academic Press, New York (1969)

- [21] J.C. Viguie, in B.N. Chapmann and J.C. Anderson (eds.), "Science and Technology of Surface Coatings", Academic Press, London (1974)
- [22] J.E. Mee, J.L. Archer, R.H. Meede and T.N. Hamilton, Appl. Phys. Letters, 10, 289 (1967)
- [23] B.A. Joyce, in J.C. Anderson (ed.), "The Use of Thin Films in Physical Investigations", Academic Press, London, (1966) p.87
- [24] S.R. Bhole and A. Mayer, RCA Rev., 24, 511 (1963)
- [25] K.R. Lawless, J. Vacuum Sci. Tech., 2, 24 (1965)
- [26] K.R. Lawless, in G. Hass and R.E. Thun (eds.), "Physics of Thin Films", Vol.4, Academic Press, New York (1967)
- [27] D.S. Campbell, in L.I. Maissel and R. Glang (eds.), "Hand Book of Thin Film Technology", McGraw-Hill, New York (1970)
- [28] J.S. Hendy, H.D. Richards and A.W. Simpson, J. Mater. Sci., 1, 127 (1966)
- [29] L. Young, "Anodic Oxide Films", Academic Press, New York (1961)
- [30] C.J. Dell'Oca, D.L. Pulfey and L. Young, in M.H. Francombe and R.W. Hoffmann (eds.), "Physics of Thin Films", Vol.6, Academic Press, New York (1971)
- [31] N.R. Pavaskar, C.A. Menezes and A.P.B. Sinha, J. Electrochem. Soc., 124, 743 (1977)

- [32] I. Langmuir, *Trans. Faraday Soc.*, 15, 62 (1920)
- [33] K.B. Blodgett, *J. Amer. Chem. Soc.*, 56, 495 (1934);
57, 1007 (1935)
- [34] K.B. Blodgett and I. Langmuir, *Phys. Rev.*, 51, 964
(1937)
- [35] V.K. Srivastava, in G. Hass, M.H. Francombe and
R.W. Hoffmann (eds.), "Physics of Thin Films",
Vol.7, Academic Press, New York (1973)
- [36] L. Holland, *Brit. J. Appl. Phys.*, 9, 410 (1958)
- [37] T. Putner, *Brit. J. Appl. Phys.*, 10, 332 (1959)
- [38] H.E. Bennett and J.M. Bennett, in G. Hass and
R.E. Thun (eds.), "Physics of Thin Films",
Vol.4, Academic Press, New York (1967)
- [39] A. Raave, "Organic Chemistry of Macromolecules",
Marcel Dekker, New York (1967)
- [40] R.B. Seymour, "Introduction to Polymer Chemistry",
McGraw-Hill, Tokyo (1971)
- [41] A. Tager, "Physical Chemistry of Polymers", Mir (Pub.),
(1978)
- [42] F.W. Billmeyer Jr., "Textbook of Polymer Science",
John Wiley and Sons, New York (1970)
- [43] P.J. Flory, "Principles of Polymer Chemistry",
Cornell Univ. Press, New York (1953)
- [44] H. Mark and G. Safford in Whitby (ed.), "Collected
Papers of Wallace Hume Carothers on High
Polymeric Substances", New York (1940)

- [45] A. Kumar and S.K. Gupta, "Fundamentals of Polymer Science and Engineering", McGraw-Hill (1978)
- [46] L.V. Gregor, in G. Hass and R.E. Thun (eds.), "Physics of Thin Films", Vol.3, Academic Press, New York (1966)
- [47] H. Melville, Proc. Roy. Soc. (London) A163, 511 (1973); A167, 99 (1938)
- [48] D.J. Valley and J.S. Wagner, IEEE Trans., CP-11, 205 (1964)
- [49] R.W. Christy, J. Appl. Phys., 31, 1680 (1960)
- [50] H. Kenig and G. Helwig, Z. Physik, 129, 1491 (1951)
- [51] M. Hudis, in J.R. Hollahan and A.T. Bell (eds.), "Techniques and Applications of Plasma Chemistry", John Wiley and Sons (1974)
- [52] M. Tibbet, A.T. Bell and M. Shen, in M. Shen (ed.), "Plasma Chemistry of Polymers", Marcel Dekker, New York (1976)
- [53] K.L. Chopra, J. Appl. Phys., 40, 906 (1969)
- [54] K.L. Chopra, A.C. Rastogi and G.L. Malhotra, Thin Solid Films, 24, 125 (1974)
- [55] A.C. Rastogi and K.L. Chopra, Thin Solid Films, 26, 61 (1975)
- [56] P.W. Palmberg, T.N. Rhodin and C.J. Todd, Appl. Phys. Letters, 11, 33 (1967)

- [57] F.E. Cariou, D.J.Valley and W.E. Loeb, IEEE Trans. PMP-1, 554 (1965)
- [58] P.P. Luff and M. White, Vacuum, 18, 437 (1968)
- [59] W. De Wilde, Thin Solid Films, 24, 101 (1974)
- [60] R.D. Collins, P. Fiveashand and L. Holland, Vacuum, 19, 113 (1969)
- [61] R. Harrop and P.J. Harrop, Thin Solid Films, 3, 109 (1969)
- [62] D.J. Morrison and T. Robertson, Thin Solid Films, 15, 87 (1973)
- [63] J.N. Jackson, Thin Solid Films, 5, 209 (1970)
- [64] H. Biederman, S.M. Ojha and L. Holland, Thin Solid Films, 41, 329 (1977)
- [65] K.G. Budinski, J. Vac. Sci. Technol., 12, 786 (1975)
- [66] L. Holland, H. Biederman and S.M. Ojha, Thin Solid Films, 35, L19 (1976)
- [67] P. White, J. Phys. Chem., 67, 2493 (1963)
- [68] M. White, Proc. Chem. Soc., 337 (1961)
- [69] T.T. Jones and H.W. Melville, Proc. Roy. Soc. London, 25 (1946)
- [70] P.R. Emtage and W. Tantraporn, Phys. Rev. Letters, 8, 267 (1962)
- [71] R.W. Christy, J. Appl. Phys., 35, 2179 (1964)
- [72] A.E. Ennos, Brit. J. Appl. Phys., 5, 27 (1954)

- [73] L. Holland and L. Laurenson, *Vacuum*, 14, 325 (1964)
- [74] I. Haller and P. White, *J. Phys. Chem.*, 67, 1784 (1963)
- [75] M. Stuart, *Nature*, 199, 59 (1963)
- [76] A.E. Brennemann and L.V. Gregor, *J. Electrochem. Soc.*, 112, 1194 (1965)
- [77] M. Millard, in J.R. Hollahan and A.T. Bell (eds.), "Techniques and Applications of Plasma Chemistry", Wiley, New York (1974) (Same as Ref.8)
- [78] A. Bradley and J.F. Hammes, *J. Electrochem. Soc.*, 110, 15 (1963)
- [79] H. Suhr, in J.R. Hollahan and A.T. Bell (eds.), "Techniques and Application of Plasma Chemistry", Wiley, New York (1974)
- [80] R.L. McCarthy, *J. Chem. Phys.*, 22, 1360 (1954)
- [81] T. Williams and M.W. Hayes, *Nature*, 209, 769 (1966)
- [82] A.R. Westwood, *Eur. Polymer J.*, 7, 377 (1971)
- [83] J. Stachura and S. Veis, *Acta Phys. Slov.*, 29, 91 (1979)
- [84] A.R. Denaro, P.A. Owens and A. Crawshaw, *Eur. Polymer J.*, 4, 93 (1968)
- [85] A.R. Westwood, *Polymer. Prepr. Am. Chem. Soc. Div. Polymer Chem.*, 10, 433 (1969)
- [86] T. Williams and M.W. Hayes, *Nature*, 216, 614 (1967)
- [87] H. Yasuda and C.E. Lamaze, *J. Appl. Polym. Sci.*, 15, 2277 (1971)

- [88] M. Millard, J.J. Windle and A.E. Pavlvath, *J. Polym. Sci.*, 17, 2501 (1973)
- [89] J.R. Hollahan and R.P. McKeever, *Advan. Chem. Ser.*, 80, 272 (1969)
- [90] J.P. Wightman and N.J. Johnston, *Advan. Chem. Ser.*, 80, 322 (1969)
- [91] D.D. Neiswender, *Advan. Chem. Ser.*, 80, 338 (1969)
- [92] L.F. Thompson and K.G. Mayhan, *J. Appl. Polym. Sci.*, 16, 2291 (1972); 16, 2317 (1972)
- [93] R.A. Connell and L.V. Gregor, *J. Electrochem. Soc.*, 112, 1198 (1965)
- [94] J.K. Stille, R.L. Sung and J. Vander Kooi, *J. Org. Chem.*, 30, 3116 (1965)
- [95] J.K. Stille and C.E. Rix, *J. Org. Chem.*, 31, 1591 (1966)
- [96] F.J. Dinan, S. Fridmann and P.J. Schirmann, *Advan. Chem. Ser.*, 80, 289 (1969)
- [97] H. Yasuda and C.E. Lamaze, *J. Appl. Polym. Sci.*, 16, 595 (1972)
- [98] A. Streitwieser, Jr., and H.R. Ward, *J. Am. Chem. Soc.*, 85, 539 (1963)
- [99] H. Yasuda, in M. Shen (ed.), "Plasma Chemistry of Polymers", Marcel Dekker, New York (1976)
- [100] H. Yasuda and C.E. Lamaze, *J. Appl. Polym. Sci.*, 17, 137 (1973); 17, 1519 (1973); 17, 1533 (1973)

- [101] H. Yasuda, M.O. Bumarnér and J.J. Hillman, J. Appl. Polym. Sci., 19, 531 (1975)
- [102] S. Tolansky, "Multiple Beam Interferometry of Surfaces and Films", Oxford Univ. Press, London (1948)
- [103] S. Tolansky, "Surface Microtopography", Intersciences Pub., Inc, New York (1960)
- [104] D.R. Lamb, "Electrical Conduction Mechanisms in Thin Insulating Films", Methuen and Co., London (1967)
- [105] M.E. Baird, Rev. Mod. Phys., 40, 219 (1968)
- [106] M. Kusaki, K. Sugiyama and M. Ieda, J. Appl. Phys., 42, 3388 (1971)
- [107] D.A. Seanor, J. Polym. Sci., A-2 6, 463 (1968)
- [108] J.G. Simmons, in L.I. Maissel and R. Glang (eds.), "Hand Book of Thin Film Technology", McGraw-Hill, New York (1970)
- [109] I.N. Sclar and E. Burstein, Phys. Chem. Solids, 2, 1 (1957)
- [110] E.J. Ryder, I.M. Ross and D.A. Kleinmenn, Phys. Rev., 95, 1342 (1954)
- [111] S.H. Koenig and G.R. Gunther-Mohr, Phys. Chem. Solids, 2, 268 (1957)
- [112] W. Kaiser and G.H. Wheatly, Phys. Rev. Letters, 3, 334 (1959)

- [113] M. Glicksman and M.C. Steele, Phys. Rev., 110, 1204
(1958)
- [114] K.L. Chopra, "Thin Film Phenomena", McGraw-Hill
(1969), Chs. 7 and 8
- [115] W. Schottky, Physik Z., 15, 872 (1914)
- [116] J.G. Simmons, J. Appl. Phys., 35, 2472 (1964)
- [117] R.H. Fowler and L. Nordheim, Proc. Roy. Soc. London,
A119, 173 (1928)
- [118] H.H. Poole, Philos. Mag., 32, 112 (1916)
- [119] H.H. Poole, Philos. Mag., 34, 195 (1917)
- [120] J. Frenkel, Tech. Phys., 5, 685 (1938)
- [121] J. Frenkel, Phys. Rev., 54, 647 (1938)
- [122] A.K. Jonscher, Thin Solid Films, 1, 213 (1967)
- [123] M.A. Lampert, Rept. Progr. Phys., 27, 329 (1964)
- [124] M.A. Lampert and P. Mark, "Current Injection in
Solids", Academic Press, London (1970)
- [125] A. Rose, RCA Rev., 12, 362 (1951)
- [126] A. Rose, Phys. Rev., 97, 1539 (1955)
- [127] N.F. Mott and R.W. Gurney, "Electronic Processes in
Ionic Crystals", Dover Pub., New York (1940)
- [128] R.H. Parmenter and W. Ruppel, J. Appl. Phys., 30,
1548 (1959)
- [129] M.A. Lampert, A. Rose and R.W. Smith, J. Appl. Chem.
Solids, 8, 484 (1959)

- [130] H.A. Pohl, in J.D. Mackenzie (ed.), "Modern Aspects of the Vitreous State", Vol.2, Butterworths, London (1962)
- [131] H.A. Pohl, in J.E. Katon (ed.), "Organic Semiconducting Polymers", Marcel Dekker, New York (1968)
- [132] H.A. Pohl and D.A. Opp, J. Phys. Chem., 66, 2121 (1962)
- [133] Ya.M. Paushkin, T.P. Vishnyakova, A.F. Lunin and S.A. Sizova, "Organic Polymeric Semiconductors", (Translation by R. Kundor), Wiley and Sons, New York (1971) Ch.1.
- [134] F. Gutmann and L.E. Lyons, "Organic Semiconductors", Wiley and Sons, New York (1967) Ch.7.
- [135] D.D. Eley and M.R. Wills, in H. Kallmann and M.Silver (eds.), "The Electrical Conductivity of Solid Free Radicals and the Electron Tunneling Mechanism", Inc., New York (1961)
- [136] A. Rembaum, A. Henry and H. Waits, "Space Programs Summary", Vol.4, Jet Propulsion Lab., Pasadena, Calif. (1963) p.103.
- [137] H. Inone, K. Noda, S. Takiuchi and E. Imoto, J.Chem. Soc. Japan, 65, 128 (1962)
- [138] A. Rembaum, J. Moacanin and H.A. Pohl, in J.B.Birks and J.A. Hart (eds.), "Progress in Dielectrics", Vol.6, Academic Press, New York (1965)

- [139] H.A. Pohl, A. Rembaum and A. Henry, J. Amer. Chem. Soc., 84, 2699 (1962)
- [140] L.I. Maissel, in G. Hass and R.E. Thun (eds.), "Physics of Thin Films", Vol.3, Academic Press, New York (1966)
- [141] K.G. Gunther, in J.C. Anderson (ed.), "The Use of Thin Films in Physical Investigations", Academic Press, London (1966) p.213
- [142] H.H. Wieder, "Intermetallic Semiconducting Films", Pergamon Press, Oxford (1970) Ch.1
- [143] L. Harris and R.M. Siegel, J. Appl. Phys., 19, 739 (1948)
- [144] W.R. Beam and T. Takahashi, Rev. Sci. Instr., 35, 1623 (1964)
- [145] I. Langmuir, Proc. Roy. Soc., SerA, 170, 1 (1939)
- [146] S.D. Sathye and A.P.B. Sinha, Thin Solid Films, 44, 57 (1977)
- [147] American Institute of Physics Hand Book, 3rd edn., McGraw-Hill Book Co., New York (1972) p.918
- [148] R.G. Cope and H.J. Goldsmid, Brit. J. Appl. Phys., 16, 1501 (1965)
- [149] G. Bonneauze, A. Lichanot and S. Gromb, J. Phys. Chem. Solids, 39, 813 (1978)
- [150] P. Junod, B. Kilcher and J. Wulfschleger, Hel. Phys. Acta, 45, 901 (1972)

- [151] A.V. Ditman and I.N. Kuklikova, *Sov. Phys. Solid State*, 19, 1403 (1977)
- [152] A. Ichimescu and L. Constantinescu, *Revue, Roum. Phys.*, 17, 163 (1972)
- [153] A. Ichimescu, *St. Cerc. Fiz.*, 25, 403 (1973)
- [154] V. Cehan, P. Petrariu and E. Luca, *Bull. Inst. Polytech. Iasi I*, 18, 171 (1972)
- [155] S.P. Sharma and J.H. Thomas, *J. Appl. Phys.*, 47, 1808 (1970)
- [156] R.B. Alder, A.C. Smith and R.L. Longini, "Introduction to Semiconductor Physics", John Wiley and Sons, New York (1964) p.197
- [157] A.K. Mukerjee, *Indian J. Phys.*, 43, 230 (1969)
- [158] A.J. Bosman, "Conference on Electronic Processes in Low Mobility Solids", Sheffield (1966) p.16
- [159] R.F.G. Gardvier, F. Sweett and D.W. Tannev, *J. Phys. Chem. Solids*, 24, 1175 (1963)
- [160] H. Remy, "Treatise on Inorganic Chemistry", Vol.2, Elsevier, Amsterdam (1956) p.272
- [161] R.R. Shively, Jr., and W.A. Weyl, *J. Phys. Coll. Chem.*, 55, 512 (1950)
- [162] K.L. Chopra, "Thin Film Phenomena", McGraw-Hill, New York (1969) Ch.7
- [163] F.J. Blatt, in "Solid State Physics", Vol.4, Academic Press, New York (1957) p.199

- [164] J.N. Zemel, J.D. Jenson and R.B. Schoolar, Phys. Rev., 140, A330 (1965)
- [165] R.G. Mankarious, Solid State Electron., 7, 702 (1964)
- [166] J. Dresner and F.V. Shallcross, J. Appl. Phys., 34, 2390 (1963)
- [167] K. Kienel, Ann. Physik, 5, 229 (1960)
- [168] C.J. Paparoditis, J. Phys. Radium, 23, 411 (1962)
- [169] S. Miyatani, J. Phys. Soc. Japan, 8, 680 (1955)
- [170] S. Miyatani, J. Phys. Soc. Japan, 15, 1586 (1960)
- [171] P. Junod, Helv. Phys. Acta, 32, 576 (1959)
- [172] S. Miyatani, J. Phys. Soc. Japan, 24, 328 (1968)
- [173] M.H. Hebb, J. Chem. Phys., 20, 185 (1952)
- [174] A.V. Ditman and I.N. Kulikova, Sov. Phys. Solid State 19, 1403 (1977): (same as Ref.151)
- [175] A. Ichimescu and L. Constantinescu, Rev. Roum. Phys., 17, 163 (1972): (same as Ref.152)
- [176] A. Ichimescu, St. Cerc. Fiz., 25, 403 (1973): (same as Ref.153)
- [177] R.G. Cope and H.J. Goldsmid, Brit. J. Appl. Phys., 16, 1501 (1965) : (same as Ref.148)
- [178] V. Cehan, P. Petraiu and E. Luca, Bull. Inst. Polytech. Iasi I, 18, 171 (1972) (.same as Ref.154)
- [179] G. Bonneauze, A. Lichanot and S. Gromb, J. Phys. Chem. Solids, 39, 813 (1978) : (same as Ref.149)

- [180] B. Tareev, "Physics of Dielectric Materials",
Mir, Moscow(1975) p.61
- [181] D.R. Goyal, O.S. Panwar, K.K. Srivastava,
K.N. Lakshminarayan, A. Kumar and D.R. Ravikar,
Indian J. Pure and Appl. Phys., 15, 10 (1977)
- [182] A. Tager, "Physical Chemistry of Polymers", Mir,
Moscow (1972) p.203
- [183] N.F. Mott and E.A. Davis, "Electronic Process in
Non-Crystalline Materials", Oxford (1971) p.41
- [184] A.K. Jonscher and A.K. Hill, in G. Hass, M.H.
Francombe and R.W. Hoffman (eds.), "Physics of
Thin Films", Vol.9, Academic Press, New York
(1977) p.10
- [185] C.L. Gupta, Indian J. Pure and Appl. Phys., 15,
684 (1977)
- [186] A. Goswami and A.B. Mandale, Japan. J. Appl. Phys.,
17, 473 (1978)
- [187] G.A. Acket and J. Volger, Physica, 32, 1543 (1966)
- [188] S. Morita, G. Sawa, T. Mizutani and M. Ieda,
J. IEE Japan, 92-A, 65 (1972)
- [189] O.H. Le Blanc,Jr., J. Chem. Phys., 33, 626 (1960)
- [190] K.C. Brown, Eur. Polymer J., 8, 117; 8, 129 (1972)
- [191] H.U. Poll, Z. Angew. Phys., 29, 260 (1970)
- [192] S. Morita, G. Sawa and M. Ieda, Japan J. Appl.
Phys., 14, 1459 (1975)

- [193] P.G. Puranik and K.V. Ranich, Proc. Indian Acad. Sci., 54, 146 (1961)
- [194] J.C. Evans, Spectrochem. Acta 16, 999 (1960)
- [195] N. Abashegovic, J. Raman. Spectrosc., 6, 6 (1977)
- [196] D.H. Whiffen, P. Torkington and H.W. Thompson, Trans. Faraday Soc., 41, 200 (1945)
- [197] K. Nakamishi, "Infrared Absorption Spectroscopy", Holden-Day (1964) Ch.2
- [198] V.M. Kolotyrkin, A.B. Hillman and K. Tasapuk, Russ. Chem. Rev., 36, 579 (1967)
- [199] A.K. Jonscher, Thin Solid Films, 50, 187 (1978)
- [200] S.J. Fonash, in C.H.S. Dupuy and A. Cachard (eds.), 'Physics of Non-Metallic Thin Films', Plenum Press, New York (1974) p.225
- [201] H. Frohlich, "Theory of Dielectrics", Oxford Press, Oxford (1958)
- [202] C. Kittel, "Introduction to Solid State Physics", Wiley, New York (1968)
- [203] S.J. Fonash, J.A. Roger, J. Pivot and A. Cachard, J. Appl. Phys., 45, 1223 (1974)
- [204] R.J. Friauf, J. Chem. Phys., 22, 1329 (1954)
- [205] J.G. Simmons and G.W. Taylor, Phys. Rev., 6, 4793 (1972)
- [206] J.R. Macdonald, J. Chem. Phys., 58, 4982 (1973)

- [207] M. Meaudre and R. Meaudre, *Solid State Electron.*,
16, 1205 (1973)
- [208] J.R. Macdonald, *J. Appl. Phys.*, 45, 73 (1974)
- [209] F. Argal and A.K. Jonscher, *Thin Solid Films*,
2, 185 (1968)
- [210] J.C. Macfarlane and C. Weaver, *Philos. Mag.*, 13,
671 (1966)
- [211] J.G. Simmons and G.W. Taylor, *Phys. Rev.*, 6,
4793 (1972) : (same as Ref.205)
- [212] J.A. Roger, C.H.S. Dupuy and S.J. Fonash, *J. Appl.
Phys.*, 46, 3102 (1975)
- [213] J.G. Simmons, *J. Phys. Chem. Solids*, 32, 1987 (1971)
- [214] J.G. Simmons, *J. Phys. Chem. Solids*, 32, 2581 (1971)
- [215] K.L. Chopra, "Thin Film Phenomena", McGraw-Hill,
New York (1969) Ch.8
- [216] C. Weaver, *Advan. Phys.*, 11, 85 (1962)
- [217] P.J. Harrop and D.S. Campbell in L.I. Maissel and
R. Glang (eds.), "Handbook of Thin Film Technology",
McGraw-Hill, New York (1970) Ch.16
- [218] C. Feldman and M. Hacskaylo, *Rev. Sci. Instr.*, 33,
1459 (1962)
- [219] A.K. Jonscher, *Nature*, 267, 673 (1977)
- [220] M.A. Careem and A.K. Jonscher, *Philos. Mag.*,
35, 1489 (1977)

- [221] E.S. Cole and R.H. Cole, J. Chem. Phys., 9, 341
(1941)
- [222] K. Kinosta, Thin Solid Films, 12, 17 (1972)
- [223] A. Tager, "Physical Chemistry of Polymers", Mir,
Moscow (1978) Ch.11
- [224] N.G. McCrum, B.E. Read and G. Williams, "Anelastic
and Dielectric Effects in Polymeric Solid",
Wiley, New York (1967) Ch.5
- [225] A.K. Jonscher, Nature, 253, 717 (1975)
- [226] G. Sawa, O. Ito, S. Morita and M. Ieda, J. Polym.
Sci., Chem. Phys. Ed., 12, 1231 (1974)
- [227] L.S. Tuzov, V.M. Kolotyrkin and N.N. Tunitskii,
Inst. Chem. Eng., 11, 60 (1970)
- [228] J.M. Tibbitt, A.T. Bell and M. Shen, in M. Shen (ed.)
"Plasma Chemistry of Polymers", Marcel Dekker
(1976) (Same as Ref.52)
- [229] J.J. Licari, "Plastic Coatings for Electronics,"
McGraw-Hill, New York (1970)
- [230] J. Chutia and K. Barua, J. Phys. D: Appl. Phys.,
13, 19 (1980)
- [231] D. Sanchez, M. Carchano and A. Bui, J. Appl.
Phys., 45, 1233 (1974)
- [232] K.O. Lee and T.T. Gaw, Phys. Stat. Solidi (a),
43, 565 (1977)

- [233] M.A. Lampert, Phys. Rev., 103, 1648 (1956)
- [234] N. Paul and M.G.K. Pillai, Thin Solid Films,
76, 201 (1981)

LIST OF SYMBOLS

A	-	Ampere, film area, Richardson-Schottky Constant
$\overset{\circ}{A}$	-	Angstrom
AC	-	Alternating Current
B	-	Constant
C	-	Capacitance
D	-	Flux density
DC	-	Direct Current
D_p	-	Degree of polymerization
d	-	Film thickness
Δd	-	Barrier width
E	-	Electric field
E_c	-	Bottom energy level of conduction band
E_F	-	Fermi energy
E_{F_0}	-	Thermodynamic Fermi energy
E_t	-	Trap energy level
ΔE	-	Activation energy
e	-	Electron or ion charge
eV	-	Electron volt
F	-	Field in volt cm^{-1}
F'	-	Fermi level
GD	-	Glow discharge

GHz	-	Gega hertz
g	-	Degeneracy factor
h	-	Planck's Constant
I	-	Current
IR	-	Infrared
i, j	-	Repeat Units
J	-	Current density
J_0	-	Constant
K	-	Degree Kelvin
KHz	-	Kilo hertz
k	-	Boltzmann's Constant
L_D	-	Debye length
l	-	Mean free path
l, l_1, l_2	-	Distance between successive defect sites
MHz	-	Mega hertz
M_i, M_j	-	Monomer Molecules
M_i^{\cdot}, M_j^{\cdot}	-	Free radicals
M_p	-	Molecular weight of polymer
M_r	-	Molecular weight of repeat unit
M-I-M	-	Metal-insulator-metal
M-P-M	-	Metal-polymer-metal
m	-	Mass of deposited film
m_e	-	Mass of electron
mfp	-	Mean free path

N_c	-	Effective density of states in the conduction band
N_t	-	Trap density
N_{t1}, N_{t2}	-	Trap levels
n_o	-	Free electron density
n	-	Total number of carriers
n_b	-	Electron density in bulk
P	-	Polarization
p	-	Specularity parameter
p_B	-	Hole density in bulk
R	-	Resistance
RF	-	Radio-frequency
SCLC	-	Space charge limited conduction
T	-	Temperature
TCC	-	Temperature coefficient of capacitance
TCR	-	Temperature coefficient of resistance
V	-	Voltage
V_{TFL}	-	Trap filled limit voltage
V_x	-	Cross over voltage from Ohm's law region to square law region
α	-	Dielectric loss peak at high temperature
β	-	Dielectric loss peak at medium temperature, a constant
γ	-	Dielectric loss peak at low temperature, d/l

- $\tan \delta$ - Dielectric loss angle
 ϵ - Dielectric Constant
 G - Trapping factor
 ϵ_0 - Constant
 λ - Wavelength
 μ - Mobility of carriers
 μ_B - Mobility of carriers in the bulk
 μ_F - Mobility of carriers in the film
 \bar{v} - Probability of defect jumping over a potential to another defect site
 \bar{v}_E^+ - Jump probability in an applied electric field
 ρ - Resistivity
 ρ_0 - Constant
 σ - Conductivity
 τ_B - Average relaxation time due to bulk scattering
 τ_B - Average relaxation time for electrons in film
 τ_S - Average relaxation time due to surface scattering
 ϕ_0 - Barrier height
 $\bar{\phi}$ - Average barrier height

ACKNOWLEDGEMENTS

The investigations presented in the thesis were carried out by the author as a full-time research scholar in the Department of Physics, University of Cochin during the years 1978-81.

It is a pleasure for the author to express her indebtedness to Dr.M.G. Krishna Pillai, Professor, Department of Physics, University of Cochin, for his able guidance and help extended to her to carry out this investigation.

The author is also thankful to Dr.K. Sathianandan, Professor and Head of the Department of Physics, University of Cochin for providing the necessary facilities and for his interest in the work.

The author wishes to express her gratitude to Dr.K. Babu Joseph, Reader, and Dr. Joy George, Professor, Department of Physics, University of Cochin for their co-operation in carrying out these investigations. The author also wishes to acknowledge with thanks Mr.C. Raghavan for the timely help.

Thanks are due to Dr.M.K. Radhakrishnan, Mr.K. Mohanachandran and Miss S. Jayalakshmi, Research Scholars, Department of Physics, University of Cochin for their whole-hearted co-operation with the author.

The author is thankful to Mr.K.P. Sasidharan who typed the thesis.

The author wishes to thank Cochin University and University Grants Commission for providing financial support in the form of Research Fellowship.

- 62970 -

